ADDIS ABABA UNIVERSITY

ADDIS ABABA INSTITUTE OF TECHNOLOGY

SCHOOL OF CIVIL AND ENVIRONMENTAL ENGINEERING

Flood Risk Mapping (Case Study of Ketar Watershed Ziway-Dugda Woreda, Ethiopia)

A Thesis in Hydraulic Engineering Stream

By Keno Abu

December 2020

Addis Ababa

A Thesis

Submitted in Partial Fulfillment of the Requirement for the Degree of Master of Science

The undersigned have examined the thesis entitled **Flood Risk Mapping (Case Study of Ketar Watershed Ziway-Dugda Woreda, Ethiopia)**' presented by **Keno Abu**, a candidate for the degree of **Master of Science,**and hereby certify that it is worthy of acceptance.

Advisor	Signature	Date
Internal Examiner	Signature	Date
External Examiner	Signature	Date
Chairperson	Signature	Date

DECLARATION

I confirm that the research work titled "**Flood Risk Mapping (Case Study of Ketar Watershed Ziway-Dugda Woreda, Ethiopia)'**" is my work. The work has not been presented elsewhere. Where material has been used from other sources it has been properly acknowledged.

Signature of Student

Keno Abu

ABSTRACT

Flood is probably the most devastating, widespread, and frequent natural hazard of the world that producing many socioeconomic and environmental consequences within the affected floodplains. In Ethiopia, there is a lot of areas under flood problem and Ketar river floodplain located at the downstream of Abura gauging stations is among the most frequently flood-affected area for which flood risk mapping is so important. The objectives of this study were to model rainfall-runoff using HEC-HMS for Ketar watershed and flood risk mapping by using HEC-RAS and HEC-GeoRAS for Ketar river floodplain, located downstream of Abura gauging station in Ziway-dugda woreda, Ethiopia. The HEC-HMS software requires daily hydrological data of 16 years Collected from a National Meteorological Agency of Ethiopia for rainfall-runoff modeling. A normal-ratio method was used for filling missing values of precipitation data and data consistency was checked bya double mass curve. The initial and constant loss for precipitation loss model, Clark unit hydrograph for excess precipitation transformation to direct run-off, monthly constant for base flow modeling, and Muskingum for flood routing modeling were chosen.Gage weight meteorological method was selected to assign the weighted precipitation to each sub-basins using the Thiessen polygon method. Among the collected 16 years of hydrological data for rainfall-runoff modeling, 11 years (1988-1998) were used in model-calibration and 5 years (1999-2003) were used in model validation. The model-performances were evaluated using performance measuring techniques including Nash Sutcliff Efficiency (NSE) and Coefficient of Determination (R^2). NSE during calibration and validation was 0.72 and 0.67 respectively whereas R^2 during these two processes was 0.87 and 0.81 respectively Flood frequency analysis was conducted using HEC-HMS' frequency storm method for 2, 5, 10, 25, 50,and 100 year return periods. The peak flood for each respective return periods were (198.5, 224.1, 242.9, 251.8, 267.5, and 283.5 m3/s). Flood risk mapping was modeled for a peak flood of each return period using HEC-RAS, HEC-GeoRAS,and Arc GIS software; and resulted in the inundated areas of 2.86, 2.91, 2.94, 2.95, 2.98, and 3.01 km2 respectively.

Key Word: Flood risk mapping, HEC-HMS, HEC-RAS, Arc GIS, Rainfall-Runoff Modeling

ACKNOWLEDGMENTS

First of all, Iwould like to thank the almighty God for his endless and invaluable help to be a person of this stage and being able to complete this Master's program. Next, my deepest appreciation and respect full thanks will go to my advisor **Dr.Daneal F/Sillassie** who share with me his expensive and priceless knowledge of Hydraulic engineering through his attractive lecture and his constructive guidance, innovative suggestions, and the leading role which contributed to the successes of this thesis research.

Again, I give my appreciation to theNational Meteorological Agency of Ethiopia (NMAE), Ministry of Water Resources, Irrigation, and Energy particularly the Hydrology and GIS Department which provided me the data and information needed for this work.

Also, Iwould like to acknowledge the Ministry of Education for the financial support made through the post-graduate program at Addis Ababa University, which is available for me during my whole study time.

Finally, I take this opportunity to thanks all my classmates (friends) and families, who helped me in one way or another, in carrying out my research through remarkable encouragement, advice, material support, and collaboration in every aspect. Inline with this, my precious and honored full thanks to Addis Ababa institute of technology staff and all who pay a contribution from the commencement of this thesis to the end.

TABLE OF CONTENTS

LIST OF TABLES

LIST OF FIGURES

ABBREVIATIONS

USACE	United State Army Corps of Engineers
GIS	Geographical Information System
CN	Curve Number
UH	Unit Hydrograph
DEM	Digital Elevation Model
TIN	Triangular Irregular Network
GUI	Graphical User Interface
ERA	Ethiopia Road Authority
SI	System international units
RVLB	Rift Valley Lake Basin
MoWRIE	Ministry of Water Resources, Irrigation, and Energy
FFA	Flood Frequency Analysis
IDF	Intensity Duration Frequency
NSE	Nash-Sutcliffe Efficiency
TEM	Terrain Elevation Model
DMC	Double Mass Curve
IUH	Instantaneous Unit Hydrograph
DTM	Digital Terrain Model
HEC-HMS	Hydrologic Engineering Center Hydrological Modeling System
HEC-RAS	Hydrologic Engineering Center River Analysis System

CHAPTER 1 INTRODUCTION

1.1 Background

Among the natural hazards capable of causing a disaster, the flood is the most hazardous, frequent, and widespread catastrophic events throughout the world today. Between 2000 and 2008, floods were affected the largest number of people worldwide, averaging 99 million people per year. This makes flooding an important subject of study, particularly in the less developed countries like Africa and the others. According to the related Programs on Flood Management, flood impacts tend to be very dangerous in African towns whereimproper land use planning and management forurbanization takes place.(ERCS, 2010)

Flood is the second and the worst environmental problem next to droughts in Africa. Most countries in Sub-Saharan Africa are exposed to one or more of the natural hazards. The large river basins which usually affected by the flood are the Congo, Niger, Nile, and Zambezi basin. The unbalanced impact of natural disasters on the poor Sub-Saharan African countries are not been well documented. The driving factors behind the increased exposure of Sub-Saharan African countries to natural hazards are population growth, poverty, food insecurity, improper use of natural resources and rapid urbanization, etc.

Ethiopia is one of the natural hazard-prone (drought, flood, etc.) countries in Sub-Saharan Africa. The impact of drought and flood combined with poverty and high population growth let several peoples become sufferersof various disasters. It is indicated by the significantly increased number of people and areas affected; several deaths; and infrastructure and property loss.The manifestation of climate change in the form of unpredictable rainfall, frequent and severe floods; and droughts have serious consequences on the livelihood, the security of smallholder farming communities, and making them more vulnerable in countries like Ethiopia.Many countries are frightened by the quite extraordinary and unusual magnitude of flooding. The problems are more acute in the river basin as well as urban areas(Niguse and Adhanom, 2019).

Floods in Ethiopia that cause significant damage to human lives and livelihood in part of the country is mainly relatedto heavy rainfall and the topographies of the highlands mountain and lowlands plain with ordinary drainage systems formed by the principal river basins. In most cases, floods occur in the country as a result of extended torrential rainfall which causes rivers to overflow and inundated areas along the river banks in the lowland plain. For instance, the major river flood-prone areas are some part of Oromia and Afar region located along the upper, middle, and down-stream plains of the Awash River; part of Somali regions along the Wabe-Shebelle, Genale,and Dawa Rivers; low-lying area of Gambella along the Baro, Gilo, Akobo, and Alwero Rivers; down-stream areas along the Omo and Bilate Rivers in SNNPR and the extensive floodplains surrounding Lake Tana and the banks of Gumera, Rib and Megech Rivers in Amhararegion (ERCS, 2012).

The Ketar watershed is entirely located in the central part ofthe rift valley of Ethiopia, Oromia national regional state, at the southeastern part. Ketar river is the major contributor of water to lake Ziway and also it is a perennial river that flows throughout the year. It is found in the southeastern part of the Meki watershed; which both of them are the feeder of Ziway Lake (Tufa et al.,2015). Also,the ketar watershed is characterized by severe land degradation resulting from soil erosion, flooding, sediment, and nutrient intrusion to the Lake Ziway. After a few years flood becomes a challenging disaster and emerging issue for the community especially during the high rainy season downstream of Abura gauging station. For instance, Villages like ‘Humbenna’ and,’ Hallo’ which is located in Ziway-dugda woreda of Arsi zone Oromia regional state are affected by flood every year during the summer season. Therefore, developing a rainfall-runoff model and flood risk mapping is an important issue to perform. This call for considering both Rainfall-runoff modeling, for Ketar watershed, and flood risk mapping, for Ketar River downstream of Abura gauging station, is to minimize its effect on community life and property by knowing the route of the problem.

Today, several mathematical methods for calculating the extent of a riverabout their flow-rate, the infiltration of water into the soil, and land-use have been developed. These mathematical model has been incorporatedinto GIS software, whose intention is to create a model that can replicate the shape of the landscape as accurately, as possible (Daniel et al., 2011). The flood risk map has a clear purpose to identify the susceptible areaand the

populations which are vulnerable in a certain region; it represents an important tool ina time of urban plan formulation and creation and intends to be used in the proscription of house construction in the affected area and to create management plans for emergencies,of certain situations of this type.(Ongdas et al., 2020)

HEC-RAS is software for one-dimension or two-dimension simulations of the development of a flood, that has stables or unstable flow-rates, sediment transport, changes of the riverbed,etc. The name of HEC-RASis derived from the creator of the software: Hydrologic Engineering Center, which stands as a subdivision of the Institute of Water Resources, U.S Army Corps of Engineers, and the "RAS" is an acronym stand for "River Analysis System". The main four rivers analysis possibilities of the software are the constant flow-rate at the surfaces of river profiles under consideration; simulations of an unsteady-flow of water; calculations of the sediment transport and modifications of the river bed and analysis of the water quality (Eric Tate et al., 1999). When using the HEC-GeoRAS extension, the data can be easily inserted into the equation, and the output can be displayed through maps of the hydrological risk (Ongdas et al., 2020).

Risk is the probability of harm that occurs at a place, community, or system as a result of an interaction betweennatural or human-induced hazards and vulnerable conditions. The impact which may occur after a disaster may be assessed by the vulnerability. It represents how susceptible an individual, a community, an asset, or a system is to the impacts of hazards. Flood usually represents the overflow of water. Overflow maybe occurs from a stream-channel onto normally unflooded land in the alluvial plains, known as riverine flooding,which is higher than normal level along the coasts and in lakes or reservoirs, called coastal flooding;and ponding of water at or near the point where the rainfall, known as flash floods. Cred classifies floods as hydrological disasters (Banstola and Sapkota, 2019).

1.2 Statement of the problem

Floods will continue to cause serious environmental and economic losses. It is indicated that flood disaster covers about one-third of all-natural disaster in terms of their numbers and economic loss. Flood and droughts are the world’s costliest natural disasters, causing an average of $6–$8 billion in global damages annually and

collectively affecting more people than any other forms of natural disasters (Asnake, 2018).

In Ethiopia, from January to February was typically wet in southwestern areas; while the continued above-average rains in March were beneficial to 'belg' crops. The rains also creates favorable ecological conditions for desert locust breeding and promoted further development(Report, May 19, 2020)

In recent years, torrential rainfall frequently causes flood disasters, and quite a few of them resulted in tremendous damage to the areas.Nowadays, extraordinary floods are common to many parts of Ethiopia every year causing a lot of losses to human lives as well as damages to property. The major of flood disasters‟ sufferers are poor people existing in nearby or surrounding the stretch of the floodplain.

Ketar watershed, located in the central part ofthe rift valley of Ethiopia, is characterized by severe land degradation resulting in soil erosion, flooding, sediment, and nutrient intrusion to the Lake Ziway. After a few years flood becomes a challenging disaster and emerging issue for the community especially during the high rainy season downstream of Abura gauging station to the entrance of Ziway lake.

For instance, Villages like 'Humbenna' and,' Hallo' which is located in Ziway dugda-woreda of Arsi zone Oromia regional State are affected by floods every year during the summer season. Therefore, developing a rainfall run-off model and flood risk mapping is an important issue to perform. This call for considering both Rainfall-runoff modeling, for Ketar watershed, and flood risk mapping, for Ketar River downstream of Abura gauging station, is to minimize its effect on community life and property by knowing the route of the problem.

1.3 Objectives of the study

1.3.1 General objective

The general objective of this research is to develop flood risk mapping of the Ketar River in Ziway-dugda woreda at downstream of Abura gauging station, and also determine the extreme flood at different return period using hydrological modeling

1.3.2 Specific objective

- To model rainfall runoff using Hydrologic Modeling System on Ketar watershed.
- HEC-HMS Hydrologic model calibration and Validation for Ketar Watershed on its outlet (Abura gauging station).
- To develop 1D steady hydraulic modeling and Flood risk mapping using River Analysis System on Ketar River starting from Abura gauging station to the downstream.
- To develop a water surface profile from different return period peak discharge
- To develop flood risk maps on Ketar river from the ketar watershed outlet to the entrance of Ziway lake

1.4 Research question

What is the magnitude of Peak flood in different return periods?

What is the output of the hydraulic model of flood profiles of the study area?

How does the flood risk map look like from the discharge of different return periods?

What are the magnitudes of inundated areas for each peak flood at different return periods?

1.5 Significance of the study

To secure human life and property of the local community it needs to obtain future information on water resources, hydrological hazard characteristics, and its impact.Accurate flood risk maps can be the most valuable tool for avoiding severe social and economic losses from floods. Timely updated floodplain maps also improve public safety by giving awareness about the flood for them as well. Early identification of flood-prone properties during emergencies allows public safety organizations to establish warning and evacuation priorities for them

This study can give full information concerningthe characters of the study catchment, peak flood magnitude and its frequency, location of the worst flood-prone area, and its

extent, for those who will go to take action like flood mitigation measures and decision making. And also it can be used as a reference for researchers who intended to carry out a further investigation on the catchment using different techniques and more advanced tools.Finally, the result will be applied in the processes to update plans, policies, and programs to minimize losses of humanlife and their properties due to flood risks in the study areas and assure community sustainability

1.6 Scope of the study

This study can cover a lot of sub-titles such as Rainfall-runoff model development, flood frequency analysis, assessment of flood risk map and identification of appropriate flood mitigation measures, 1D steady and unsteady hydraulic modeling and flood hazard mapping, etc. However, because of constraints in time and limited availability of essential data, and complexity in computation, the study mainly focus on hydrologic model development, HEC-HMS based flood frequency analysis, 1D Steady hydraulic modeling, and Flood risk mapping

CHAPTER 2 LITERATURE REVIEW

2.1 Definition of Flood

Floodis defined as the inundation of land-surface by the rise and overflow of a body of water which may cause some damage to property and sometimes injuries and death. Water resources specialists frequently relate flood to a flow with a magnitude close to its annual peak value. Floods are the most dangerous and destructive acts of nature. They cause widespread damage to agriculture, residences, and public utilities and amount to the loss of billions of dollars each year besides the loss of human as well as animal lives. (Saha and Praneeth, 2016).

A flood occurs most commonly when water from heavy rainfall, melting ice and snow, or from a combination of these exceeds the carrying capacity of a river-canal system or the lake into which it runs. Usually, the combined flow of several water-swollen tributaries causes flooding along a riverbank or shoreline. However, all floods are not destructive. The annual floodwaters of the Nile and some other larger rivers historically deposited fertile soil along the surrounding floodplain, which is used extensively for agriculture. The damming of the Nile and other rivers in modern times, however, often has greatly reduced this deposition. It can be slow or fastrising but generally develop for days.

There is a relationship between human interactions and hydrological characteristics, such as a decrease of infiltration, an increase of overland flow, increase in frequency and height of flood peak, increase in variability of discharge (range) and decrease lag time. The dangers of floodwaters are associated with several different characteristics of the flood such as depth of water, velocity, duration, sediment load, rate of rising, and frequency of occurrence.

2.2 Types of Flood

One of the keys points to understand the flood risk is to know the types of floods. There are several different types of a flood, and each of them has different impacts in terms of

how it occurs, the damage it causes, and how it is forecasted. Floods can be categorized according to the speed of the water, geography, or the root cause of floods (Wana, 2018).The four common types of floods are as follows:

River Flood: is occurs when too much rainfall above the extended length of time and bring a riverexceeding their capacity and as a result water levels rise over the banks of the river. It can also be caused by intensive snowmelt and ice-jams. The damage from a river flood can be extensive as the overflow affects smaller rivers downstream, always causing dams and dikes breaking and swamping nearby areas.

Flash Flood: Thisis a special type of flood that can happen anywhere which is caused by extremely intense precipitation within a short period. It usually lasts only a few hours. Flash flood is very risky and harsh because of the force of the water and the moving of debris which is frequently sweptup in the flow. The ferocity, rapidity, and intensity of the high water make it (flood) very dangerous. The severity of the flash flood is resolved by how much of the precipitation in the area howthe length of time it stays during precipitation to build up, the previous saturations of local soil, and the terrain around the river system.

Urban Flood: Urban flood, is resulted from excessive rainfall creating the flood event independents of spilling over the water body. Urban flood is an inundation of urban areas when heavy rainfall exceeds the capability of a sewer system and drainage canals. It can cause severe damage to infrastructure: roads can be blocked, water can get inside buildings through walls and floors, or cause backup through toilets and sinks.

Coastal flooding:is a type of floodthat occurs in the area where the coast of a sea and ocean, or other large open waterbody recline on. It'stypically happened from great tidal conditions bring about by harsh weather conditions. Storm surge formed when the high wind from the hurricane and other storm drive water onshore is the primary give rise to coastal flooding and frequently the most significant intimidation relatedto a tropical storm.

2.3 Flood cause and impacts

There are many events that can cause flooding; these are like rains, river overflow, strong wind in coastal areas, dam breaking, ice, and snow-melt, etc. Flood has

impactson socio-economic and environmental as well. Flooding can produce a variety of negative effects on social, economical as well as environmental activities. As a result the loss of lives and livelihoods, loss of properties, reduction in production and purchasing power, Hindering economic growth and development, and the environment also suffers from the problem when the flood has happened.

Floods also affect the economic level by affecting the earth's global supply chain networks.A supply- chain network is used to highlight interactions between organizations and also be used to show the flow of information and materials across organizations. However, with lean and compounded supply chains, there is much more susceptibility to systematic risk. This idea of risk is relevant to the supplychain. While a more well-organized production and transportation systemsare more capital demand and cost-efficient, in the event of a natural catastrophe like a flood, the overall system may expose disturbance and collapse (Haraguchi and Lall, 2013).

2.4 Flood risk mapping

The flood risk map has a clear intension to identify susceptible area and populations which are vulnerable in a certain region; thatrepresents an important tool at the time of urban planning useful and intended to be used in the prohibition of houses constructions in the damaged areas and also management plan creation for emergencies.

The flood risk map is prepared from the hazard map and flood vulnerability analysis; since flood risk comprises hazard and vulnerability. The significance of a Flood Risk maps are:-

- It is a practical reference point for decision-making concerned in the management of land and water resources.
- It is not a principal device or tool for policymaking, rather it could be joined as a system for proper administering of floodplain and related area based on their comparative land-use and land cover characteristics.
- It is a typical input for the common planning of pieces of land; so, the issue concerning legal or political, or any other governmental instruments are not connected to a mapping process. It’s more of a guide to proper resource management than a restrictively-centered mechanism for land management. This

is necessary as water level fluctuates relative to water-input and water-output within the catchment (Getahun and Gebre, 2015).

Integration of spatial devices of GIS for flood inundation mapping has made it possible to delineate water level, inparticular, water level spatially, and superimpose with land use and land cover data to generate areas that will be inundated.

Flood risk is the combination of flood hazards and vulnerabilities at a particular location that needs systematic assessment, collection, and analysis of variables. GIS and its extension (HEC-GeoRAS) have emerged as an important device in flood mapping and analysis because it enables the preparation of maps of inundated areas (Niguse and Adhanom, 2019).

2.4.1 Flood hazard mapping

Flood hazard mapping is a flood map showing the flood hazard, i.e. the intensity of flood situations and their related exceedance probability. Frequently, a flood hazard map shows synthetic-event for scenarios of inundation area with a certain recurrence interval, the spatial distribution of the depth of water,and flow velocity. The hazard feature of the flood risk is related to the hydraulic and hydrological parameters.GIS is an important tool for delineating flood hazards and flood risk susceptibilityof mapping by considering the determinant factors. Floodhazard for a given area depends on physical and socio-economic factors (Niguse and Adhanom, 2019).

Flood hazard maps are commonly used in floodplain information reports and requirementsfor updating when changes have occurred in the channels, on the floodplains, and in upstream areas. These changes include structural and channel or floodplain modifications in upstream areas. Development of new buildings on the floodplain, obstructions, or other land-use changes can affect the water surface elevation,stream discharges and flow velocities, thereby changing the elevation profile defining the floodplain

2.4.2 Flood vulnerability

The vulnerability can be defined as the degree to which people, property, environment, social and economic activities are subjected to harm or being exposed to any destructive factors or cause. It generally refers to that characteristic of society which specifies the potential for the damage to occur from different types of hazards for hazard problem.

The flood vulnerability is affected by the land use/cover characteristics of the areas under the influence of flood i.e., a flood of the same exceedance probability will have different levels of vulnerability according to the land use characteristics and potential for damage. Therefore, the vulnerability analysis consists of identifying the land use areas under the potential influence of a flood of a particular return period.

2.5 Rainfall-Runoff modeling

Rainfall-runoff modeling shows the relationship between precipitation received by and surface runoff generated from the catchment area. The model will estimate the surface runoff in the channel or river system as a function of precipitation for the target catchment. Rainfall-runoff modeling helps to imagine what occurs in the water system due to the alterations in previous surfaces, vegetation, and meteorologic event(Wana, 2018).

The models are used as a device for a wide range of activities, likethe modeling of the flood event, the monitoring of water levels in different water conditions, or flood prediction. Hydrological models can be categorized as probabilistic and deterministic. The probabilistic models will produce outputs that have partial randomness whereas the deterministic models on the other hand do not give randomness. Further, deterministic hydrological models are classified into three major classes.These are the lumped, distributed, and semi-distributed model.

Rainfall-runoff correlation is a complex phenomenon to represent in the mathematical form. Today's advanced rainfall-runoff computing software has overcome most of the real-world complexity of rainfall-runoff correlation which is possible to stand for even complex situations in a fairly better way.

2.6 Detail of selected software (model selection)

Selection of the best and appropriate model is an essential part of any research work. The choice of models is not limited to the criteria of the models described below. It is often difficult to determine the relative merits and demerits of models proposed for operational use. The choices of a model for a specific hydrological situation has implications in water-resources planning, development, and management. There are various criteria for choosing the most suitable model. The choice depends mainly on the requirement and

needs of the research or the project under interest. The following areamong the factors and criteria involved in the choice of a model (Dawit, 2015).

a) Required output of the model
b) Availability of input data
c) Prices and availability of the model
d) The model structure
e) The lengths of the records of the various types of data;
f) The availability and size of computers for both the development and operation of the model;
g) The ability of the model to be updated based on current hydro-meteorological conditions.

There are different flood modeling tools that have a distinct model structure and solution procedures. The most commonly used 1D flood modeling tools are; HEC-RAS, FLDWAV, FLUCOMP, ISIS,and MIKE11. Although today's researchers select 1D, 2D interaction flood models, and the use of a one-dimensional flood model has also great significance in the research areas. In this research 1D,a hydraulic model with HEC-GeoRAS and GIS is used because the model has the capacity to simulate flood plain areas with great accuracy

The selection of modeling software is often made on much more realistic grounds. The most important factor in the choosing of software is the familiarity of the potential user with techniques employed by software. Inferior techniques applied by the knowledge of engineers will often produce much more reliable results than a sophisticated model that the user does not understand and therefore treats as a "black box"(Alaghmand et al., 2012).

Data availabilities are another important consideration. For instance, complex flow routing cannot be performed in a stormwater system without extensive data, which may lead the engineer to a simple technique that is not so data intensive. The need for data should not be ignored, however. If the problem is sufficiently complex, there may be no option to the use of a sophisticated model and its attendant data collection requirements

The following are the best known operational models defined criteria to be fulfilled:

1. An operational model must have documentation. This must include a user's manual that describes input data requirements, outputs to be expected, and computer requirements. Besides, the theory and numerical procedures used in the model predictions should be stated. Documentation is the characteristics that most often differentiate a model that can be accessed and used by others from the other computerized procedures described in the literature.
2. An operational model must have support which is normally provided on commercial terms by the original software developer. Support indicates that the user can obtain answers, by telephone or written correspondence, to problems that arise during model implementation and use.
3. An operational software program should have been widely used by other than just the software developer. Regardless of its technical virtues, a procedures described in a single journal article or report with no experience or "review" by the engineering community is a poor candidate for the user by a third party

2.7 Software Description

2.7.1 Arc GIS

A GIS integrated with enterprise database management systems could manage large volumes of geospatial data to provide spatially distributed parameters for modeling However, the use of GIS for modeling data management and integration is generally held back by the differences in scale, precision, data structure, data meaning, representation of the reality, and others, between a GIS and a simulation model (Wana, 2018; Zelalem, 2011).

Major characteristics that differentiate GIS from other types of information systems are that it is a set of computer-based systems for managing geographic data and using these data to solve spatial problems. The objectives of collecting geographic data and changing them into useful information through a GIS transcend the traditional boundary of data processing and information management.

Geographic information system GIS helps us to better understands the world around us. It enables us to develop spatial intelligence for logical decision making. GIS is a special class of information systems. By this heritage, it contains all the characteristics of information systems. Input, data management, manipulation and

analysis, and output is four sets of capabilities that GIS provides to handle geo-referenced data.

The ability to perform complex spatial analyses rapidly provides a quantitative as well as qualitative advantage.By making refinements to successive analyses planning scenarios, decision models, change detection and analysis, and other types of plans can be developed. The analysis of complex, multiple spatial, and non-spatial data sets in an integrated manner forms the major part of a GIS's capabilities. The data used in a GIS represent something about the real world at some point in time. They are always an abstraction of reality because we don't need or want every bit of data; just the one we think would be useful. The application of GIS in combination with remote sensing is very broad. A critical factor governing the incorporation of remotely sensed data into a GIS is the digital nature of the data. One of the most expensive and time-consuming aspects of any GIS is data input since much of the data to be inputted during the transition from analog to digital handling of geographical data must first be digitized. In this study, Arc GIS was used as the work environment in conjunction with both HEC-Geo HMS and HEC-Geo RAS to prepare the input data both for HEC-HMS and HEC-RAS.

2.7.2 HEC-HMS

HEC-HMS is hydrologic modeling system software developed by the USACE HEC. It is the physically-based and conceptually semi-distributed models intended to computethe rainfall-runoff process in a wide range of geographic areas such as large river basin, water supply, and flood hydrology to small urban and natural watershed runoff. Hydrographs created by the program can be used directly or in conjunction with other software for the study of water availability, flow forecasting, urban drainage, future urbanization effect, reservoir spillway design, floodplain regulation, flood damage reduction, wetlands hydrology,and systems operations. The software is designed for interactive use in a multi-tasking, multi-user network environment, and can be utilized with both XP and Microsoft Windows (Feldman, 2000).

The hydrologic model HEC-HMS is designed to compute the rainfall-runoff processes of dendritic drainage basins and the surface runoff response of a basin to rainfall by dividing the basin into interrelated hydrologic and hydraulic components. Simple mathematical relationships are used to represent model component functions, including meteorological, hydrologic, and hydraulic processes, which are divided

into precipitation, interception, infiltration, direct run-off, base-flow, and finally flood routing. Each element in the model performs different functions of the rainfall-runoff process within a given sub-basin.

The advantages of using HEC-HMS are that it draws on more than 30 years of experience in hydrologic simulation. It is freely available for download from the HEC website and is supported by the US Army Corps of Engineers. It provides a graphical user interface making it easier to use the software and the program is broadly used and accepted for many official purposes, such as floodway determination for the FEMA (Federal Emergency Management Agency) (Yuan and Qaiser, 2011).

Model components are used to simulate the hydrologic response in the catchment. The main model components are basin models, meteorological models, and control specifications.

The main inputs to the model are Watershed stream network and size, Infiltration loss method (i.e. SCS curve Number, Initial and Constant, Deficit and Constant, Exponential, Green-Ampt, Smith Parlange, and Soil Moisture Accounting), Transform method for transforming excess precipitation into runoff (i.e. SCS unit hydrograph, Clark unit hydrograph, Snyder unit hydrographs, ModClark, Kinematic wave, User specified unit hydrograph), Routing methods (i.e. Muskingum, Kinematic Wave, Lag, Modified Puls, Muskingum-Cunge, and Straddle Stagger), Meteorological data (i.e. precipitation) and the time span of the simulation. The outputs from the model include the hydrographs and flow volume(Yuan and Qaiser, 2011).

2.7.3 HEC-GeoHMS

HEC-GeoHMS (Hydrologic Engineering Center's Geospatial Hydrologic Modeling System) has been developed as a geospatial hydrology tool kit for engineers and hydrologists. The program is an extension of Arc GIS and allows users to visualize spatial information, document basin characteristics, do spatial analysis, delineate sub-basins and streams, construct inputs for hydrologic models, and assist with report preparation. Eight data sets can be derived from a DEM that collectively describe the drainage patterns of the watershed (Fleming and Doan, 2009). HEC-GeoHMS provides the connection for translating GIS spatial information into the hydrologic model. The end result of GIS processing is a spatial hydrology database that consists of the digital

elevation model (DEM), soil types, land use information, rainfall, etc. HEC-GeoHMS operates on the DEM to derive sub-basin delineation and to prepare several hydrologic inputs, 30m resolutions DEM were used for this case. HEC-HMS accepts the hydrologic inputs as a starting point for hydrologic modeling (Asadi and Porhemat, 2013)
HEC-GeoHMS is a geospatial hydrology toolkit designed to prepare data for HEC-HMS simulations. HEC-GeoHMS creates input files which can be used for HEC-HMS simulations HEC-GeoHMS extension in ArcGIS was used to delineate the boundary of the area by considering the geographical reference points of the hydrological gauging station as the outlet point of the Ketar watershed. Further HEC-GeoHMS processing of the DEM produced five subbasins, two routing reaches, twojunctions, and the major physiographic characteristics.

2.8 HEC-HMS Technical Capabilities

The basic framework for simulation of basin runoff is similar to that in HEC-1. We can also import data from an HEC-1 input file. Hydrologic elements are set in a dendritic network, and calculations are performed in the upstream to the downstream sequence. Computations are performed with System International Unites (SI) units. However, one can enter input and view the output with units in the U.S. Customary system, and can readily convert input/results from one unit system to the other

There are three model setup requires specification in the execution of a simulation or run. The first model setup is the Basin Model - encompasses parameters and data connectivity for hydrological elements, such as sub-basin, routing of reach, junction, reservoir, source, sink, and diversion. The second model setup is Precipitation Model - consists of meteorological data and information needed to process it. The model may represent historical or hypothetical conditions. The third model setup is called Control Specifications manager - specifies time-related information for a simulation. A Project is used to hold the different data sets and can contain many of each type. The program is multi-platform capable, meaning it operates on more than one kind of computer operating system (Tassew et al., 2019).

2.9 HEC-HMS Parameters

HEC-HMS model requires three main input process parameters. Among them is the Precipitation loss method for overland flow, which accounts for the infiltration losses. There are multiple methods available in HMS including SCS Curve Number, Initial and Constant, Deficit and Constant, Exponential, Green-Ampt, Smith Parlange, and Soil Moisture Accounting (Yuan and Qaiser, 2011).

After the precipitation losses are accounted for, a transform method must be specified for transforming overland flow into surface runoff. The different methods available for the transform method in HMS are SCS, Clark or Snyder unit hydrographs, Kinematic wave, ModClark, and User specified unit hydrograph. As mentioned in the GeoHMS section, the Clark unit hydrograph method was selected. It requires two parameters. Once excess precipitation has been transformed into overland runoff and routed to the outlet of a subwatershed, it enters the stream at that point and is added to streamflow routed from upstream. There are many techniques available in HMS for routing of streamflow. These are Kinematic Wave, Lag, Modified Puls, Muskingum, Muskingum-Cunge, and Straddle Stagger.From the above methods, the Muskingum method was selected for this study.

The different parameters in the Muskingum method are K, X, and the number of sub-reaches (n) which need to be specified. Muskingum K is the travel time through the reach that ranges from 0.1 to 150hr. Muskingum X is the weighting between inflow and outflow influence, it ranges from 0 to 0.5. The number of sub-reaches affects attenuation where one sub-reach gives more attenuation and increasing the number of sub- reaches decreases the attenuation (Yuan and Qaiser, 2011).

2.10 HEC-HMS Component

HEC-HMS model components are used to compute or simulate the hydrologic response in the watershed. It includes basin models, meteorological models, control specifications, and input data. A simulation calculates the precipitation-runoff response in the basin model which is given input from the meteorological model. The control specifications define the period of time and time steps of the simulation run. Input data components,

such as time-series data, paired data, and gridded data are often needed as a parameterin the basin and meteorological models. (Wana, 2018).

The four main components of HEC-HMS are Basin model manager, Meteorological model manager, Control specifications manager, and Input data time series manager.

Basin model: Basin model manager represents the physical watershed. The user develops a basin model by adding and connecting hydrologic elements. It is based on a Graphical user interface (GUI) and can import map files from the GIS environment through an Arc GIS extension called HEC-Geo HMS to use as background map files later in the hydrologic modeling process (Fleming and Brauer, 2016). Basin model mainly comprises different hydrologic elements of the model that include: sub-basins that used to represent a physical watershed, junctions used to combine streamflow from elements located upstream of the junction, reach that helps in conveying stream flow basin model.

On the other hand,the basin model contains different methods that are used in computing precipitation loss, excess precipitation transformation to direct runoff, baseflow estimating, and flood routing methods.

Table 2-1: Method available in basin model for HEC-HMS Processing

Loss methods	Deficit and constant method Exponential method Initial and constant method SCS-CN method Green and Ampt method Smith parlange method and Soil moisture accounting method
Transform methods	Clark UH method ModClark method Kinematic wave method Snyder UH method SCS UH method Specified UH method
Baseflow	Constant monthly Bounded recession Linear reservoir and None linear Boussinesq

Flood routing	Kinematic wave Lag Muskingum Modified puls Muskingum cunge

Generally, the Basin model, for instance, contains the hydrologic element and their connectivity that represent the movement of water through the drainage system

The Basin model principally serves to convert atmospheric conditions into streamflow at specific locations in the watershed. HEC-HMS treats the different phases of rainfall-runoff processes with separate mathematical models. All components of the loss models, direct runoff models, base flow, and routing models are accessed from the basin model component of HEC-HMS (Fleming and Brauer, 2016).

Ketar watershed has five sub-basins with the gauge located at Abura gauging station. The basin map is extracted from the GIS with the coordinate of the gauging station. The Basin Model uses the following spatial data: River Reach Files for Stream network with junctions and diversions, Stream parameters (Muskingum K and X), Sub-basin data components: Loss parameters, routing parameters, and baseflow values and computation methods and downstream points.

Meteorological model: The precipitation and evapotranspiration data necessary to simulate watershed processes are stored in the meteorological model manager. The meteorological model manager calculatesthe precipitation input necessary by each sub-basin element. This model can make use of both points and gridded precipitation and has the capability to model frozen and liquid precipitation along with evapotranspiration (Fleming and Brauer, 2016). An evapotranspiration method is only required when simulating the continuous or long term hydrologic response in a watershed. The meteorological component is also the first computational element utilizing which precipitation input is spatially and temporally distributed over the river basin (Feldman, 2000).

Control Specification model: The Control Specifications is defined as the time-related information in the simulation, including the starting dates, ending dates, and the computational time interval. The function of control specifications is to set the starting and ending dates and times and time (computation) intervals. The time step

for HEC-HMS model calibration for the catchment is divided into different time steps as for calibration, simulation, and verification

2.11 HEC-HMS Processing

The four main components of the program which HEC-HMS processing mainly focused on are basin model, meteorological model, control specification model, and time-series data. HEC-HMS basin model consists of about four elements: sub-basin, reach, junction, sink (outlet), and different methods that represent precipitation loss modeling, direct runoff modeling, base flow modeling, etc.

Another HEC-HMS component that is categorized under HEC-HMS processing is meteorological modeling. Meteorological data analysis is performed by the meteorological model and includes precipitation and evapotranspiration. (Wana, 2018).

2.11.1 Precipitation Loss Modeling

Runoff from a watershed mainly depends on rainfall, infiltration, and watershed characteristics and it can be measured daily, monthly, or annually.According to the HEC-HMS user's manual (2016),the hydrologic modeling system tool encompasses different methods for precipitation loss modeling. These methods are:SCS-Curve Number method, Gridded Deficit Constant method, Green-Ampt method, Gridded Soil Moisture Account method, Initial and Constant Method and Soil Moisture Account Method

Initial and constant loss rate include two Parameters of constant rate and Initial loss which show the physical characteristics of soil, land use, and antecedence conditions of basin. If the basin is in saturated conditions, initial abstraction tends to zero. When the soil of the basin is dry, initial abstraction will increase and show the maximum height of rainfall that cannot be changed into runoff (Saleh et al., 2011)**.** For this reasons, the initial and constant loss rate method is selected for this study.

2.11.2 Direct Runoff Modeling

There are different methods that can be used for excess precipitation conversion to direct runoff in HEC-HMS hydrologic modeling system. These are Clark unit hydrograph, kinematic wave, SCS-unit hydrograph, Snyder unit hydrograph, mood Clark, user-specified s-graph, and user-specified unit hydrograph methods.

Among these techniques, Clark's unit hydrograph method is regarded as the first runoff routing technique based on a time–area diagram that reflects the shape of the drainage area. In this method, Clark first created an IUH by dividing the watershed into isochrones to develop a time–area histogram. This then needs to be translated into a time–discharge histogram with instantaneous unit excess rainfall and attenuated by routing through a linear reservoir. Lastly, the IUH can be converted into a unit hydrograph for any desired period of time by subdividing it into periods of the desired unit length and averaging the ordinates over the preceding periods of time (Cho, 2018).Clark unit hydrograph method requires only two input data, time of concentration and storage coefficient. The time of concentration is used in the development of the translation hydrograph where as storage coefficient is used in the linear reservoir that accounts for storage changes.

This method also incorporates the processes of attenuation and the translation of runoff through a time-area relationship. Clark's unit hydrograph method combines the continuity Eq. (2.1) and the storage-discharge relationship Eq. (2.2) for a linear reservoir to approximate watershed outflow at any given time step. The continuity and storage-discharge relationship for linear reservoirs are respectively.

$$\frac{dSt}{dt} = It - Qt \qquad 2\text{-}1$$

$$St = RQt \qquad 2\text{-}2$$

Where St is the storage at time t and It and Qt are the inflow and outflow at time t, respectively, and R is the storage coefficient of the watershed (Che et al., 2014). Therefore, Clark's Unit Hydrograph method for direct runoff computation was chosen because of not only due to simplicity and minimum data requirements but also it gives a good performance than the other modules and also suitable for conceptual models to transform rainfall to runoff process.Since, HEC-HMS is a conceptual model.

2.11.3 Base flow Modeling

The Base flow models simulate the slow subsurface drainage of water which is the runoff from precipitation that was stored temporarily in the watershed, plus the delayed subsurface runoff from the current storm. The base flow is added to the direct runoff (obtained with the transformation model) to obtain the total flow, which is routed through the stream reach to the outlet. In addition to this baseflow defines a minimum

river depth over which additional runoff accumulates. Models that neglect base flow may underestimate water levels and therefore fail to identify inundated reaches. To model the base flow, HEC-HMS offers alternative models, which can be combined with other loss, and direct runoff models(Eliyas, 2018).

From a total of four different base flow methods, the constant monthly base flow method was selected for this study, because of its simplicity in the HEC-HMS program; and it represents baseflow as a constant flow for all months. It does not conserve mass within the subbasin and is intended primarily for continuous simulation in subbasins where the baseflow is nicely approximated by a constant flow for each month. An average of minimum values for all of the month of January was calculated and entered for the month of January. Likewise, the value was also entered for each of the remaining months from February to December as a baseflow.Therefore, in this study, the mean monthly constant is adapted for base flow calculation methods.

2.11.4 Flood Routing Model

Flood routing is a mathematical method for predicting the change in magnitude and celerity of a flood wave as it propagates down rivers or through reservoirs. The two basic methods inrouting thenatural channels for flood waves are based onhydrological and hydraulic routing. The hydrologic methods are based on a storage continuity equation, whereas the hydraulic methods are based on the Saint-Venant equations contains the continuity and momentum equations(Samani and Shamsipour, 2004). On the other hand Routing by a lumped system method is called hydrologic routing, whereas routing by a distributed system method is called hydraulic routing (Olivera and Maidment, 1999). A flow routing model is used in the estimation of outflow hydrograph by routing of flow events from an upstream flow gauging station to a downstream station. Flood routing procedure may be classified as either hydrological or hydraulics. The choosing of a routing model is also influenced by the required accuracy, the type and availability of data, the available computational facilities, computational cost, the extent of flood wave information desired, and familiarity of the users with the given model. In practical applications, hydrological routing methods are relatively simple to implement reasonably accurately.

Among the HEC-HMS different flood routing methods, the Muskingum technique was chosen for the Ketar watershed. The Muskingum method is the most popular flood

routing method. It requires two parameters, namely: flood wave travel time (k) ranges from (0.1-150 hrs) and weighted coefficient of discharge (x) ranges from (0.0-0.5)(Hossain, 2014). The initial Muskingum-K value lies between the specified ranges was calculated using equation 2.5 and manually assigned for sub-watershed and later calibrated. The Muskingum flood routing method uses the following popular hydrologic flood routing equation.

$$\frac{dS}{dt} = I-Q \qquad 2\text{-}3$$

$$S = k[xI+(1-x)Q] \qquad 2\text{-}4$$

Where: dS/dt –the rate of charge of storage per unit time; Q-outflow S-storage, x-weighted coefficient of discharge, k-wave travel length.

The wave travel time (k) for each reach was calculated from the following equation as the initial value. Running the model with this initial value, later the parameters were optimized.

$$k = \frac{\mathbf{v}}{\mathbf{l}} \qquad 2\text{-}5$$

Where: K= flood wave travel length, V- permissible velocity, l-reach length. Here the permissible velocity value should be in the range that neither causes erosion of the channel nor letting deposition of sediment.

2.12 HEC-GeoHMS Processing

For the DEM in using GeoHMS, it must first be processed to create certainly required layers. These include the flow direction and flow accumulation, stream definition, and segmentations, slope grid, catchment grid delineation, catchment polygon, drainage line, and adjoint catchment layers which can be created by using either HEC-GeoHMS or Arc Hydro Tools. The layers are used further in HEC-GeoHMS processing(Yuan and Qaiser, 2011).

2.13 Tools Description

2.13.1 HEC-RAS Hydraulic Model

HEC-RAS is a hydraulic model developed by the HEC (Hydrologic Engineering Center) of the US. Army Corps of Engineers. The model is used indetermining of water surface profile for different flow scenarios.The peak discharge generated by the HEC-HMS models is used to find out the flow profiles and flood plain profiles for the selected flood return periods. HEC-RAS is intended for steady flow water surface profile computationand unsteady flow simulation. The method can model subcritical and supercritical as well as mixed-flow regimes for streams consisting of a full network of channels, a dendrite system, or a single river reach (Brhane, 2012).

The software is capable of performing one-dimensional steady and unsteady-flow modeling and comprises a graphical user interface, divide hydraulic analysis component, data storage, and management capabilities as well as graphics and reporting facilities. The four rivers analysis components of the HEC-RAS system include the steady-flow water surface profile computations, unsteady flow simulation, sediment transport computations, and water quality analysis.

The main inputs to the model are River geometric data, Manning's 'n' value determined by the Cowan method(in this paper) for floodplain and main channel, Boundary conditions (i.e. slope, normal depth), and Stream discharge values of the different return period. The outputs from the model include Water surface elevations, Rating curves, Hydraulic properties (i.e. energy grade line slope and elevation, flow area, velocity), Visualization of streamflow which shows the extent of flooding (Yuan and Qaiser, 2011).

HEC-RAS, combined with Hydrologic Engineering Center's Geographical River Analysis System (HEC-GeoRAS), offers engineers a powerful tool in the process of hydraulic modeling and analysis. The three required components for HEC-RAS projects are the Geometry, the Flow, and the Plan data. The Geometry data, for instance, consists of a description of size, shape, and stream cross-sectionconnectivity. Likewise, the Flow data containthe discharge rate. Lastly, the plan data contain information relevant to the run specification of the model, together with a description of the flow regimes (subcritical, supercritical, or mixed).

The HEC-RAS program, like the other software, is also downloaded free of charge from the HEC (Hydrologic Engineering Center). HEC-RAS is the software predominately used in the field of hydraulic analysis for floodplain delineation.

2.13.2 HEC-RAS Capabilities

HEC-RAS is designed to perform one-dimensional (1D), two-dimensional (2D), or combined 1D and 2D hydraulic calculations for full networks of natural as well as constructed channels. It has a capability of performing:-

Steady flow modeling: Steady flow water surface profiles are the components of the modeling system that is proposed to calculate the water surface profiles for steady gradually-varied flow and can handle a single river reach, a dendritic system, or full networks of channels. The steady flow components are capable of modeling subcritical and supercritical, and also mixed flow regimes water surface profile. (Gary W.Brunner, 2016).The basic computational steps are based on the solutions of the one-dimensional energy equation. Energy loss is evaluated by frictional (manning's equation) and contraction/expansion. The momentum equation is used in the situation where the water surface profile is rapidly-varied. These situations include mixed-flow calculations (hydraulic jump), hydraulic of a bridge, and evaluating profile at river confluences (stream junction) (Gary W.Brunner, 2016).

Unsteady Flow modeling: This component of the HEC-RAS Modeling system is capable of simulating 1D unsteady flow; 2D unsteady flow; or combined 1D and 2D unsteady flow modeling through full networks of the open channel. The hydraulic calculation for cross-section, bridge, culvert, and other hydraulic structures that were developed for the steady flow components was integrated into the unsteady flow modules. Additionally, the unsteady flow component can model storage areas and hydraulic connections between storage areas; 2D flow areas; and between streams reaches.

Sediment Transport/ Movable Boundary conditions: This component of the modeling system is proposed for the simulations of one- dimensional sediment transport calculation resulting from scour and depositions over moderate time periods.

Water Quality Analysis: This component of the modeling system is planned to allow the user to perform a riverine water quality analysis.

Water surface profiles are computed from one cross-section to the next by solving the Energy equation with an iterative procedure called the standard step method. The Energy equation is written as follows:

$$Z_2 + Y_2 + \frac{a2v2}{2g} = Z_1 + Y_1 + \frac{a1v1}{2g} + h_e \qquad 2\text{-}6$$

Where Z1 and Z2 are elevations of the main channel

Y1 and Y2 are the depth of water across the section

2.13.3 HEC-RAS Parameters

For hydraulic analysis of the stream channel geometry and water flow, HEC-RAS uses several input parameters. These parameters are used to establish a series of cross-sections along the stream. In each cross-section, the locations of the stream banks are identified and used to divide into segments of the left floodway (overbank), main channel, and right floodway. HEC-RAS subdivides the cross-sections in this manner, because of differences in hydraulic parameters. To illustrate, the wetted perimeters in the floodway is much higher than in the main channel. Therefore, the frictional forces between the water and channel bed have a greater influence on flow resistances in the floodway, leading to a lower value of the Manning coefficients. As a result, the flow velocity and conveyance are substantially higher in the main channel than in the floodway showing higher values of manning's resistance coefficient (Zelalem, 2011). At each cross-sections, HEC-RAS uses many input parameter to describe a shape, elevation, and relative location along the stream:

- River stations (cross-sections) numbers
- Lateral and elevation coordinate for each terrain points
- Left and right bank stations locations
- Reach length between the left overbank, stream centerline, and right overbank of adjacent cross-sections.
- Manning's roughness coefficient.
- Channel contractions and expansions coefficients
- Geometric descriptions of any hydraulic structures, like a bridge, culvert, and weir.

The data needed for HEC-RAS models are:

i) Geometry Data: Cross-section data represent the geometric boundary of the stream. Cross-sections are located at relatively short intervals along the stream to describe the flow carrying capacity of the stream and its adjacent floodplain. It is advisable to take a cross-section at a constant interval.Cross-sections are essential at sample location throughout the stream and at locations where alterations occur in discharges, slope, shape, roughness at the location where levee begins and end; and at hydraulic structures (bridge, culvert, and weirs). The required information for a cross-section consists of: the river, reach and river station identifiers; a description; X and Y coordinates (station and elevation points); downstream reach lengths; manning's roughness coefficients; main channel bank stations; and finally contraction and expansion coefficients

ii) Flow Data: Steady Flow Data consist of: the number of profiles to be computed; the flow data; and the river system boundary conditions. At least one flow must be entered for every reach within the system. Additionally, flow can be changed at any location within the river system. Flow values must be entered for all profiles. Flow values can be imported directly from the HEC-HMS run for different hypothetical design storms or entered manually from the model run results. The flow data for the Ketar River is takenfrom the one that is computed by the HEC-HMS. Because of sedimentation and frequent washing of the River channel due to the nature of the topography and water losses for irrigation purpose at the upstream of outlet point, the observed flow is assumed less.

iii) Plan Data: Usually, the first step in performing a simulation is to put together a plan. The Plan defines which geometry and flow data are to be used, as well as provide a description and short identifier for the run. If the geometry and flow data do not exist, then this action is performed after their creation. Also included in the plan information are the selected flow regime and the simulation options(Zelalem, 2011).

iv) Manning's constant: was taken from relevant text chow (1959) in combination with site observation of earth characteristics of the study area and finally combine the result of the two by Cowan method to determine the channel and floodplain for this study. The roughness of a surface affects the characteristics of runoff, whether the water is on the surface of the watershed or in the channel. The "n" values will be assigned based on the characteristics of the Ketar River channel and Ketar River floodplain area.

v) Boundary conditions: are needed to establish the starting and end of the water surface of the river system upstream and downstream. Starting water surface is essential for the program to begin the calculation. In subcritical flow regimes, the boundary condition is only needed at the downstream end of the river systems whereas for supercritical flow calculation boundary conditions are only needed at the upstream ends of the river systems and lastly for the mixed flow calculation boundary condition must be entered both at upstream and the downstream end of the river system. Four categories of boundary conditions are known watersurface elevation, normal depth, critical depth, and rating curve.

2.13.4 HEC-GeoRAS and TIN

HEC-Geo RAS is an Arc GIS extension developed by the U.S. Army Corps of Engineers (USACE) designed specifically to improve the data input process for HEC-RAS. Operating within the Arc GIS environment, Geo RAS uses spatial data to develop, organize, and automatically enter input data into the HEC-RAS model (Ackerman, 2009).

The key data element that HEC-Geo RAS uses to develop the input data is terrain data, commonly referred to as a Triangular Irregular Network (TIN). One source for data used to develop TIN is a Digital Elevation Model(DEM.). DEMs exist in grid (raster cell) format which can be displayed within Arc GIS if the proper extensions are installed. The quality of this data is based on its resolution or cell size. The smaller the cell is, the greater the resolution and accuracy. However, the smaller the cell size, the greater the memory and computation requirements. The usefulness of DEMs for developing terrain models should be determined based on the resolution (cell size) and the level of hydraulic analysis to be performed. The more approximate the analysis is to be, the greater the cell size that may be used. This can best be represented by the TIN of the study area. The TIN is the representation of the topographical surface in terms of regularly spaced x, y, z, coordinates. In the TIN model, each point has defined x, y, and z coordinates. The coordinate z represents the height.

2.14 HEC-GeoRAS Processing

To create the geometric data file for HEC-RAS, HEC-GeoRAS requires a digital terrain model of the river system in the Triangulated Irregular Network (TIN) format. The DEM

file was converted to the TIN format using the 3D Analyst toolbox in Arc GIS. After the conversion of DEM to TIN, extracting the geometric data in HEC-GeoRAS is conducted for the study area. The procedures were like River Digitization by following different steps and finally GeoRAS Data is exported to RAS. (Yuan and Qaiser, 2011).

2.15 Flood Inundation Mapping

Inundation mapping is performed using the water surface elevations on the cross-sectional cut lines feature class and is limited to bounding polygon features. These two feature classes must be created before performing the inundation mapping. Floodplain delineation also requires the digital terrain model (Ackerman, 2009)

2.15.1 Water Surface TIN Generation

The first step in the floodplain delineation process is to create a water surface TIN from the water surface elevations attached to each cross-section. A water surface TIN for each profile will be created in respective of the terrain model. The Arc GIS triangulation method will create the surface using cross-sectional cut lines as hard brake lines with constant elevation.

2.15.2 Floodplain delineation

Floodplain delineation is performed using the water surface TIN and terrain model to calculate the floodplain boundary and inundation depths. The floodplain delineation process using HEC-GeoRAS is an iterative process that should be used to refine the hydraulic model in HEC-RAS.

The floodplain delineation method rasterizes the water surface TIN using the rasterization cell size and compares it to the DTM/GRID. The floodplain is calculated where the water surface grid is higher than the terrain grid. The bounding polygon is used to limit the floodplain only to the area modeled in HEC-RAS.

The DEM (digital elevation model) was processed to create the TIN (triangular irregular network). After that, the river cross-sections, stream centerline, stream bank lines, flow lines, and other river geometry information will be extracted from the TIN for the HEC-GeoRAS model. At the same time, the land use will be processed to get the Manning‘s n value for the individual cross-sections. After the RAS geometry data preparation, the

HEC-GeoRAS model will be used to generate the RAS GIS import file (final river geometry file) that can be used as input for HEC-RAS.

Checking the cross-section; editing the river geometry, and making final corrections of the river geometry file in the HEC-RAS model. After the compilation of the final river geometry file, the simulated flowin different return period will be imported from HEC-HMS into HEC-RAS and the HEC-RAS generate water level for different return periods. The water surface level for each return period will be exported in HEC-GeoRAS for final inundation area mapping along the river (Getahun and Gebre, 2015).

CHAPTER 3 MATERIALS AND METHODS

3.1 Location of the study area

Ketar watershed is a part of the Ziway– Shala basin, an internal drainage basin located in the central part of the Main Ethiopian Rift Valley.Geographically it is located between 7.16^{o} to 8.31^{o} N latitudes and 38.69^{o} to 39.62^{o} E longitudes. The total area of the Ketar watershed is 3255.8 km^{2}and was used for hydrologic modeling for this study. Topographically, the Ketar watershed is ranging from 1620 m at the outlet near Ziway lake to about 4178 m on the high mountainous areas at its sources(Sime et al., 2020).

The originality of Ketar River is from the Kaka Mountain, Rift Valley Basin Ethiopia, and Ziway lake gets around 60% of inflow water from Ketar River.The whole Ketar river length of the study area (8.95km), starting from Abura gauging station to the entrance of Ziway Lake, is considered for hydraulic modeling (Flood Risk Mapping) in this paper as stated in the figure below.

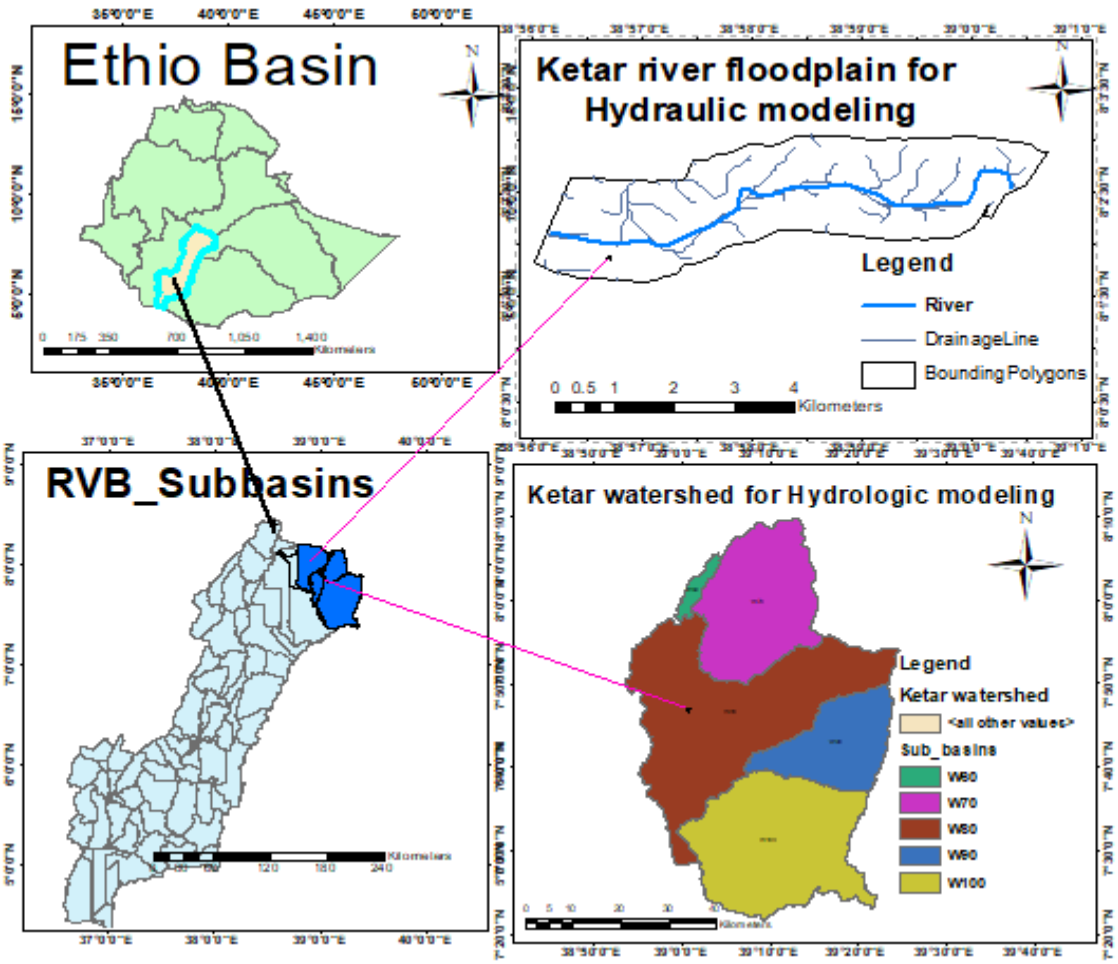

Figure 3-1:Location of the study area.

3.2 Topography and slope

The topography of the Ketar River as a whole is characterized by its physical variation, especially the difference between the eastern and western parts. Most of the eastern part is mountainous like Kaka and the western at the entrance of Lake Ziway is a nearly flat area. Also, the northern and southern part of the river is hilly terrain and agricultural land which supply high erosion to the Lake Ziway. Ketar River is a perennial river that contributes high water for Lake Ziway.The elevation of flood risk mapping area, Ketar River at the downstream of Abura gauging stations, catchment ranges from 1623 to 1690 m amsl and the slope of the floodplain was approximated 0.168% flat or gentle slope. The river length of the study area located at the downstream end of the Ketar watershed is about 8.95 km long (from Abura gauging station to the nearest Ziway lake).

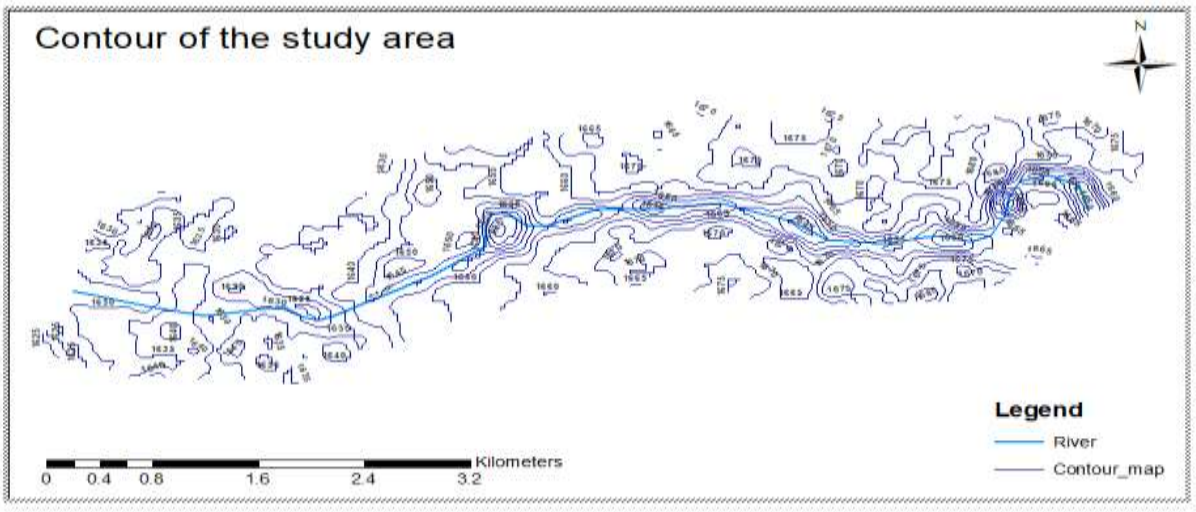

Figure 3-2:-Topographical map of the study area.

3.3 Input data used

Data that are important in this study consists of meteorological data, flow data, cross-sectional data, manning's roughness coefficient of the site, land use/land cover data, spatial data (DEM), and soil data. The flow data was collected from the ministry of water, irrigation, and energy at the hydrology department whereas the cross-sectional data were collected from a detailed survey of the Ketar River on-site and also by extract cross-sections from Ketar DEM 30m resolution. The manning's roughness coefficient value we found from relevant literature Chow (1959) and site observation and finally apply the Cowen method to determine the value of 'n' for the main channel and floodplain. The land use/land cover and soil type of the study area were taken from the GIS department of the Ministry of Water, Irrigation and Energy in addition to field visit.

Table 3-1: Input variables for model and their data sources

Variables	Data sources
Soil map	RVLB Master plan, Ministry of WaterResources, Irrigation and Energy of Ethiopia
Digital Elevation Model	RVLB Master plan, Ministry of WaterResources, Irrigation and Energy of Ethiopia
Streamflow	Hydrology and irrigation department of the Ministry of Water and Energy of Ethiopia
Precipitation	From the National Meteorological Agency of Ethiopia(NMAE).
River Cross-Sectional data	DEM 30x30m and Google Earth, also survey data on the site

Manning roughness	From different relevant Literatures and field observation and the cowan method
The land use/land cover	RVLB Master plan, Ministry of Water Resources, Irrigation and Energy of Ethiopia

3.3.1 Meteorological data

Meteorological data is among the most important data type required for runoff modeling. Hydrologic modeling system (HEC-HMS) requires daily meteorological data which includes precipitation, maximum and minimum temperature, solar radiation, relative humidity, wind speed, and so on. For this study, the precipitation data of five meteorological stations (Asella, Bekoji, Kulumsa, Ogolcho, and Keter Genet) found within the watershed was collected from theNational Meteorological Agency of Ethiopian(NMAE) from the year 1985 to 2018.

3.3.2 Land use and land cover

Land use and land cover are essential influences on runoff. If a basin has very dense vegetation cover, the vegetation will intercept precipitation and store it, reducing the volume of water entering a river.(Anees et al., 2017).The dominant land use and land cover in the Ketar watershed are cropland/grassland mosaic, agricultural land generic, corn, cropland/woodland mosaic, and range bush(Tufa et al.,2015).

As it stated in the figure below there are eight classes of land use land cover for Ketar river catchment, starting from Abura gauging station to the entrance of Ziway lake, an area considered for flood risk mapping.

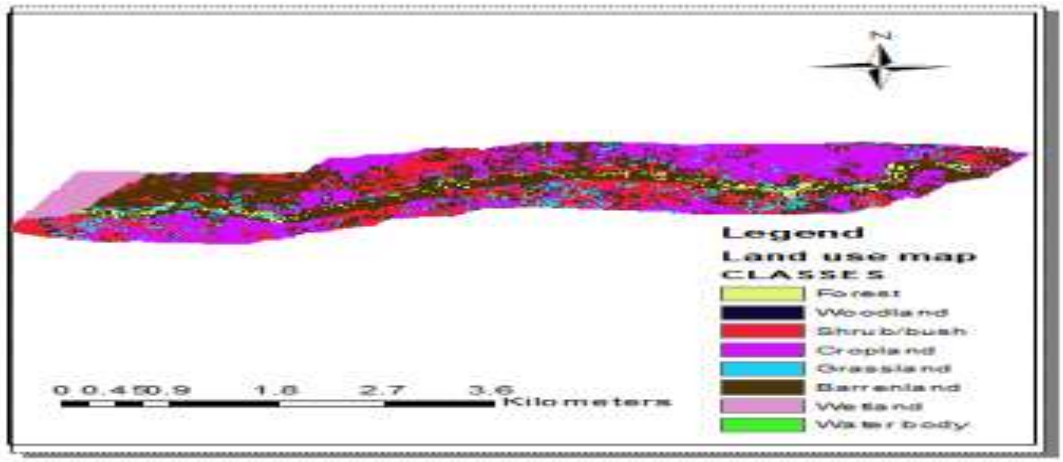

Figure 3-3: Land use/cover map of the study area.

Table 3-2: Land use/cover analysis based on their area coverage.

S.No	Land Use Type	Area(km2)	Percentage (%)
1	Forest	8.85	7.81
2	Woodland	26.77	23.64
3	Shrub/bush	28.08	24.80
4	Cropland	22.62	19.98
5	Grassland	13.37	11.81
6	Barren land	12.33	10.89
7	Wetland	0.36	0.32
8	Water body	0.85	0.75
	Total	**113.23**	**100**

The result of the land use land cover map (from table 3.2:) shows that the shrub/bushland use land cover map had the highest value of 24.80% followed by woodland 23.64% and cropland 19.98%, Grassland 11.81%, barren land 10.89%, Forest 7.81% and others (wetland and water body) occupying 1.08% of the area.

3.3.3 Spatial data (DEM)

Digital Elevation Model (DEM) is the digital representation of the land surface elevation with respect to any reference datum. It is a continuous spatial representation of the earth's surface. DEM is used to usually utilized to refer to any digital representation of a topographic surface. It is the simplest form of digital representation of Topography which is used to determine terrain attributes like elevations at any points, slope, and aspect. In addition to these terrain features such as drainage basin and channel,the network can also be differentiated from the DEMs. DEM is widely utilized in hydrological and geological analyses, monitoring of hazards, exploration ofnatural resources, agricultural management, etc. Also, hydrologic applications of the DEM include groundwater modeling, estimation of the volume of proposed reservoirs, determining landslide probability, flood-prone area mapping,etc.(Sime et al.,2020).

Traditionally watershed characteristics were obtained from maps or field surveys which are time-consuming and expensive. But today DEMs are widely used for developing the watershed characteristics (Olusina, 2013).For this paper, a DEM was used to develop

elevation related characteristics for the study site with the help of a GIS-based tool called HEC-GeoHMSand HEC-GeoRAS for hydrologic and hydraulic modeling respectively.

The Ketar watershed was delineated and then divided into sub-watersheds from the DEM.Flow directions, Flow accumulations, stream definitions and segmentation, catchment grid, and polygon processing, drainage line, and adjoint catchment processing, etc.was developed from DEM. After HEC-HMS input file preparation was completed, it was exported to HEC-HMS and run the model. For hydraulic modeling, the area considered was Ketar River and its floodplain starting from Abura gauging station to the entrance of Ziway Lake which is about 113.23 km^2. The obtained data (DEM, raster format) is converted to the TIN and geometric data extraction was done by using HEC-GeoRAS. This was the process of preparing data for processing (HEC-RAS) and post-processing (HEC-GeoRAS) again

3.3.4 Soil data

The soil database describes the surface and upper subsurface of a watershed. In this study the soil data was collected from the Ethiopian Ministry of Water, Irrigation, and Energy,Department of GIS was used. The five dominants or majors groups of soil were found in the Ketar watershed. These are dystric regos,Haplic xerosols, Eutric Nitsols, Haplic aerosols, and pellic vertisols. Eutric Nitsols covers the central parts of the watershed. Eutric Nitsols cover a large area of the Ketar watershed and followed by Haplic xerosols (silt loam) (Sime et al., 2020).

Ketar River starting from Abura gauging station to the entrance of Ziway lake (the study area for hydraulic modeling in this paper) consists of soil classes like Vitric Andosols, Calcaric Fluvisols, etc. Their descriptions and analysis is as follow

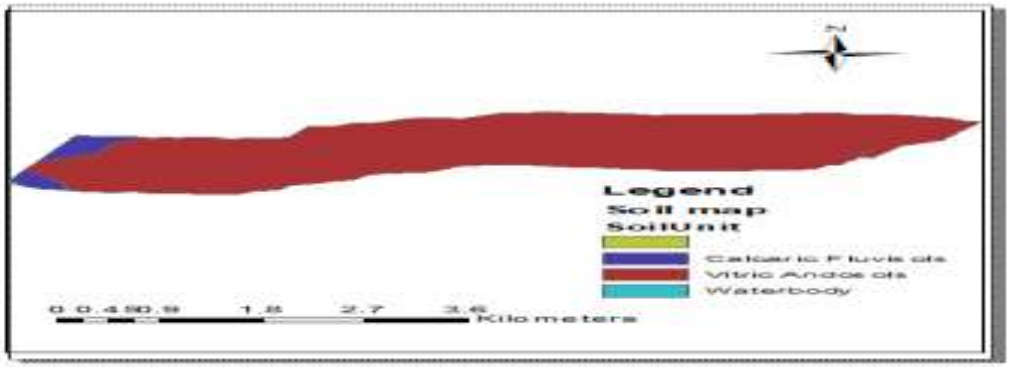

Figure 3-4 Soil classes of the study area

Table3-3:Soil map analysis based on their area coverage.

S.No	Soil Types	Area_ha	Percentage (%)
1	Calcaric Fluvisols	2416.767	1.78
2	Vitric Andosols	91182.83	67.21
3	Waterbody	42063.77	31.01
Total		**135663.4**	**100**

The result of the Soil type map (table 3.3:) indicates that the Vitric Andosols had the highest value of which is about 67.21% followed by water body 31.01% and Calcaric Fluvisols 1.78% of the total area

3.3.5 Hydrological (flow) data

Hydrological data is another most important input data required for rainfall-runoff modeling and its main function is for hydrological model calibrations and validations. As that of meteorological data, HEC-HMS requires daily hydrological data. The hydrological data used in this study was collected from the Ethiopian ministry of water resource, irrigation, and energy for the Abura streamflow gauging station that is found at the outlet of the Ketar watershed. Two additional neighbor's stream gauging stations data were collected for missing data filling and data quality test (i.e. Arata and Fite gauging station). The collected daily time series of stream discharge of the study area was between 1985 – 2007 years.

The discharge gauge is foundat the outlet of Ketar watershed at Abura gauging station on the upstream of lake Ziway in Ketar watershed; where the hydraulic modeling (flood risk mapping) was developed. The Abura gauging stations is located at longitude 38^0 58' 59'' E and latitude 8^0 2' 32'' N,which is found at the outlet of the watershed near the lake Ziway

3.3.6 Survey (cross-sectional) data

Cross-section data represent the geometric boundary of the stream. Cross-sections are necessarily at representative locations throughout the stream and at locations where changes occur in discharge, slope, and shape roughness at locations where levees begin and end; and at the hydraulic structure (bridge, culvert, and weirs).The required

information for a cross-section consists of the river name, reach name; river station identifiers, a description x and y coordinates (stations and elevation points), downstream reach length, manning's roughness coefficients, main channel bank stations, and contraction and expansion coefficients.

In this paper survey data of the cross-sections of the Ketar River from Abura gauging station to the entrance of Ziway lake on-site and by extracting the cross-section with DEM 30m resolution,58 cross-section points had been extracted to givethe better and accurate result of the site. The cross-sections of the river were not uniform but mostly looks like irregular shape, as a result, its depth and width also varies from cross-section to cross-section along to the downstream.

3.3.7 Manning's roughness coefficient

The manning's roughness coefficient for the Ketar river is calculated by the Cowan method. The concept and application of this method includes the site observation of the researchers, reading, and understanding of manning's value given for different earth characteristics from literatures and finally combining the two concepts and determining the manning values for the study area and this mechanism is the Cowen method

3.4 Methodology

The conceptual workflow diagram for the overall of the study design is as follows

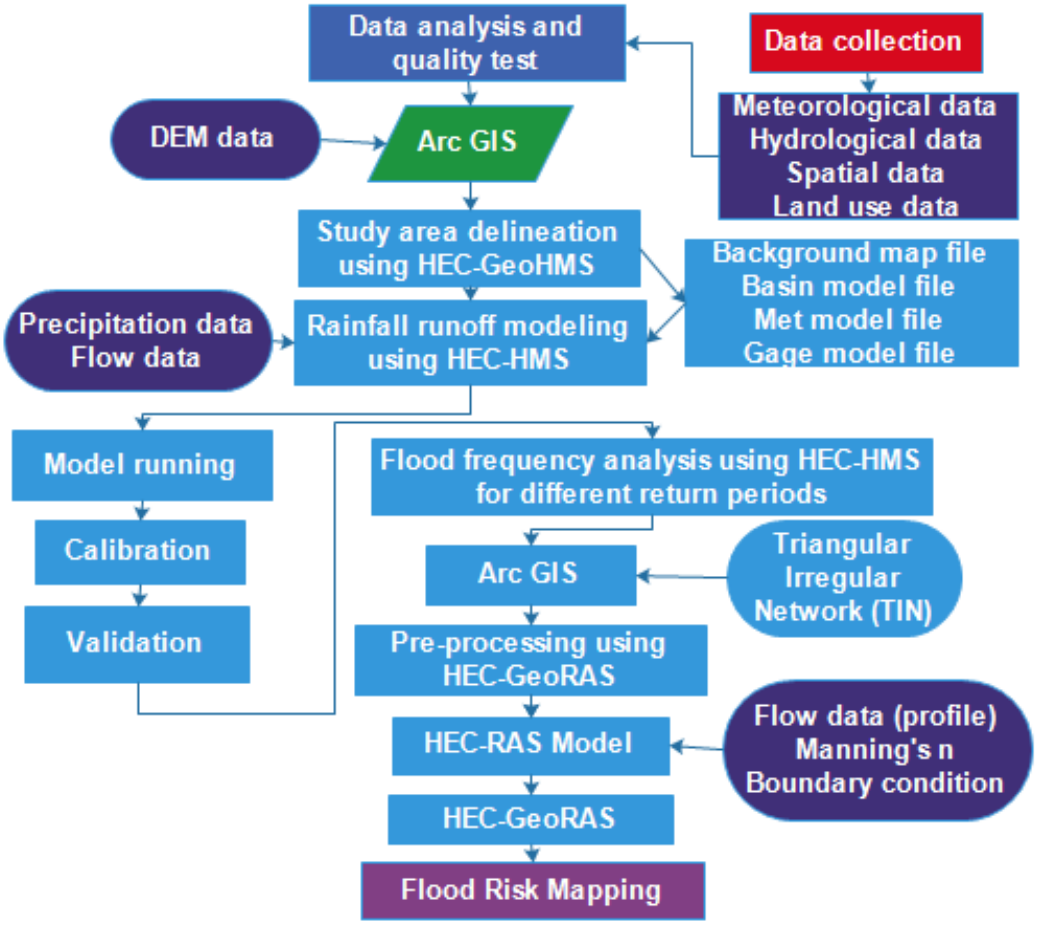

Figure 3-5:-General schematic workflow diagram.

3.5 Data analysis and quality test

3.5.1 Filling of Missing Precipitation Data

Rainfall data play a central role in developing rainfall-runoff models.Measured precipitation data is important to many problems in hydrological designs and analysisone of the first steps in any hydrological and meteorological study is accessing reliable data. However, precipitation data is frequently incomplete. This incompleteness of the precipitation data may occur as a result of the damage on measuring devices, errors in measurements, geographical data gaps, a change of measurement site, changes in data collector, the measurement irregularity, or severe tropical changes in the climate of thezones(Sattari and Joundi. 2016).

Therefore, the estimating of missing data in the hydrological and meteorological study is essential inthe timely implementation of rainfall-runoff modeling and also for reasonable flood risk mapping. The correct estimating of the missing data makes a great contribution in correctly assessing the capacity of flood control structures in rivers and also the flood-prone extent of the specified flood plain. The following are some of the missing data estimating techniques.

The Arithmetic Mean Method: The Arithmetic Mean method is the simplest method mostly used in filling the missing meteorological data. This method is applicable if and only if the normal yearly precipitation around the gauges are less than 10% of the normal yearly precipitations at station X. This assumes equal weights from all nearby rain gauge stations and uses the arithmetic mean of precipitation records of them as an estimate

$$Px = \frac{1}{m}[P1 + P2 + P3 + \cdots + Pm] \qquad 3\text{-}1$$

Where Px is the estimated value of the missing data (precipitation at the concerned station), P is the value of the same parameter at m^{th}nearest weather station, and m is the number of the nearest stations. The Average Arithmetic Mean method is acceptable if the gauges are uniformly distributed over the area and the individual gauge measurement does not vary greatly about the mean(MulukenLE,2020).

Linear Regression (LR) Method: LRis a method used in the estimation of data at a station with a similar condition. In statistics, linear regression is an approach for modeling the relationship between scalar dependent variable y and one independent parameter denoted X(Sattari and Joundi.,2016). To do this, the correlation coefficients between the target station and each of the neighboring stations are initially calculated and then ranked. Then the missing data are estimated by a linear regression equation with the station that has the highest correlation coefficient. The correlation and the equation of the regression line are obtained by using Microsoft Excel.

Normal ratio method: This method is applicable if any surrounding gauging station has the normal annual precipitations greater than 10% of the gauge under consideration. This weighs the effect of each surrounding station. If the normal precipitation varies considerably then Px is estimated by weighting the precipitation at various stations by the ratio of normal annual precipitations (MulukenLE, 2020). It is the most

powerfulmeans of missing data filling techniques and is expressed by the equation given below. The normal ration method gives Px as:

$$Px = \frac{Nx}{m}\left[\frac{P1}{N1} + \frac{P2}{N2} + \frac{P3}{N3} + \cdots + \frac{Pm}{Nm}\right] \qquad 3\text{-}2$$

Where Px -Estimate for the ungauged station or precipitation of station with a missing value

Pi -Rainfall values of rain gauges used for estimation or precipitation of nearby station

Nx -Normal annual precipitation of X station or station with missing data.

Ni-Normal annual precipitation of surrounding stations

m -number of surrounding stations excluding of station under consideration.

Since all the stations under consideration here in this study satisfy the assumption raised under the normal ratio method, it was adopted to fill the precipitation missing data gap by this method. Having filling the entire precipitation data gap, the Monthly average rainfall of each meteorological stations considered under the Ketar watershed was shown on the figure 3.6

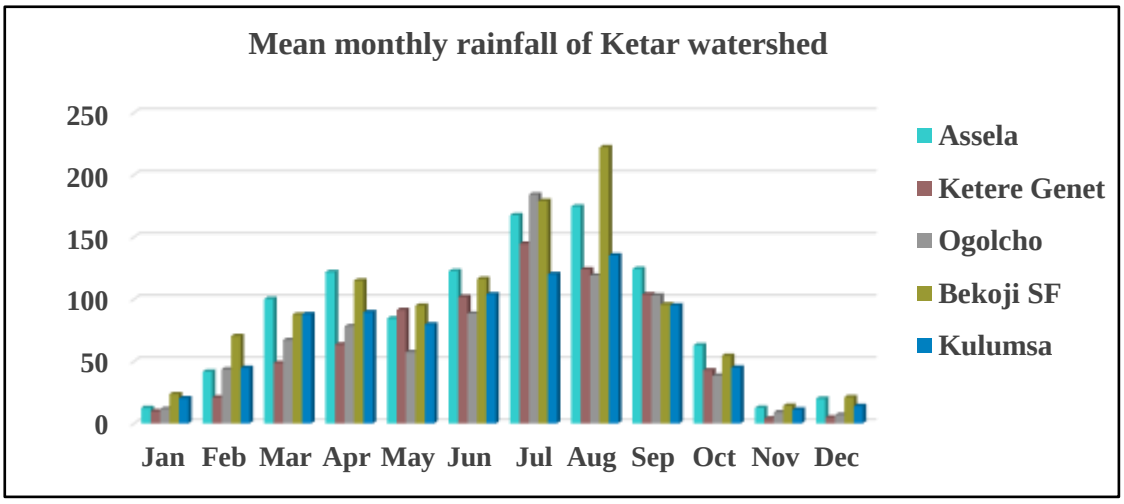

Figure 3-6: Monthly average rainfall of each meteorological station.

As the collected data from the National Meteorological Agency indicates, the average monthly precipitation was varied with each station and station obtains a minimum of 3.78mm to a maximum of 222.06mmper month as indicated on the figure 3.6

Table 3-4: Selected gauging stations for Ketar watershed

No	Station Name	Latitude	Longitude	Elevation
1	Assela	7.57	39.08	2350
2	Bekoji	7.32	39.15	2810
3	Keter Genet	7.5	39.06	2400
4	Ogelcho	8.04	39.02	1760
5	Kulumsa	8.08	39.08	2200

3.5.2 Filling of Missing Streamflow Data

Availability of data on hydrologic variables such as river flow is necessary for the planning and management of water resources.However, several river basins in developing countries have no full datasets on river flow due to the gauging station'sdegradation, the coupled of gauging stations with unnecessary data compilation and storage procedures. Different methods are available inthe filling of missing data however, these methods differ in performance depending on the characteristics of initial data points (Salim et al., 2018).

Regardless of the availability of many methods in the filling of missing hydrological data, it is commonly believed that no single method can be considered universally best. Every method hasits own advantage and disadvantage depending on the characteristics of the data set. In this study, the linear regression method has been selected to fill the gaps of missing river flow data on Abura gauging stations of the Ketar River catchment.Since, this method is developed based on correlation between the station with missing data and the adjacent stations of the high correlation coefficient.

The process was by developing a correlation between the station with missing data (Abura gauging station) and selecting any of the adjacent stations (Fite or Arata gauging station) of the high correlation coefficient with the Abura gauging station. After selecting the highly correlated neighboring station, (independent variable) from the Fite or Arata gauging station with the targeted station (dependent variable), Abura, the regression equation is developed to fill the missing value of flow data for the Abura gauging station.

Linear regression analysis: If X and Y are two related variables, then linear regression analysis helps us to predict the value of Y for a given value of X or vice versa, expressed by

$$Y = \boldsymbol{\beta}x + \boldsymbol{\alpha} \qquad 3\text{-}3$$

Where β is the slope of the LR equation and α is the Y-intercept

3.5.3 Data Consistency test

Estimating missing precipitation is one problem that hydrologists need to address. A second problem occurs when the catchment rainfall at rain gages is inconsistent oversome time and correction or adjustment of the measured data is necessary to provide a consistent record. A consistent record is one where the characteristics of the record have not changed with time. Inconsistency of data may be resulted from: change in gauge location, exposure, instrumentation, or if an observational procedure is not real and on time. To solve the inconsistency problem the most widely applied technique called double mass curve is used. Double-Mass Curve (DMC) analysis is a graphical method to identify or adjust inconsistencies in the station's record by comparing its time trends with those of other stations nearby.

The theories of the double-mass curve are based on the fact that a graph of a cumulative of one variable (dependent variable) against the cumulative of another variable (independent variable) during the same period will plot as a straight line to indicate the proportionality of data. The slope of the line will represent the constant of proportionality between the variables. A brake in a slope of a double-mass curve indicates that the change is a constant of proportionalities between the two variables have occurred or maybe that the proportionality is not a constant at all rates of cumulative.

As an example, in the case of this study, a break in slope of the double mass curve for Ogelcho station was detected from 1988-1989 and its correlation coefficient with cumulative of all other remaining stations of the Ketar watershed was so poor as indicated on the figure 3.7

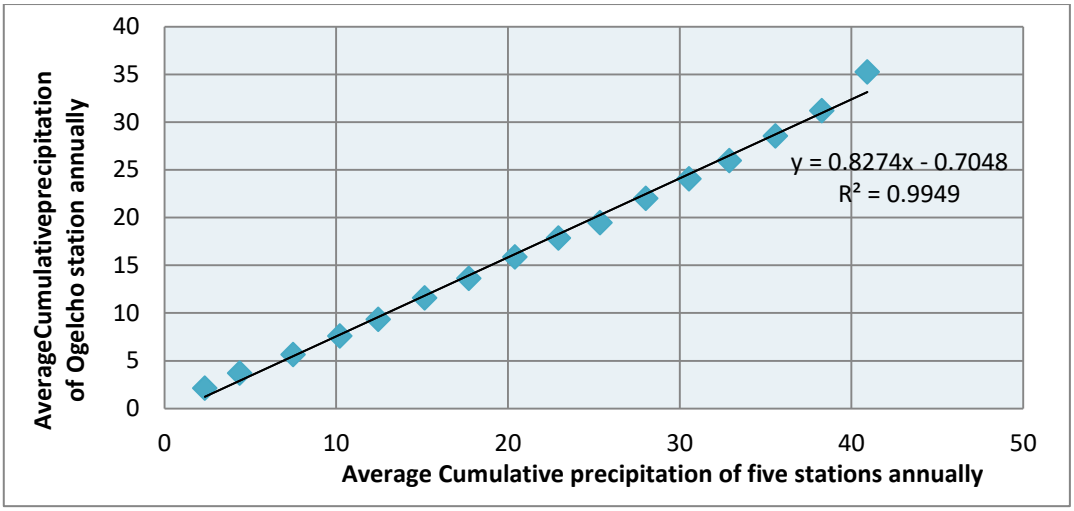

Figure 3-7: DMC for consistency checking before adjustment

In the case of the above inconsistency condition, the double mass curve is a means foran adjustment that was expressed in the following procedures. First, determine correlation factor that can be taken as the slope of the graph which was calculated as below from reading of average cumulative as X-entry and cumulative rainfall of Ogelcho station as Y-entry from the above graph for 1988 and 1989 and the adjusted precipitation was the product of the obtained correction factor and the observed precipitation.

$$\text{Slope} = \frac{\text{Vertical increase}}{\text{Horizontal increase}} = \frac{\Delta y}{\Delta x} \qquad 3\text{-}4$$

$$\text{Slope} = \frac{35.2775 - 31.21383}{40.923 - 38.28637} = 1.541236 \qquad 3\text{-}5$$

Multiplying all the precipitation values within the proposed range, i.e. precipitation data from 1988 to 1989 by the computed correlation factor (equation 3.5), the adjusted value was tabulated as in table 3.5.

Table 3-5: Ogelcho meteorological station before precipitation adjustment

Year	Before adjustment	After adjustment
1989	31.21383	29.98285
1988	35.2775	32.1644

Then, the graph of the newly adjusted precipitation data for the specified station was sketched as shown in figure 3.8.

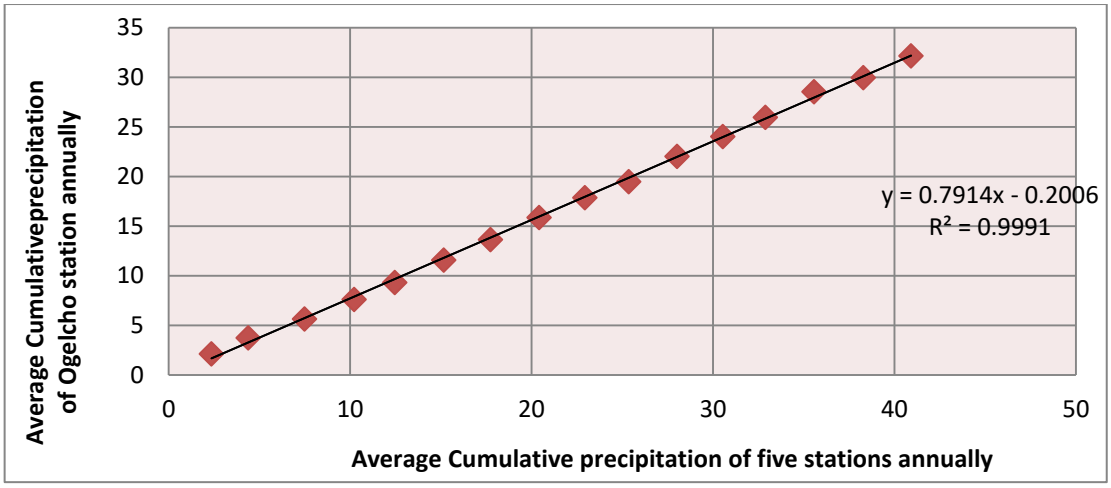

Figure 3-8: DMC for consistency check-up after adjustment

Now reading the value of slope before an adjustment and after adjustment from both the above graphs, the double mass curve can help to fix the newly adjusted precipitation data through the following equation.

$$Pcx = Px * \frac{Mc}{Ma} \qquad 3\text{-}6$$

Where: Pcx= corrected precipitation at any time period T1 at station x

Px= original recorded precipitation at time period T1 at station x.

Mc= Corrected slope of the double mass curve.

Ma= Original slope of the double mass curve.

Applying this technique for the stations with inconsistent precipitation data, it was illustrated in figure 3.9 that the precipitation of all the stations under the specified sub-basin was consistent.

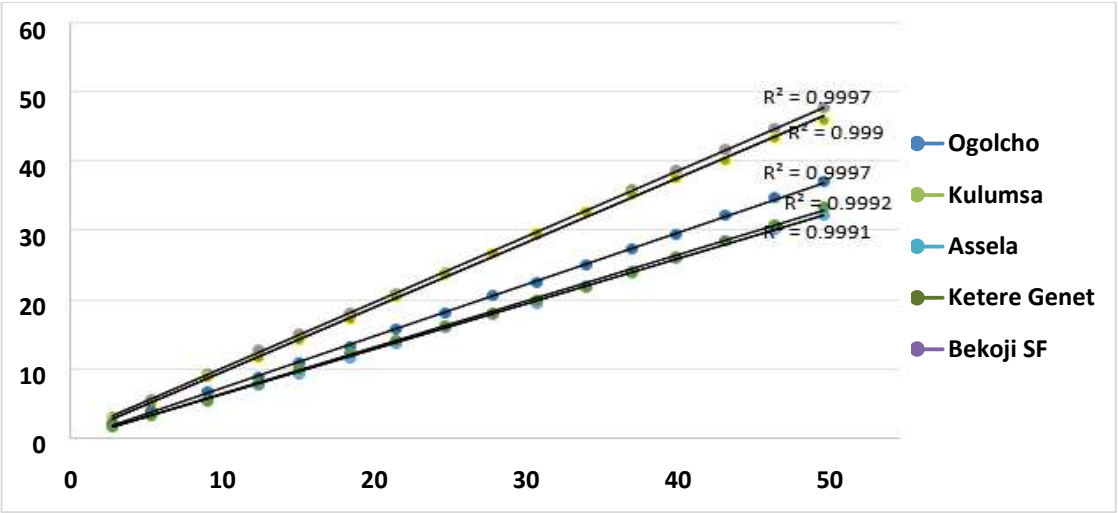

Figure 3-9: DMC and correlation coefficient for each station

3.6 Rainfall-Runoff Model

Rainfall-runoff modeling shows the relationship between precipitation received from the catchment and surface runoff generated. Channel or river system as a response to rainfall input data for the catchment under the study and it produces the runoff as an output.

The Rainfall-runoff of this study was modeled using theHEC-HMS(hydrologic engineering center hydrologic modeling system) developed by the U.S Army Corp of Engineers (USACE). It is the physically-based and conceptual semi-distributed model designed to simulate the precipitation-runoff processes in a wide range of geographic areas such as large river basin, water supply, and flood hydrology to small urban and natural watershed runoff (Mokhtari et al., 2016). For rainfall-runoff modeling, HEC-HMS requires a Background map file of the study area, Basin model file, Gage file, Met file, etc. and all these can be generated by HEC-Geo HMS.

3.6.1 Study area delineation: HEC-GeoHMS

HEC-Geo HMS has been developed as a geospatial hydrology tool kit for engineers and hydrologists. The program is an extension of Arc GIS and allows users to visualize spatial information, document watershed characteristics, perform spatial analysis, delineate sub-basin and streams, construct inputs to hydrologic models, and assist with report preparation.

HEC-Geo HMS operates on the DEM to derive sub-basin delineation and to prepare several hydrologic inputs (Mokhtari et al., 2016). A 30m high-resolution DEM with HEC-Geo HMS 10.3 was used for this study. HEC-HMS accepts the hydrologic input files as a starting boundary condition for the hydrologic modeling system. HEC-Geo HMS consists of different menus that provide different functions especially, during preprocessing in the Arc GIS work environment. These menus are: preprocessing, project setup, basin processing, basin characteristics, basin parameters, HMS and utility, etc. (Figure 3.10).

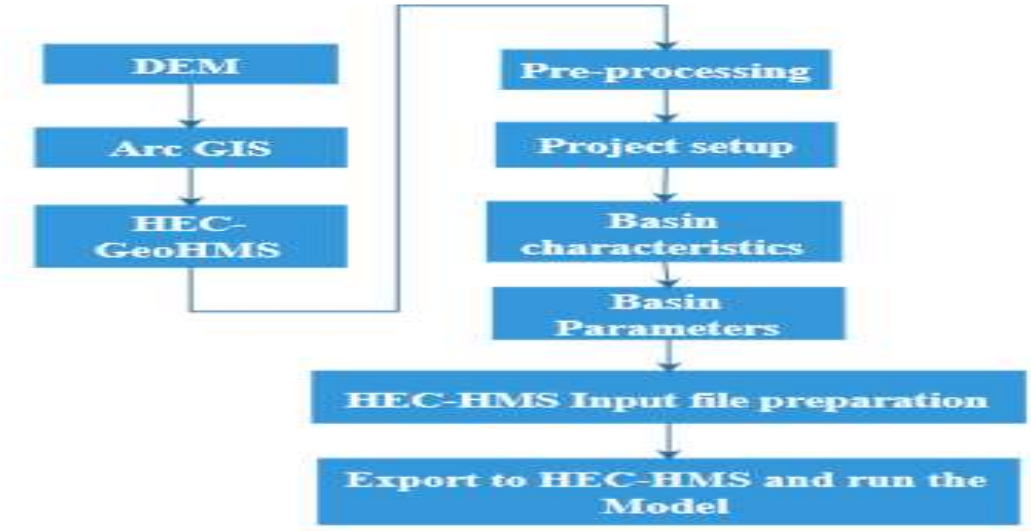

Figure 3-10**:** HEC-GeoHMS Preprocessing workflow diagram

After the successful completion of HEC-Geo HMS processing a background shapefile consists of Basin model file, Met model file, and Gage model file together with watershed hydrologic elements were exported to HEC-HMS to use as an input file for further analysis.

3.6.2 Determination of Areal Rainfall

For analyses involving areas larger than a few square miles, it may be necessary to make estimates of average rainfall depths over sub-watershed areas since a rain gauge represents only point sampling of the areal distribution of a storm.In practice, however, hydrological analysis requires knowledge of the rainfall over an area (Brhane,2012).

There are many methods available to determine the areal rainfall over the catchments from the rain gauge measurement: Arithmetic Mean, Thiessen Polygon, Isohyetal, Percent Normal, GridPoint, Hypsometric, etc. are available for estimating average

precipitation over a drainage basin, (Shaw, 1988). Choice of methods requires judgment in consideration of the quality and nature of the data, and the importance, use, and required precision of the result.

A Thiessen polygon method is the most widely used method compared to others and is used in this study. In this method, weights are given to all the measuring gauges based on their areal coverage of the watershed, thus eliminating the discrepancies in their spacing over the basins. All the stations in and around the basins are considered and a linear variation in the precipitation between two gauge stations is assumed. In this procedure, areas and lines between adjacent stations were drawn on a map of the area by using Arc GIS 10.3 software with Arc toolbox extension. The perpendicular bisector of these lines forms a pattern of polygons with one station in each polygon. The area with which each station is taken represents the area of its polygon and is used as a factor for weighting the station precipitation. The contribution of the rainfall from each gauging station is limited by its weighting factor.

According to Thiessen, the average rainfall, Rareal,over the area can be computed from equation 3.7

$$\text{Rareal} = \sum_{i=1}^{n} \frac{\text{RiAi}}{\text{At}} \qquad 3\text{-}7$$

Where Ri is the rainfall at station i^{th}, Ai is the polygon area of station i^{th}, At is the total catchment area, and n is the number of stations.

The area functions Ai/At are known as the Thiessen coefficients and once they are determined for a given stable station network, the areal rainfall can be computed for the set of rainfallmeasurements. The four nearby location of the rainfall stations are as shown below

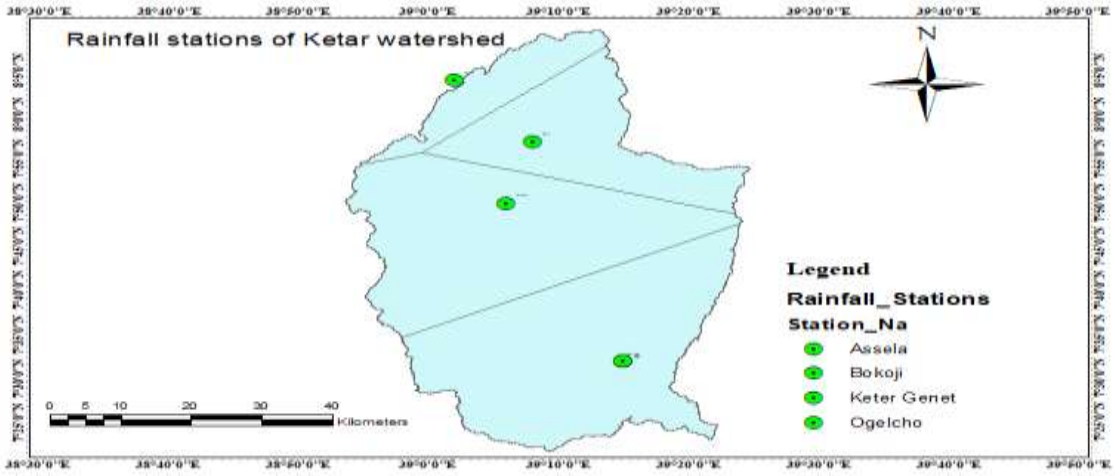

Figure 3-11: Thiessen polygon of Rainfall Stations.

Table 3-6: Station's Areal weight of Thiessen polygon

S.No	Name of polygon	Area of the polygon (km2)	Areal Weighted (Ai/At)
1	Assela	601.3	0.184681
2	Ogelcho	248.04	0.076183
3	Keter Gent	1149.82	0.353152
4	Bekoji	1256.72	0.385984
Total		**3255.88**	1

After determining the areal precipitation for each polygon represented by station name as in Figure 3.11, the areal precipitation for each sub-basin's polygon was computed using the area of each station polygon as the total area and calculating area of each sub-basin polygon using Arc GIS 10.3.

Table 3-7: Area and weighted area contributed from each gauging station.

S/No	Name of subbasin	Shape Area(km2)	Station Name	Weighted Area
1	W60	43.2	Ogelcho	1
2	W70	414	Assela	0.617722
		173	Ogelcho	0.25844
		82.9	Keter Genet	0.123838
3	W80	82.5	Bokoji	0.066853
		184	Assela	0.149048
		31.78	Ogelcho	0.025755
		936	Keter Genet	0.758345
4	W90	268.23	Bokoji	0.66552
		3.8	Assela	0.009363
		131	Keter Genet	0.325117

5	W100	906	Bokoji	1
Total		**3256.41**		

3.6.3 Model Performance Evaluation

Nash–Sutcliffe model efficiency coefficient (NSE): is used to assess the predictive power of hydrological models or used to analyze the correlation between simulated and observed hydrological data. It can range from $-\infty$ to 1. An efficiency of 1 indicates a correct match of simulated(modeled) discharge to the measured (observed) data. The efficiency of 0 shows the model prediction is as perfect as of the average of the observed data, whereas the efficiency less than zero occur when the observed average is a better predictor than the modeled or, in another word, when the residual variances (expressed by a nominator) is greater than the data variances (expressed by a denominator). Essentially, the closer the model efficiency is to 1, the more accurate it is.

The disadvantage of this efficiency criterion is an overestimation of the model performance during peak-flows and an underestimation during the low-flow condition. It can be expressed as follow:

$$\mathrm{NSE} = 1 - \frac{\sum_{I=1}^{n}(\mathrm{Qsi}-\mathrm{Qoi})^2}{\sum_{i=1}^{n}(\mathrm{Qoi}-\bar{\mathrm{Q}}\mathrm{o})^2} \qquad 3\text{-}8$$

Where, $\mathrm{Qsi} - \text{Simulated flow value at the } i^{th} \text{time interval}$

$$\mathrm{Qoi} - \text{Observed flow value at the } i^{th} \text{time interval}$$

$$\bar{\mathrm{Q}}\mathrm{o} - \text{Mean observed flow value.}$$

Coefficient of Determination (R^2): The coefficient of determination is a measure of the proportion of variances of the forecasted outcomes. It estimates how well the dispersion of the measured data is predicted by the model. With a value of 0-1, the coefficient of determination is computed as the square of the correlation coefficients (R) between the sample and forecasted (predicted) data. The coefficient of determination indicates how well a regression model fits the data. A value of 1 shows every point on the regression lines fit the data; a value of 0.5 shows only half of the variations are discussed by the regression. A zero coefficient of determination (R^2) indicates that the dependent variable

cannot be forecasted from the independent variable. The equation of coefficient of determination can be expressed as follow:

$$R^2 = \frac{\sum_{i=1}^{n}[(Qsi-\bar{Q}s)(Qoi-\bar{Q}o)]^2}{\sum_{i=1}^{n}(Qsi-\bar{Q}s)^2 \sum_{i=1}^{n}(Qoi-\bar{Q}o)^2} \qquad 3\text{-}9$$

Where $Qsi - \text{Simulated flow value at the } i^{th} \text{ time interval.}$

$$Qoi - \text{Observed flow value at the } i^{th} \text{ time interval.}$$

$$\bar{Q}o - \text{Mean observed flow value.}$$

$$\bar{Q}s - \text{Mean Simulated flow value.}$$

3.6.4 Sensitivity Analysis

Sensitivity analysis is a method to determine which parameters of the model have the greatest impact on the model results. There are different parameters of the event model that were subject to the sensitivity analysis. In an initial and constant loss rate method, which is used to handle the infiltration loss in the sub-basins, the three parameters in the basin are initial loss, constant rate, and percent impervious area. Percent impervious area is taken as 0%. Therefore, the remaining two parameters (initial loss and constant loss) of the initial and constant loss rate method were calibrated. The Clark unit hydrograph method which is used to model the transformation of precipitation excess into direct surface runoff has Clark time of concentration and storage coefficient parameters. This parameter was calibrated as well.

3.6.5 Flood Frequency Analysis

Flood frequency analysis is the most essential statistical method in understanding the nature and magnitude of peak flow in a river or flood plain. It gives the probability model curve to the year flood peak which is recorded by the period observation and data of flood occurred in 16 years (1988-2003).

This technique is important to forecast the return period and help to save the public and government properties. There are different classes of techniques for the estimation of Flood Frequency Analysis (FFA).Before the demarcation of flood inundation area of the flood plain, analyzing peak discharge is vital to get Probability distribution.

Ethiopian Roads Authority (ERA) divided the country into eight Meteorological regions based on their rainfall pattern similarity and develops intensity-duration frequency curves (IDF curve) for 24hr rainfall depth for each Meteorological region as a function of the 2,5,10, 25,50,100, 200 and 500 years return period of the storm events.

According to ERA classification, the Ketar watershed was found in rainfall region A3 (RR-A3) and the 24-hour rainfall depth for each return period was taken fromtable 3.8.

ERA has developed 24-hour rainfall depth for different rainfall regions of Ethiopia for corresponding return periods (table 3.8). Using the 24-hour rainfall depth of RR3 provided in table 3.8 that was specified for the Ketar watershed the rainfall depth of 1, 2, 3, 6, 12, and 18 hours were developed using equation 3.10 and used in HEC-HMS for peak flood estimation.

Table 3-8: 24 hrs rainfall depths (mm) vs. return period (yr)

24hr Rainfall Depth (mm) vs. Frequency(yr)								
Return period Years	2	5	10	25	50	100	200	500
RR-A1	50.30	66.02	76.28	89.13	98.63	108.06	117.48	130.00
RR-A2	51.92	65.52	74.45	85.70	94.07	102.45	110.91	122.27
RR-A3	47.54	59.61	67.66	77.92	85.62	93.34	101.13	111.58
RR-A4	50.39	63.83	72.28	82.55	89.97	97.20	104.32	113.63
RR-B1	58.87	71.26	79.29	89.35	96.84	104.37	112.02	122.41
RR-B2	55.26	69.95	79.68	92.03	101.29	110.61	120.07	132.87
RR-C	56.52	71.04	80.54	92.52	101.48	110.50	119.66	132.06
RR-D	56.23	76.84	90.37	107.46	120.23	133.05	146.00	163.44

Note: RR- Rainfall Region

$$\frac{\mathbf{R_t}}{\mathbf{R_{24}}} = \frac{\mathbf{t}}{\mathbf{24}} * \frac{\mathbf{(9b+24)^n}}{\mathbf{(b+t)^n}} \qquad 3\text{-}10$$

Where: Rt-t hr rainfall depth, R24- 24hr rainfall depth, b and n are constant-coefficient in

Which b = 0.3 and n = (0.78 – 1.09) and t – rainfall duration.

3.7 Hydraulic Modeling: HEC-RAS

The hydraulic model is a numerical model that is used to represent the hydraulic behavior of water. It may be broadly classified into one-dimensional (1D), two-dimensional (2D), and three-dimensional (3D) schemes. 1D mathematical models are the most commonly used for flood inundation mapping and use the Saint Venant equations and therefore rely on many high-resolution morphological parameters (cross-sections) (Saleh et al., 2011).

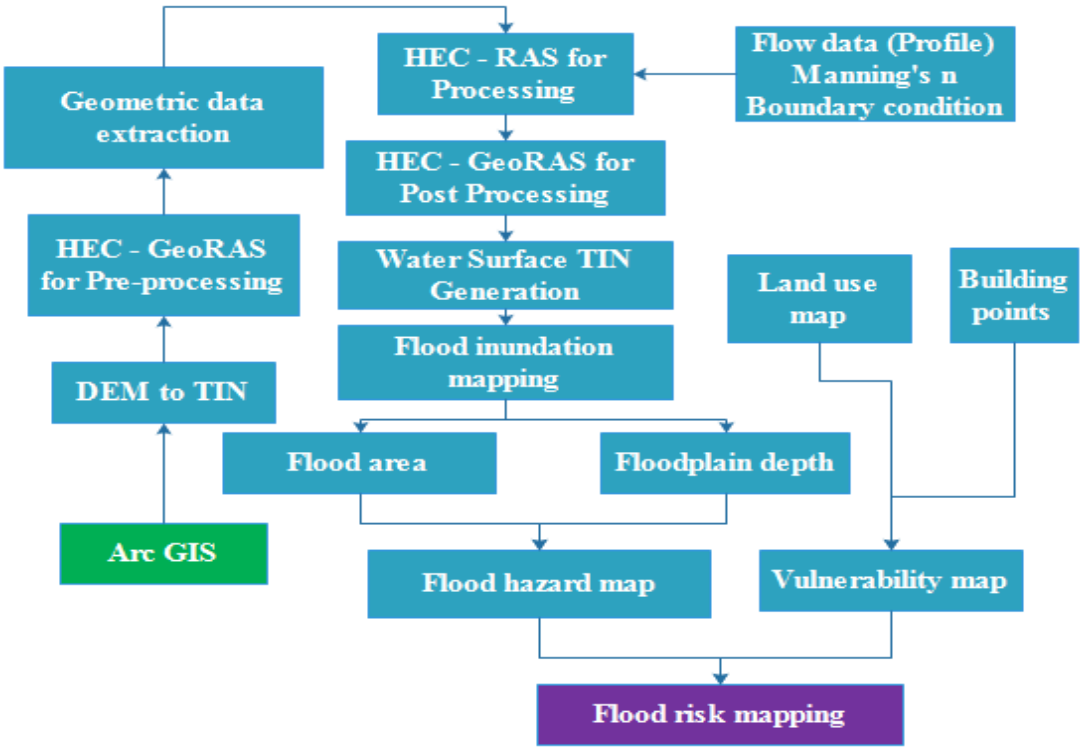

Figure 3-12:General workflow in Hydraulic model.

In this study,the HEC-RAS 5.0 version was used to develop one-dimensional steady flow hydraulic modeling. HEC-RAS is a computer program that models the hydraulics of water flow through natural rivers and other channels. One of the functions of the HEC-RAS program is to determine surface elevations at any point of interest. The data needed to perform these computations are the geometric data, steady flow data (profiles) and boundary conditions, and manning's roughness coefficient.

3.8 HEC-GeoRAS and TIN

HEC-Geo RAS is an Arc GIS extension developed by the U.S. Army Corps of Engineers designed specifically to improve the data input process for HEC-RAS. Operating within the Arc GIS environment, HEC-Geo RAS uses spatial data to develop, organize, and automatically enter input data into the HEC-RAS model using the terrain digital elevation model of the study area. The key data element that HEC-Geo RAS uses to develop the input data is terrain data, commonly referred to as a Triangular Irregular Network (TIN). The triangular irregular network (TIN) used for this study was converted from a digital elevation model obtained from the MoWRIE of Ethiopia with a high resolution of 30m. HEC-Geo RAS works together with Arc GIS and it contains about four main menus: RAS Geometry, RAS Mapping, Assign river code and reach code to River, select flow path, and assign line type attributes.

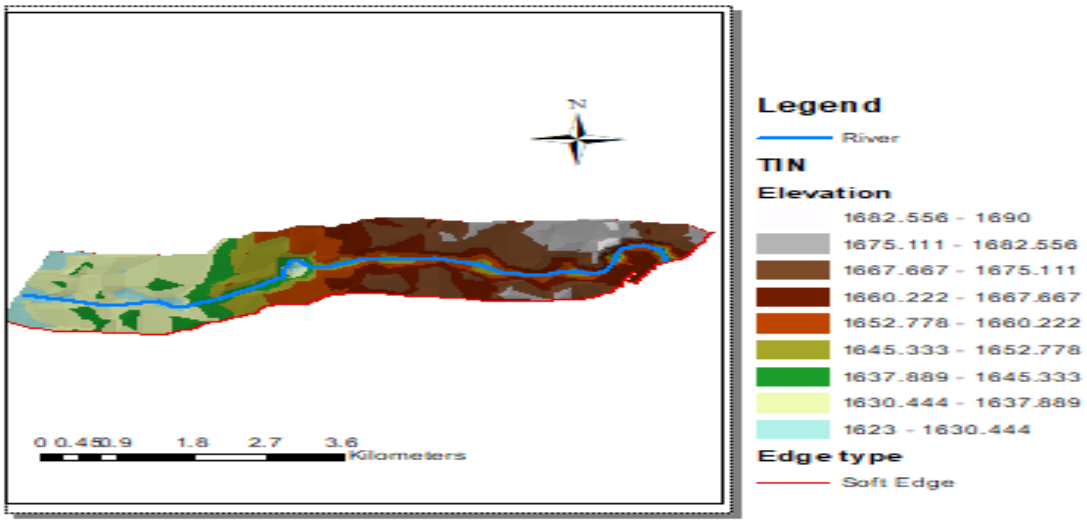

Figure 3-13: TIN of study area developed by Arc GIS

3.8.1 Terrain Preprocessing using HEC-GeoRAS and TIN

The goal of this activity was to develop the basic spatial data required to generate the HEC-RAS Geometry Import File. Terrain preprocessing requires a terrain elevation model (TEM) that is commonly referred to as a triangular irregular network and it is used to prepare input data like river station, channel length left and right over the bank, and reach length for HEC-RAS. The initial point of preprocessing was RAS geometry that includes options like create RAS layers, Layer setup, stream centerline attribute, XS Cutline attribute, and Manning's n value.

RAS geometry: Boundary geometry for the analysis of flow in the natural stream is specified in terms of ground surface profiles (cross-sections). Cross-sections should be perpendicular to the anticipated flow lines and extend across the entire floodplain (these cross-sections may be curved or bent). Cross-sections are required at locations where changes occur in discharge, slope, shape, or roughness; at locations where levees begin or end and at bridges or control structures such as weirs. Each cross-section is identified by a Reach and River Station label.

In general, the delineation of cross-sections located close to river junctions was not easy: each cross-section have to cross the stream centerline exactly once, the bank lines exactly twice (left and right), and the flow paths exactly three times (left, right, and centerline) and they should not intersect each other.

The cross-section is digitized from left to right, with respect to looking in the downstream direction. After the creating of the river cross-section,stream centerline attributes (like topology, length/stations, and elevation) and XS cut line attributes were added in order to compute river station at each cross-section, channel length, and left and right overbank length (table 3.9). Executing river geometry cross-section using Arc GIS combined with HEC-Geo RAS, the constructed river geometry cross-section was exported to HEC-RAS in Arc GIS format. Exporting the river geometry cross-section to HEC-RAS, it was displayed as geometric data with all the river cross-section (figure 3.14).

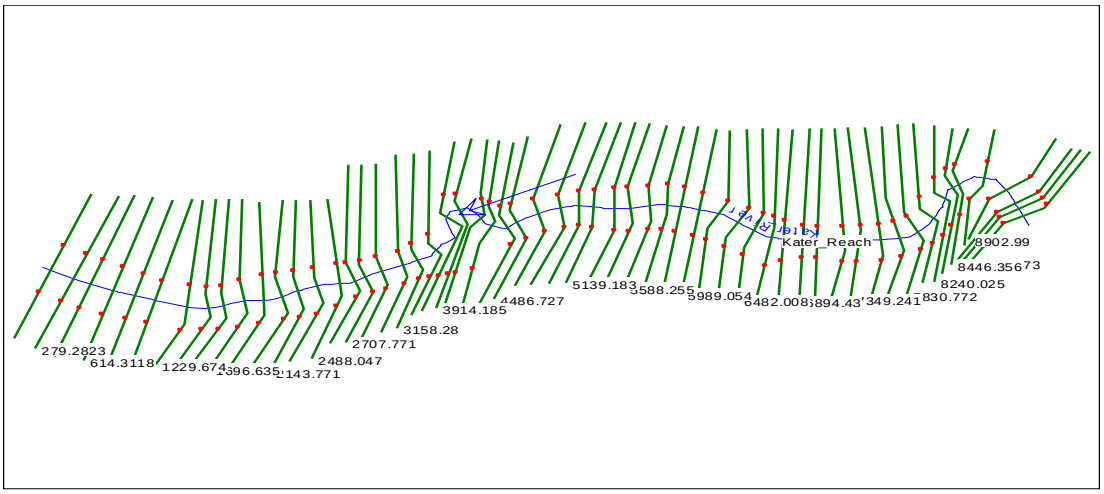

Figure 3-14: River geometric XS and station exported from HEC-Geo RAS.

Having exporting the entire river cross-section from HEC-Geo RAS to HEC-RAS, it is possible to see river stations, channel, left and right overbank length in table form as in table 3.9. Also, the HEC-RAS can provide different outputs like the total discharge of the channel, channel elevation, water surface elevation, critical water surface elevation, energy gradient elevation, energy gradient slope, channel velocity, flow area, top width, and channel Froude number for each river station (APPENDIX-C).

Table 3-9: River station with Leftover bank, Right and Channel length

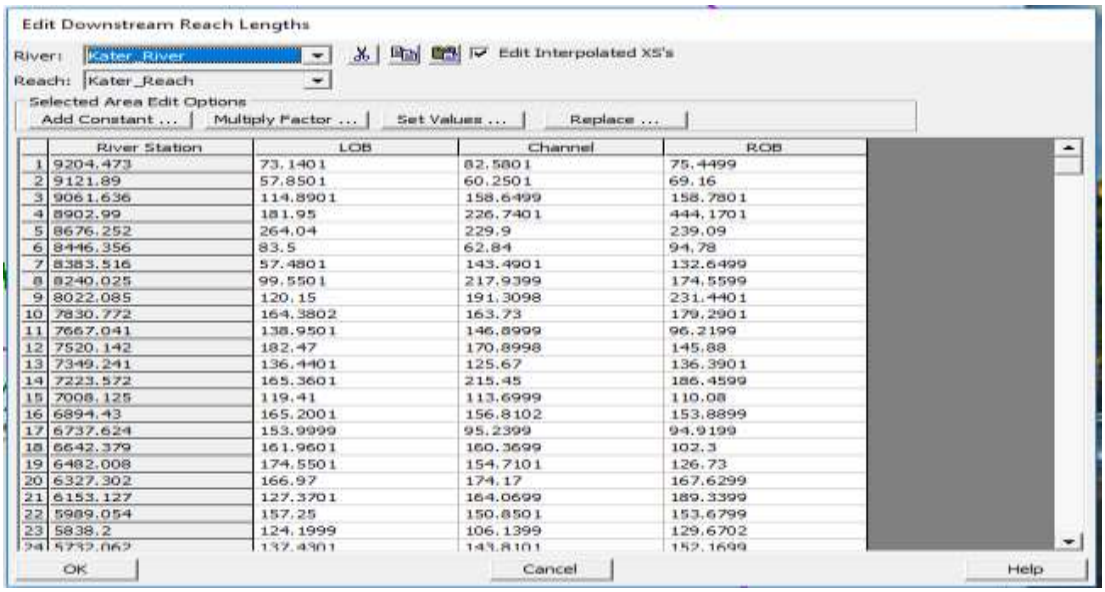

	River Station	LOB	Channel	ROB
1	9204.473	73.1401	82.5801	75.4499
2	9121.89	57.8501	60.2501	69.16
3	9061.636	114.8901	158.6499	158.7801
4	8902.99	181.95	226.7401	444.1701
5	8676.252	264.04	229.9	239.09
6	8446.356	83.5	62.84	94.78
7	8383.516	57.4801	143.4901	132.6499
8	8240.025	99.5501	217.9399	174.5599
9	8022.085	120.15	191.3098	231.4401
10	7830.772	164.3802	163.73	179.2901
11	7667.041	138.9501	146.8999	96.2199
12	7520.142	182.47	170.8998	145.88
13	7349.241	136.4401	125.67	136.3901
14	7223.572	165.3601	215.45	186.4599
15	7008.125	119.41	113.6999	110.08
16	6894.43	165.2001	156.8102	153.8899
17	6737.624	153.9999	95.2399	94.9199
18	6642.379	161.9601	160.3699	102.3
19	6482.008	174.5501	154.7101	126.73
20	6327.302	166.97	174.17	167.6299
21	6153.127	127.3701	164.0699	189.3399
22	5989.054	157.25	150.8501	153.6799
23	5838.2	124.1999	106.1399	129.6702
24	5732.062	132.4301	143.8101	152.1699

After exporting the river cross-section from Arc GIS through HEC-Geo RAS, geometric data like manning's roughness coefficient, flow data generally called profile and boundary condition were added.

The manning's roughness coefficient n used for this study was determined by the Cowan method for the main channel and floodplain. Flow data (profiles) was obtained from peak flood frequency analysis developed in HEC-HMS for 2, 5, 10, 25, 50, and 100 year return period. Upstream and downstream normal depth was selected as a boundary condition after calculating the upstream and downstream slope from the cross-section profile plot. Steady flow analysis with mixed flow regime was selected and the model was run. Having run the model, the 3D view of the multiple river cross-section plots were presented as in figure 3.15.

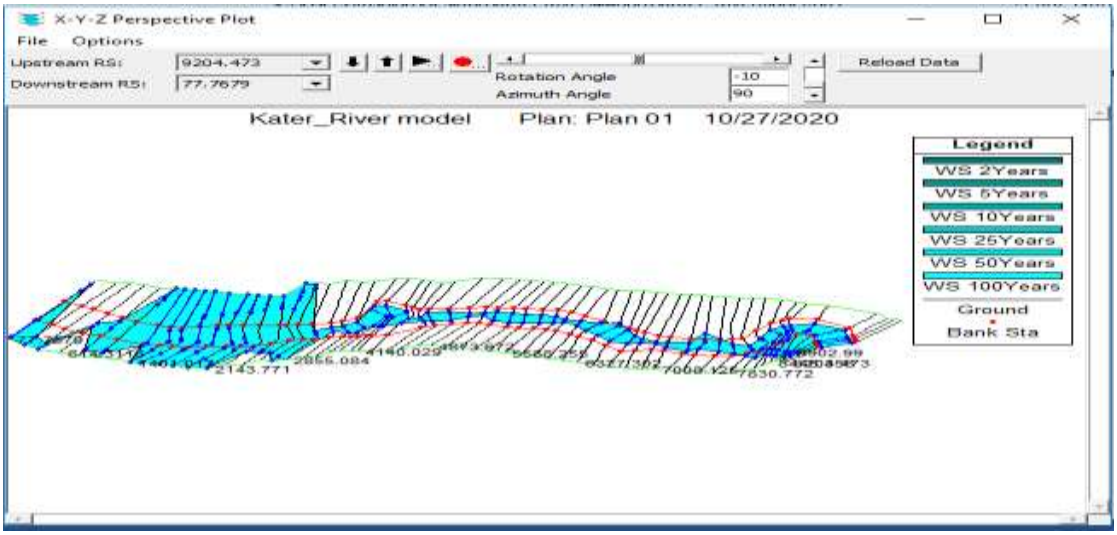

Figure 3-15: 3D view of multiple river cross-sections

.After running the HEC-RAS successfully, the GIS data such as water surface and water surface extent, velocity, river centerlines, and the entire river cross-section for all profiles were exported to GIS as 'RASexport.sdf' format, Kater_Rivermodel.RASexport.sdf, (figure 3.16).

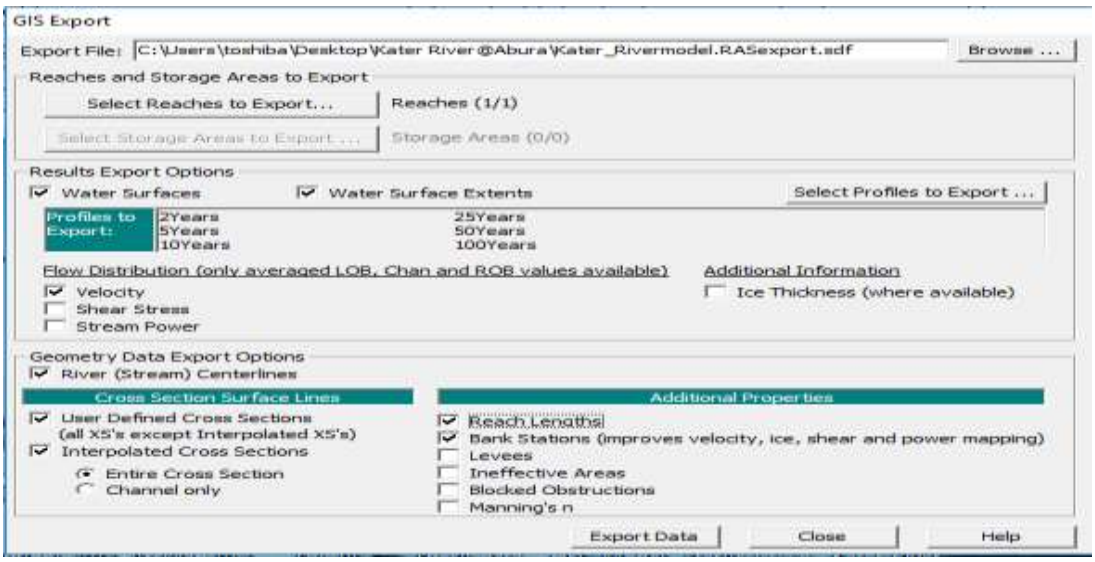

Figure 3-16: GIS data exported from HEC-RAS to Arc GIS

3.8.2 Importing and editing geometric data

The first component is the channel geometry. To analyze streamflow, HEC-RAS represents a stream channel and floodplain as a series of cross-sections along the channel. To create the geometric model, the Geometric data has been imported from GIS to the HEC-RAS. However, the geometric data processed may not appropriate with the

actual data, so that it is necessary to edit them in HEC-RAS software. Therefore cross-section data editor should be displayed with the downstream reach lengths (left overbank, right over the bank, and the main channel) should be edited.

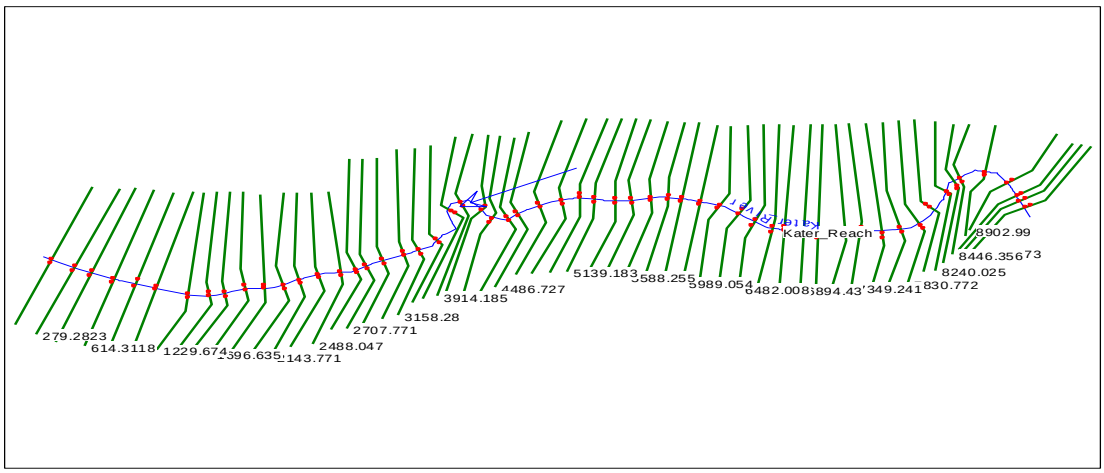

Figure 3-17: Edited geometry Data of the Flood Plain

3.8.3 Roughness coefficient for river channel and floodplain

Manning roughness coefficient used to represent the resistance to flood flows in channels and flood plains. Determination of the correct value for Manning's n is very important to compute water surface profiles. Many factors that affect the manning's values are Surface roughness, Vegetation, Channel irregularities, and alignment, Scour and deposition, Obstructions, Size and shape of the channel, Stage, and discharge, Seasonal changes, Temperature, and Suspended material and bedload, etc(Asnake,2018).The Cowan method is a potentially more accurate techniquethat is required for a number of hydraulic computations. Thus the manning's value was determined from this method. The first step involved was defining land-use characteristics for the main channel and flood plain of the study areas andthen, the "n" values were assigned based on their characteristics. Each characteristic was given n-value based on table values for similar conditions and engineering judgment using a field survey of the Ketar River channel and floodplain area under consideration was also taken into account.

This method is a table look-up solution, with the basic n value and each of the corrections obtained from a table. The method involves the selection of a base value of n and then correcting the base value based on the following five factors:

1. The degree of regularity of the surfaces of the channel cross-section.

2. The character of variations in the size and shape of cross-sections.

3. The presence and characteristics of obstructions in the channel.

4. The effect of vegetation on flow conditions.

5. The degree of channel meandering.

The general procedure for estimating n involves first, the selection of a basic value of n for a channel and floodplain materials involved, then, through a critical consideration of the factors listed above, the selection of a modifying value associated with each factor. The modifying values are added to the basic value to obtain n for the channel under the study.

The actual value of the reach roughness coefficient equals the sum of the values of the basic value n1 and the modifying values n2 to n6. The calculations can be performed on the computation sheet.

Table 3-10:Computation sheet for manning's roughness coefficient

Variable	**Description Alternatives**	**Recommended value**	**Actual value of Channel**	**Actual value of Floodplain**
Basic **n1**	Earth	0.02	n1 = 0.022	n1 = 0.022
	Rock	0.025		
	Fine gravel	0.024		
	Coarse gravel	0.028		
Irregularity **n2**	Smooth	0.000	n2 = 0.005	n2 = 0.01
	Minor	0.005		
	Moderate	0.010		
	Severe	0.020		
Cross-section **n3**	Gradual	0.000	n3 = 0.005	n3 = 0.005
	Occasional	0.005		
	Alternating	0.010 – 0.015		
Obstructions **n4**	Negligible	0.000	n4 = 0.0125	n4 = 0.0125
	Minor	0.010 – 0.015		
	Appreciable	0.020 – 0.030		
	Severe	0.040 – 0.060		
Vegetation **n5**	Low	0.005 – 0.010	n5 = 0.015	n5 = 0.0375

	Medium	0.010 – 0.020		
	High	0.025 – 0.050		
	Very high	0.050 – 0.100		
Meandering **n6**	Minor	0.000	n6 = 0.000	n6 = 0.000
	Appreciable	0.15 * ns		
	Severe	0.30 * ns		
Total Reach n			0.0595	0.087

Therefore, the total reach "n" values were obtained for the main channel of Ketar River and its floodplain. Finally, were performed the computation sheet calculation of a manning roughness coefficient value of 0.0595 for the main channel and 0.087 for the left and right bank of the floodplain.

3.8.4 HEC-RAS Calibration

Model calibration is the procedure of adjustment of parameter values of a model to reproduce the response of reality within the range of accuracy specified in the performance criteria. It is a comparison between a known measurement (measured water levels) and the measurement using the model (simulated water levels) to check the accuracy of model. The HEC-RAS model was calibrated for predicting water levels and hence determining a single value of manning's coefficient 'n'.In order to check the ability of the calibrated model in predicting the water levels for different river flows the model should be validated (verified) using measurement data other than the one used in calibrating model.

In calibration process, the manning's coefficient 'n' was altered continually until the variations between observed and simulated water levels were within the acceptable limits. The calibration procedure gave the correct value of the manning's coefficient of the river. It was performed by comparing the result of the water level in each cross section obtained by the model with the observed levels until the differences between observed and simulated water levels become small as far as possible. Finally, to provide the additional accuracy measurement, the root mean square error, mean absolute error and correlation coefficient were tested between observed and simulated water surface elevations. However, in this study the absence of observed water level data makes difficulties in calibration process of the model.

3.8.5 Expansion and contraction coefficient

According toUSACE, (2010) the contraction and expansion coefficient for a natural channel that has a gradual change in cross-section is estimated to be 0.1 and 0.3 respectively. By understanding this concept, since Ketar River is a natural channel, it has the same value as stated above. Ketar River is gradually varied. Therefore, to perform flow calculation in the channel, 0.1 was used for the contraction coefficient whereas 0.3 was used for the expansion coefficient.

3.9 Flow data

The flow data has been extracted from an HEC-HMS hydrologic model. Steady flow condition is adopted even though it is rare to find the steady flow condition in the natural channel flow condition. This component of the HEC-RAS modeling system is capable of simulating one-dimensional steady flow through a full network of open channels. For the case of Ketar river floodplain, the peak flows estimated by HEC-HMS for 2, 5, 10, 25, 50 and100 years return period is used at the outlet of the catchment (Ketar watershed).

3.9.1 Entering and editing flow data

Flows are typically defined at the most upstream location of the river. After analysis of the flow data in HEC-HMS at different return periods, it is used as an input for HEC-RAS Software. Each flow that needs to be simulated is called a profile in HEC-RAS. For carrying out the analysis here, the peak flood having 2, 5, 10, 25, 50, and 100 year return period of flow was used.

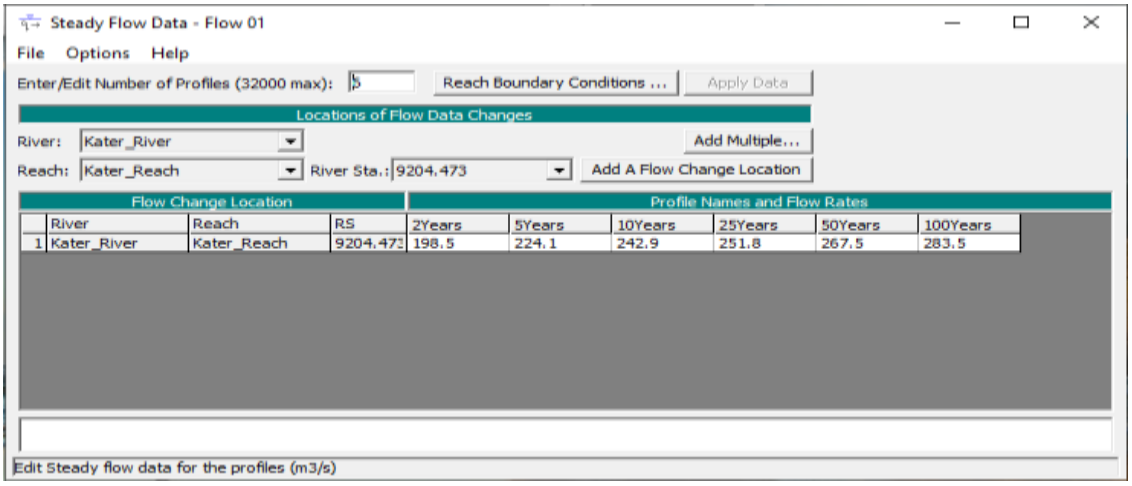

Figure 3-18: Steady Flow Condition Using Six Flow Profiles

3.9.2 Boundary condition

Boundary conditions are essential to establish the starting water surface at the ends of the river system upstream and downstream. A starting water surface is needed in order for the programs to begin a calculation. In the subcritical flow regimes, boundary conditions are only needed at the downstream ends of the river system. If the supercritical flow regimes are going to be calculated, boundary conditions are only essential at the upstream end of the river systems. If the mixed flow regimes calculations are going to be made, then the boundary condition should be entered at all ends of the river system.

According to the model, there are four types of boundary conditions namely:

- Known water surface elevation
- Normal depth
- Critical depth and
- Rating curve

For this thesis, normal depth had been selected. A normal depth should be determined for the upstream and downstream end profile of the study area. The slope of the channel bottom for upstream and downstream was 0.075 and 0.018 respectively which can be calculated from the river cross-section profile plot.

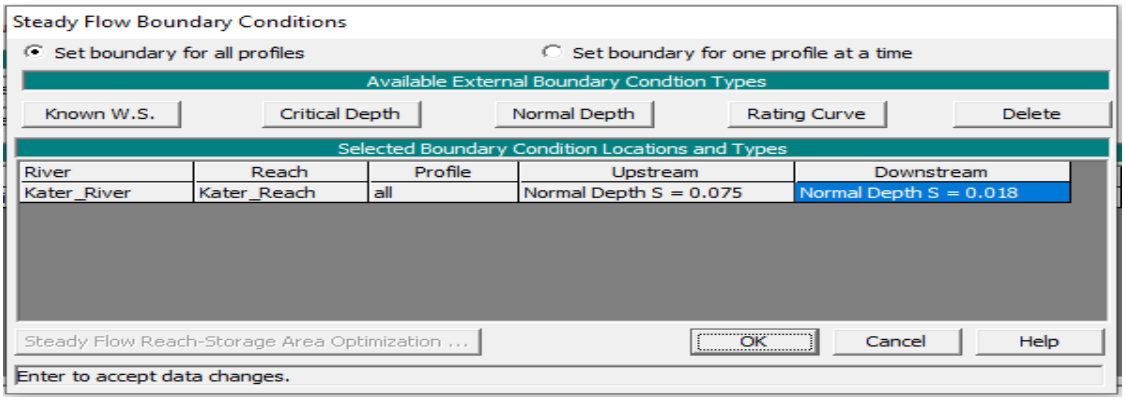

Figure 3-19: Boundary Condition in Steady Flow.

3.9.3 Steady flow simulation

Simulate the model, with the type of flow to be calculated should be distinguished. So that for this paper, the steady flow analysis was selected. Not only the type of flow but also the regime of flow should be identified as well. Therefore, in this case, the mixed flow regime was selected because it starts flow calculation from the upstream and downstream ends of the river system.

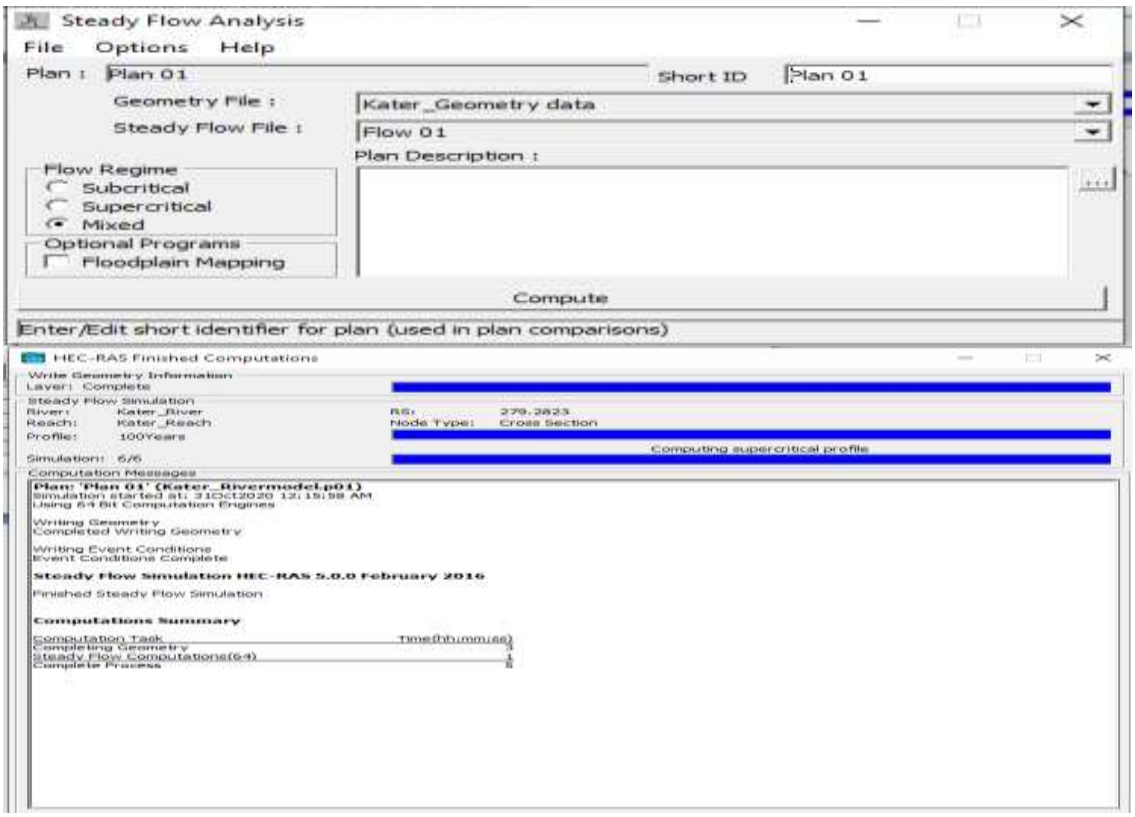

Figure 3-20 Steady flow simulation in HEC-RAS

3.10 Post Processing:HEC-GeoRAS

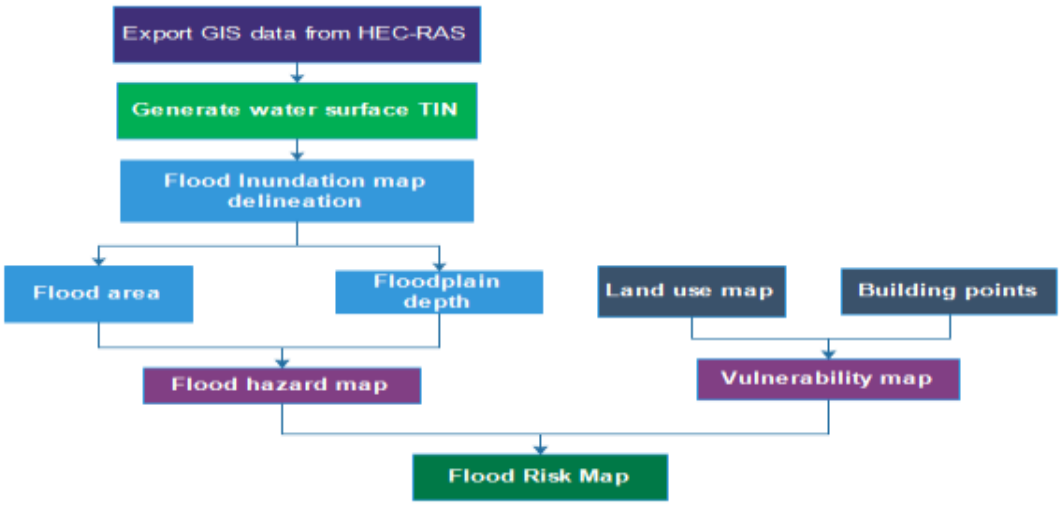

Figure 3-21: Workflow diagram in Post-processing.

In this section, the delineation of floodplains was accomplished by integrating the RAS-GIS output file (RASexport.sdf) and the TIN layer on GIS. The next step was overlaying the terrain TIN with water surface TIN. From this, inundation depths and floodplain boundaries are extracted.

RAS GIS output conversion: HEC- Geo RAS cannot recognize the direct output of RAS GIS file format and must be converted into HEC-Geo RAS file format. By using the 'Import RAS SDF File' toolbar of HEC-Geo RAS, the RASexport.sdf file format was converted intoXML file format so that the Arc GIS can recognize it.

Layer setup: by using the layer setup window of HEC- Geo RAS, the type of analysis (in this case steady flow analysis), input (RAS GIS file, terrain TIN), and output data directory were identified.

3.10.1 Generation of water surface TIN

The first step was to create a water surface TIN from the cross-section water surface elevations using HEC-Geo RAS. All Six water surface profiles were selected from the window then for each selected water surface profile, a water surface TIN is created without consideration of the terrain model. The TIN was created using the Arc GIS triangulation method. This allowed for the creation of a surface using cut lines as hard brake lines with constant elevation.

3.10.2 Floodplain map delineation

Floodplain delineation used the Water surface TIN and terrain model to calculate the floodplain boundary and inundation depth. At this stage the water surface TIN was first converted into a GRID, and then DTM/ GRID was subtracted from the water surface grid. The area with positive results (i,e. water surface is higher than the terrain) is the flood area, whereas the area with negative results is dry. All the cells in the water surface grid that result in positive values after subtraction were converted to a polygon, which is the final flood inundation polygon.

3.10.3 Determination of floodplain area

Areas inundated by flooding occur wherever the elevation of the floodwater exceeds that of the land. To delineate these areas, we will create surface models of the floodwater and land surface and then compare the elevations. HEC-RAS represents the floodplain as a computed water surface elevation at each cross-section (Zelalem,2011).

3.11 Calibration of Flood mapping,

Flood mapping in hydraulic modelling is calibrated by using satellite data (image) and remote sensing tools. Since, satellite image and remote sensing data with Arc GIS is used to identify the potential area for flood problem. As it described in the chapter one in the document before, the flood in the study area occurs only during summer season of heavy rainfall and in the others season it is totally dry. As I try to see from satellite data of landsat 8 during different months in the summer season the mapping area is totally covered by cloud and the flooded area is invisible; where as during others seasons there is no flood and the area is totally dry. This make the difficulties in flood mapping calibration by using flood map obtained from satellite image and remote sensing data.

CHAPTER 4 RESULT AND DISCUSSION

4.1 Rainfall-Runoff Model

4.1.1 Back Ground Map File

The background map file represents the physical watershed under consideration. For this study, a background map file that contains about 5 Sub-basins with 2 reaches and 2 junctions was generated using HEC-Geo HMS in Arc GIS (Figure 4.1). It encompasses Basin model file, Met model file, Gage model file those were used as an input in HEC-HMS during rainfall-runoff modeling and also it comprises methods for modeling each HEC-HMS components. Basin model file contains sub-watersheds, reaches, junctions, and outlets with methods for precipitation loss modeling, excess precipitation transforming, base flow modeling, and channel routing methods.

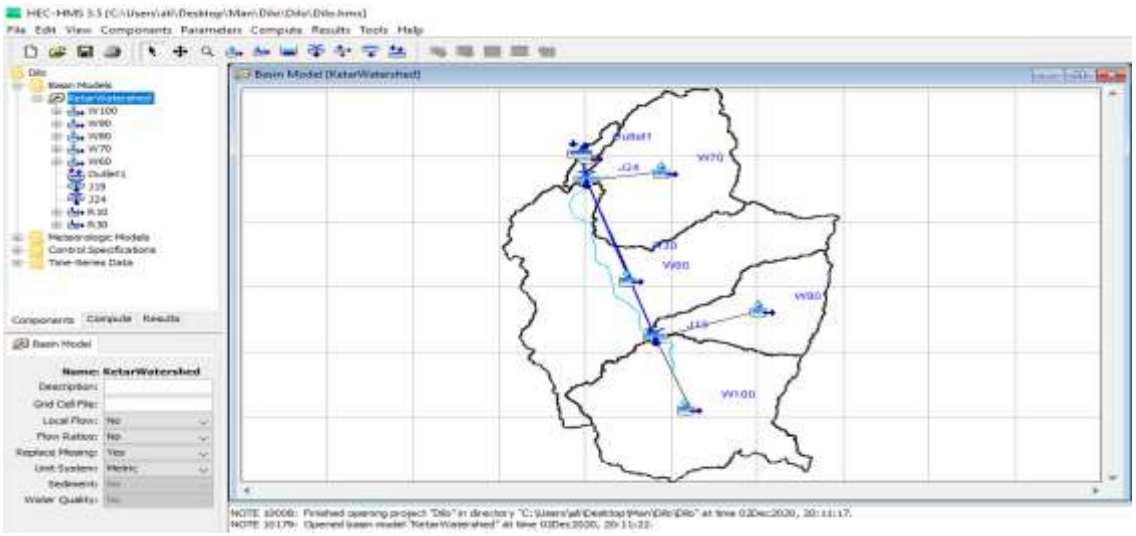

Figure 4-1: Background map file of the Ketar watershed

The observed flow at Abura gauging station was used and set into the HEC-HMS to compare the computed flow with the actual flow and to give personal judgment. After all the required data were prepared and entered into the hydrologic modeling system (HEC-HMS), the model was run and the first simulation result at the outlet was investigated and there is poor agreement between the computed and observed flow. Therefore it requires parameter optimization or model calibration.

4.1.2 Parameters Optimization (calibration)

Parameter optimization is a systematic process of adjusting model parameter values and other variables in the model until the computed model results match acceptably with observed data. The quantitative measure of goodness of fit between the computed result from the model and observed flow is called the objective function. Objective function measures the degree of variation between simulated and observed hydrographs which is equal to zero if hydrographs are identical. The key to automated parameter estimation is a search method for adjusting parameters to minimize objective function value and find optimal parameter value. The minimum objective function is obtained when the parameter values best able to reproduce the observed hydrograph are found.

The two search methods available for minimizing objective function and finding optimal parameters values are the Univariate gradient method that evaluates and adjusts one parameter at a time while holding the other parameters constant and the second search method is Nelder and Mead's method uses downhill simplex to evaluate all parameters simultaneously and determine to adjust. Among the parameters used in HEC-HMS for rainfall-runoff modeling of this study, flood wave travel time (Muskingum-K) and weighted coefficient of discharge (Muskingum-X) were the most sensitive parameters, and the calibration was carried out considering these parameters.Table 4.1: indicates the initial and optimized value of the parameters and objective function sensitivity value.

Table 4-1: HEC-HMS optimized parameters for Ketar watershed

Elements	Parameters	Units	Initial Value	Optimized Value	Objective Function Sensitivity
R10	Muskingum K	HR	150	65.333	0.05
R10	Muskingum X		0.13293	0.12511	0.02
R30	Muskingum K	HR	75.254	33.446	0.02
R30	Muskingum X		0.14126	0.13567	0
W60	Clark Time of Concentration	HR	25.812	38.901	0
W70	Clark Time of Concentration	HR	132	129.62	0
W80	Clark Time of Concentration	HR	307.98	206.2	0
W90	Clark Time of Concentration	HR	411.58	268.9	0
W100	Clark Time of Concentration	HR	338.96	221.45	0.03
W60	Constant Loss Rate	MM/HR	0.851	0.85765	-0.01

W70	Constant Loss Rate	MM/HR	0.851	0.56994	-0.07
W80	Constant Loss Rate	MM/HR	0.851	1.2825	-0.03
W90	Constant Loss Rate	MM/HR	0.851	0.85378	-0.01
W100	Constant Loss Rate	MM/HR	0.851	0.85904	-0.13

A total of 16 years of historical data from 1988 to 2003 was used. For calibration, 11 years (1988-1998) and for Validation, 5 years (1999-2003) of daily data was used for the HEC-HMS model. After a number of iterations, the observed and simulated flow shows a good agreement as in Figures4.2 and 4.3 with a maximum value of 164.7m3 /s and 188.2m3 /s respectively.

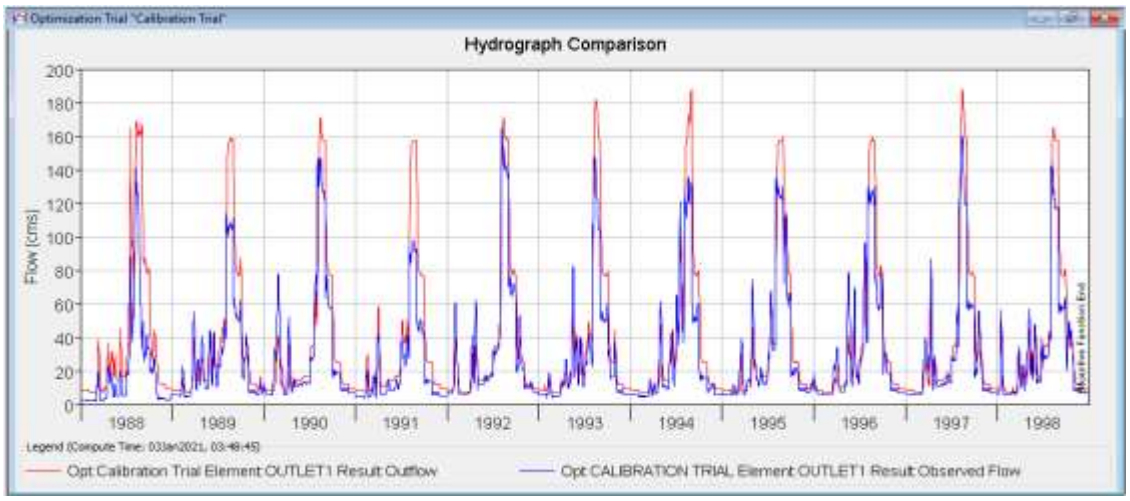

Figure 4-2: Daily simulated and observed flow hydrograph from HEC-HMS

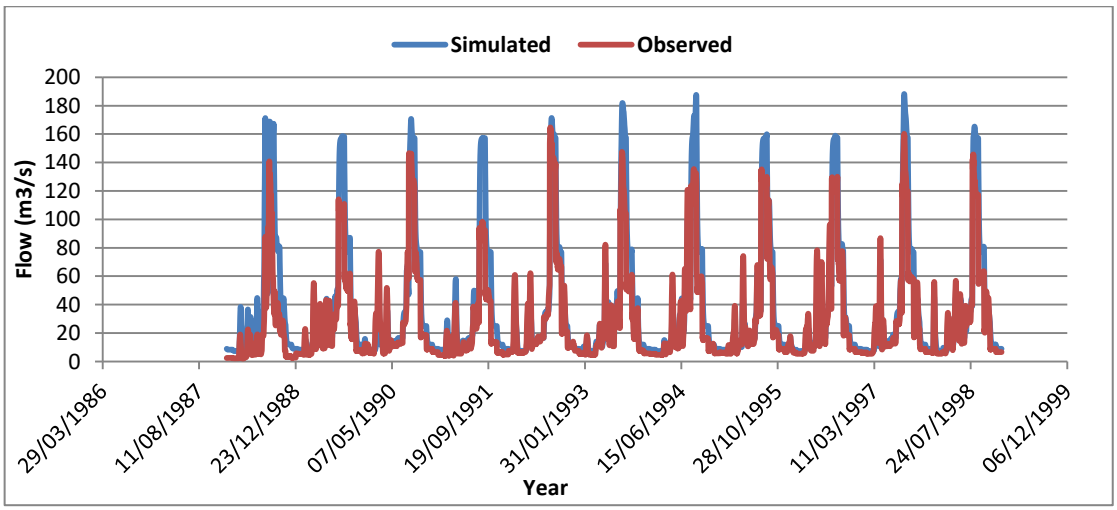

Figure 4-3: Daily hydrograph comparison during calibration

As mentioned in chapter three the model performance evaluation was performed using the two well-known model performance checkup techniques. These were Nash Sutcliff's efficiency and coefficient of determination.

The Nash Sutcliff efficiency and coefficient of determination during the model calibration were 0.72 and 0.87 respectively and graphically, the Coefficient of determination during model calibration was illustrated in the figure 4.4.which performed by using Microsoft excel.

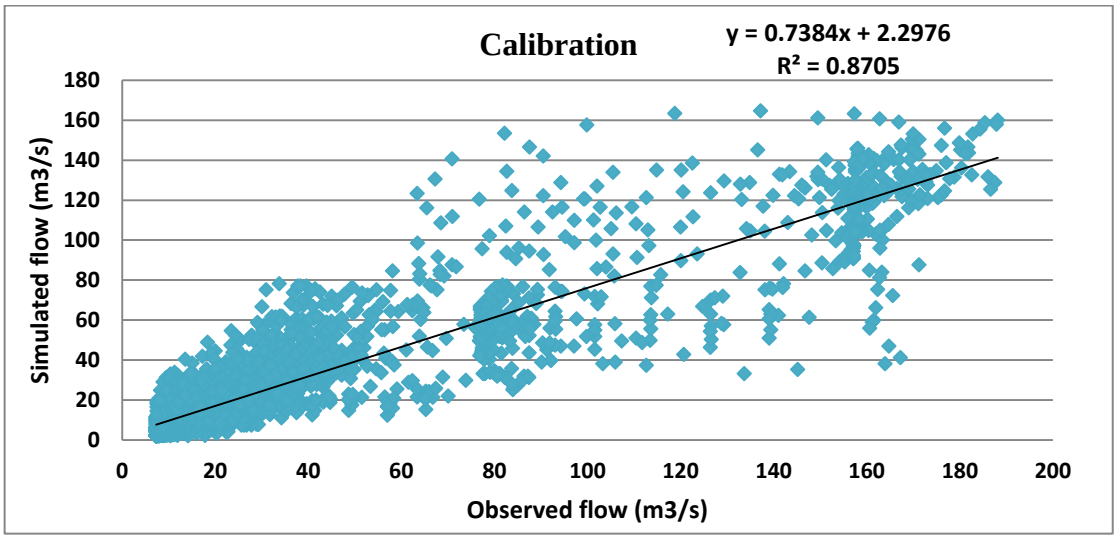

Figure 4-4 Coefficient of determination during calibration

4.1.3 Validation

After the calibration was completed and all model parameters were adjusted, 5 years (1999-2003) hydro-meteorological data (i.e. precipitation and observed flow) were entered and model validation was carried out to check whether the model with an adjusted parameter was valid or not. After processing the input data the model was generated good results without any adjustment; especially, the sensitive parameters. The obtained result was almost identical as it was shown in Figures 4.5 and 4.6. The Nash Sutcliff efficiency and coefficient of determination during the model validation were 0.67 and 0.81 respectively and graphically, the coefficient of determination during model validation was illustrated in figure 4.7.

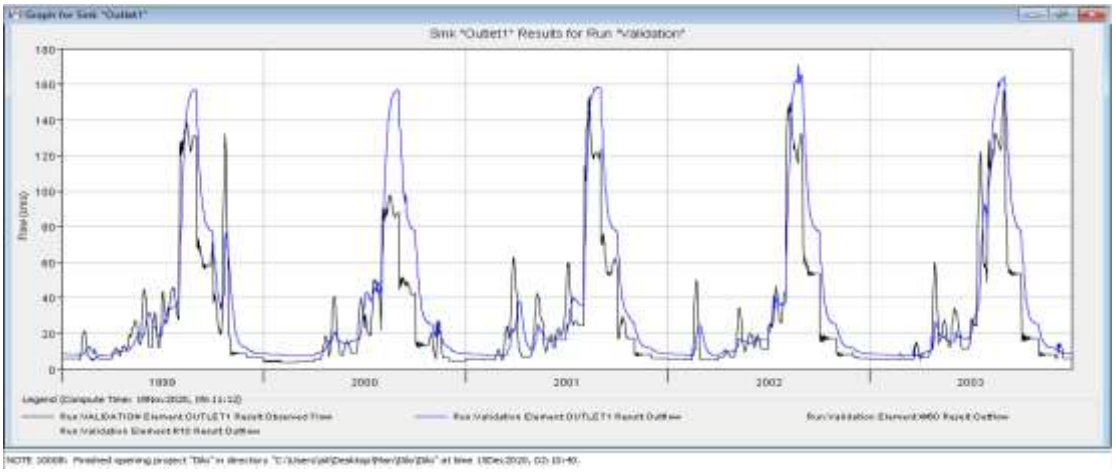

Figure 4-5: Daily simulated and observed flow hydrograph during validation.

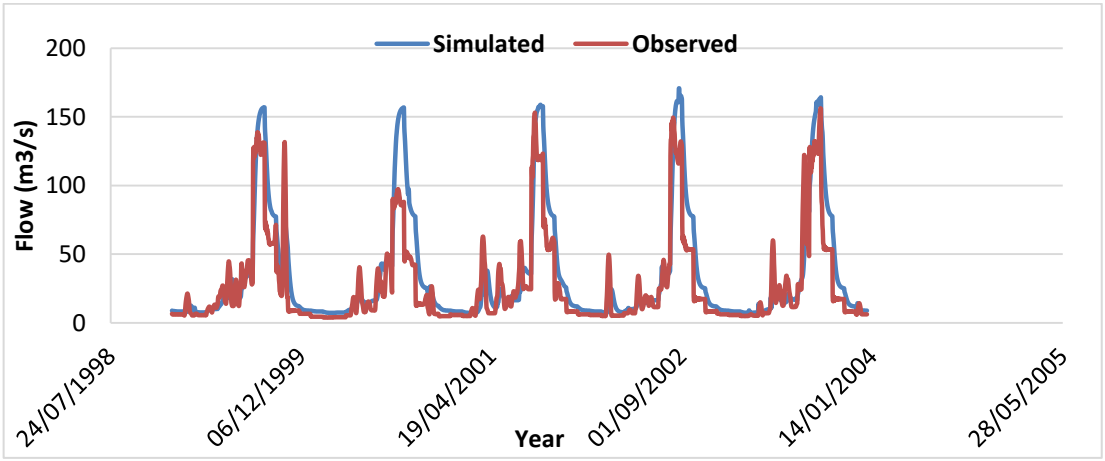

Figure 4-6: Daily hydrograph comparison during validation

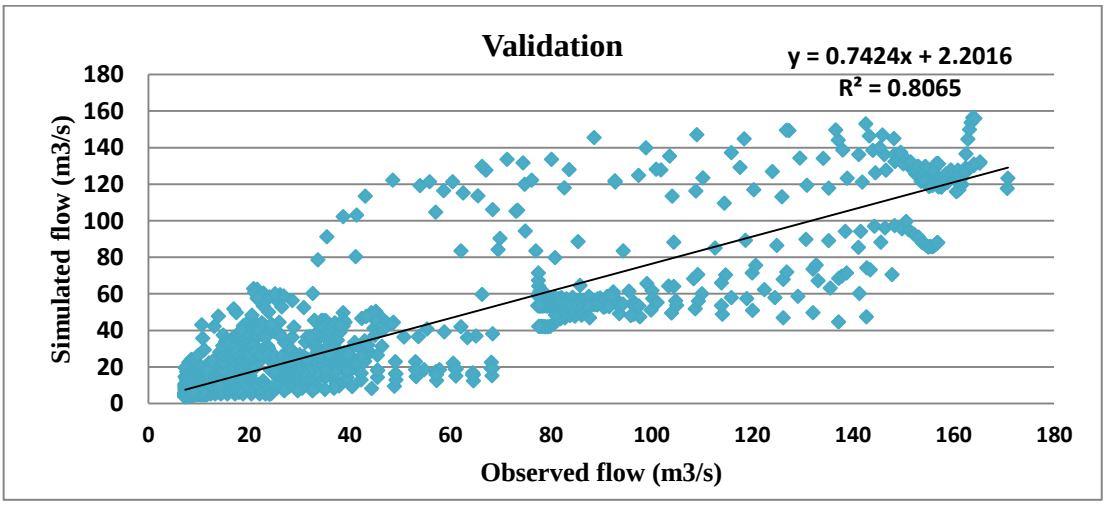

Figure 4-7: Coefficient of determination during validation

With the final result, one can say that the HEC-HMS model can perform well if accurate and reasonable data was used for model development; and also the parameter used must be reasonable and should be physically based as they vary with the different watersheds.

4.2 Flood Frequency Analysis

The 1hr, 2hr, 3hr, 6hr, 12hr,18hr, and 24hr duration rainfall depth for the corresponding return period was computed using equation 3.10 and tabulated as in table 4.2. Ascan be seen from the table, every return period under consideration has maximum rainfall depth during the 24hr.

Table 4-2: Rainfall depth vs. Return period for Ketar watershed

Rainfall Intensity duration	Rainfall depth versus return period (mm)					
	2	5	10	25	50	100
1	30.61	38.38	43.57	50.17	55.13	60.1
2	35.91	45.03	51.11	58.86	64.68	70.51
3	38.43	48.19	54.7	63	69.22	75.46
6	41.99	52.66	59.77	68.83	75.63	82.45
12	44.93	56.34	63.95	73.64	80.92	88.22
18	46.48	58.28	66.16	76.19	83.72	91.27
24	47.54	59.61	67.66	77.92	85.62	93.35

The above-computed rainfall depth for each rainfall duration corresponding to the return period was used in HEC-HMS to develop peak discharge for each return period. After model setup was adjusted using different parameters and model validation was carried out using daily time series data, a 1hr,2hr,3hr,6hr,12hr, 18hr and 24hr rainfall depth provided in table 4.2 was inserted into HEC-HMS for the computation of 2,5,10,25,50 and 100 year return period peak flood (table 4.3).

4.2.1 Output of HEC-HMS by frequency storm

The model has the capability to produce and generate values for different flow conditions (return periods). Given the above input parameters, the flow values are found accordingly. From the result table,the minimum peak flow for the Ketar River occurred for 2 year return period for 24-hour storm duration, and the maximum obtained with a

100-year frequency storm for the same duration. The value being 198.5m3/s and 283.5m3/s for 2 years and 100 year return period respectively.

Table 4-3: 24hr rainfall depth and its peak flood developed by HEC-HMS

S/No	Return period	24hrs rainfall depth (mm)	Peak flow (m3/s)
1	2	47.54	198.5
2	5	59.61	224.1
3	10	67.66	242.9
4	25	77.92	251.8
5	50	85.62	267.5
6	100	93.35	283.5

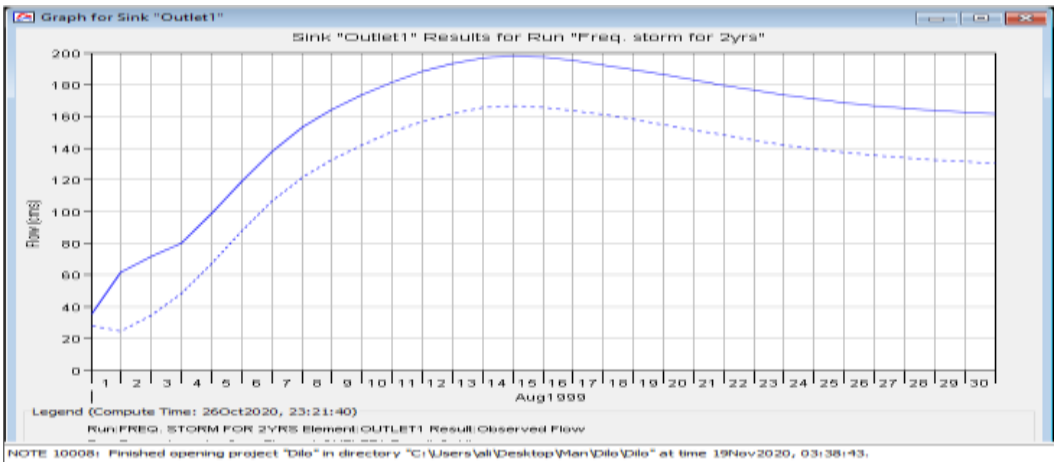

Figure 4-8: 2 years Flow hydrograph by HEC-HMS frequency storm

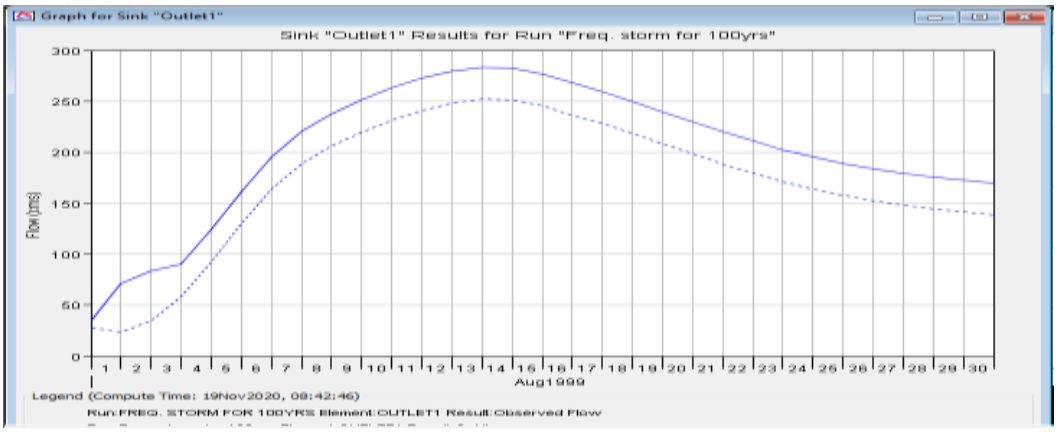

Figure 4-9: 100 years flow hydrograph by HEC-HMS frequency storm.

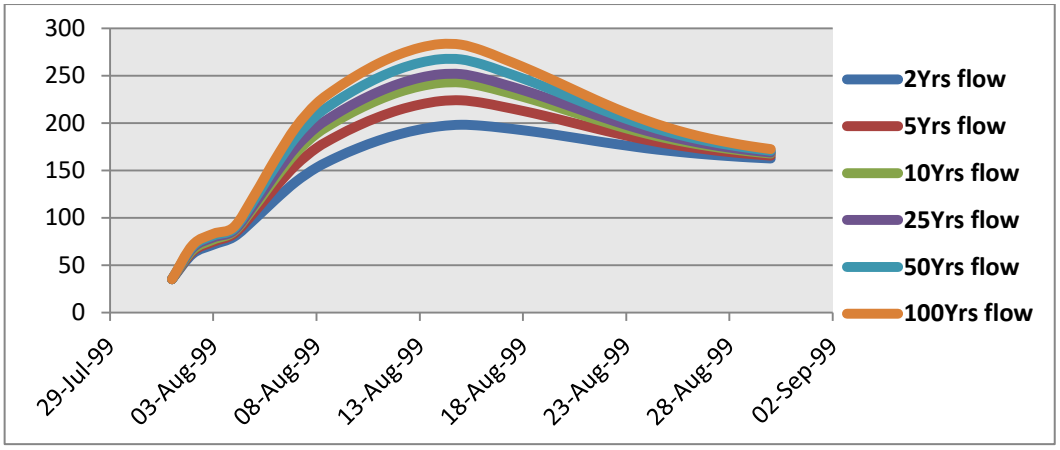

Figure 4-10: Flow hydrograph for all six return period.

4.3 Abstaction of flow on the upstream of outlet point

There is an existence of high abstraction (losses) for irrigation purpose by the local people located at the upstream of the outlet point (Abura gauging station) which undermine the observed discharge of the river. This condition makes the simulated (modelled) and the observed (measured) peak flow become far apart. As a result this high difference disturb and lower the acceptance levels of the model performance evaluation parameters (NSE and R^2) values which is obtained from different calibrated parameters and the calibration process close the simulated and observed flow with low or medium model performance value. Consequently, the peak flood determined by HEC-HMS frequency storm resulted from different calibrated parameters and 24hr rainfall depth also affected as well. Figure below shows the location of abstraction or losses for irrigation purpose, the outlet point (Abura gauging station) and the study area for hydraulic modelling.

Figure 4-11:Location of water losses, outlet point and ketar river floodplain

4.4 HEC-RAS Output

Having a peak flood for different return periods from HEC-HMS, river geometry and river cross-section data extracted from digital terrain model as in the figure 4.11, manning's roughness coefficient (n = 0.087 for right and left bank and n = 0.0595 for channel bed) were determined by cowan method and boundary condition (normal depth and mixed flow regime for this study), the hydraulic modeling was developed for steady-state 1-Dimensional flow condition to simplify the complexity in model computation.

4.4.1 River cross-section

River cross-section represents the river geometry like river centerline, bank line, flow path line and XS Cut line along the flood plain. For this study, 58 XS Cutlines were manually drawn in Arc GIS and HEC-Geo RAS with the help of Arc GIS assigns the river stations for every XS Cutline (figure 4.11) and also calculated the channel length, left and right overbank length.

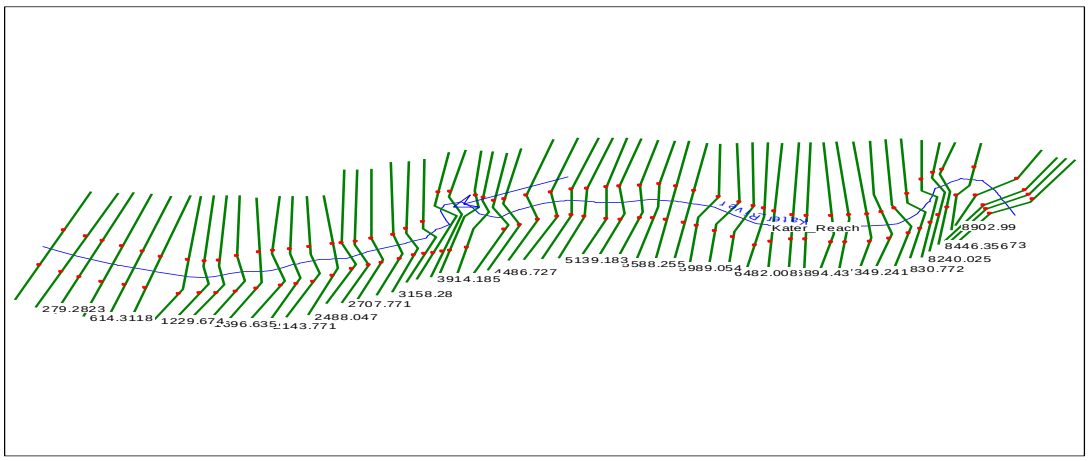

Figure 4-12: Exportedstation and cross-section from Arc GIS to HEC-RAS

4.4.2 Cross-sectional view

Having entering all the necessary data and running the RAS model for mixed flow regime, the representative graphical outputs of the HEC-RAS model for 2 and 100 years flow profile is shown in Figures 4.12 and 4.13 asa sample cross-section at station9204.473

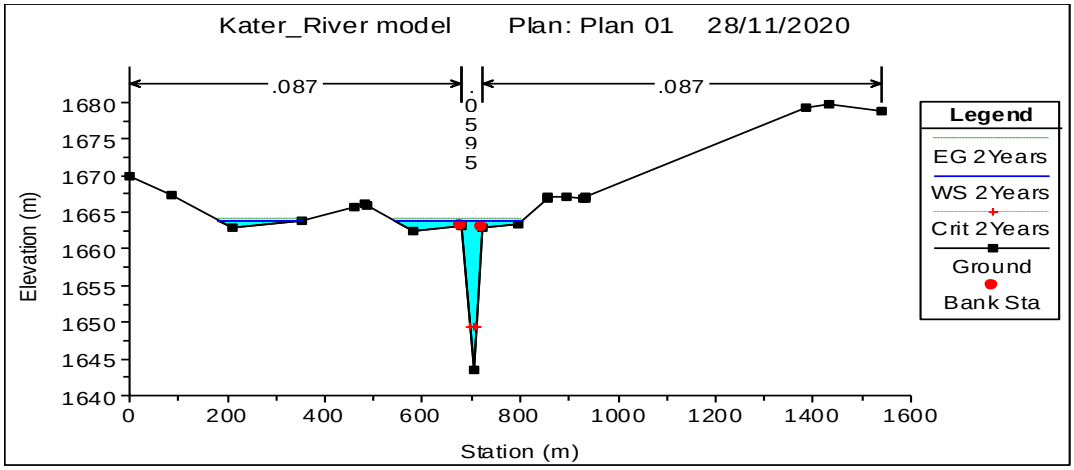

Figure 4-13: Cross-sections view at river station 9204.473 for 2-year profile

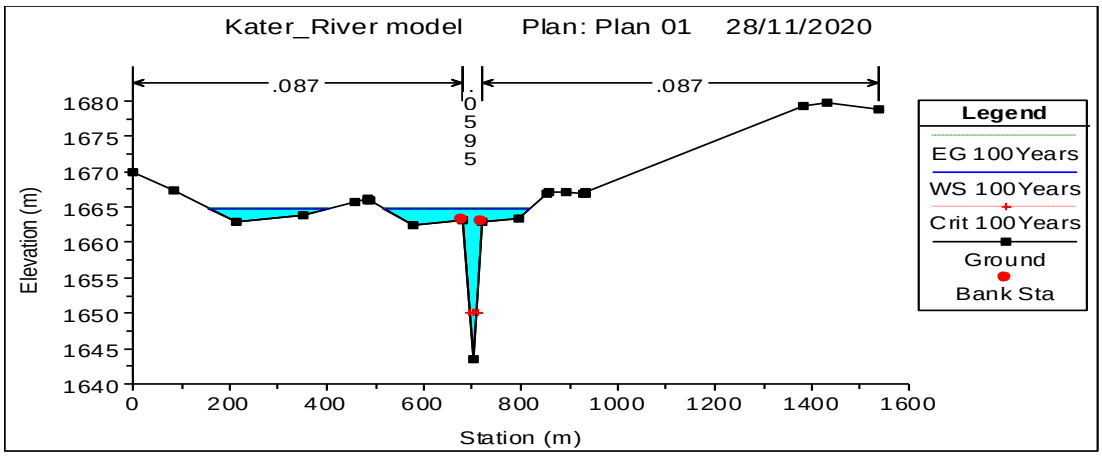

Figure 4-14: Cross-sections view at river station 9204.473 for 100-year profile

4.4.3 Water Surface Profile

The water surface profiles of the different return periods, i.e. 100, 50, 25, 10, 5, and 2 years, are shown in Figure. 4.14. The water surface profile for 2 and 100 years return periods is shown in APPENDIX-C since peak floods obtained from them,2 and 100 years peak floods, are the most minimum and maximum value to characterized the parameters (water surface profile).

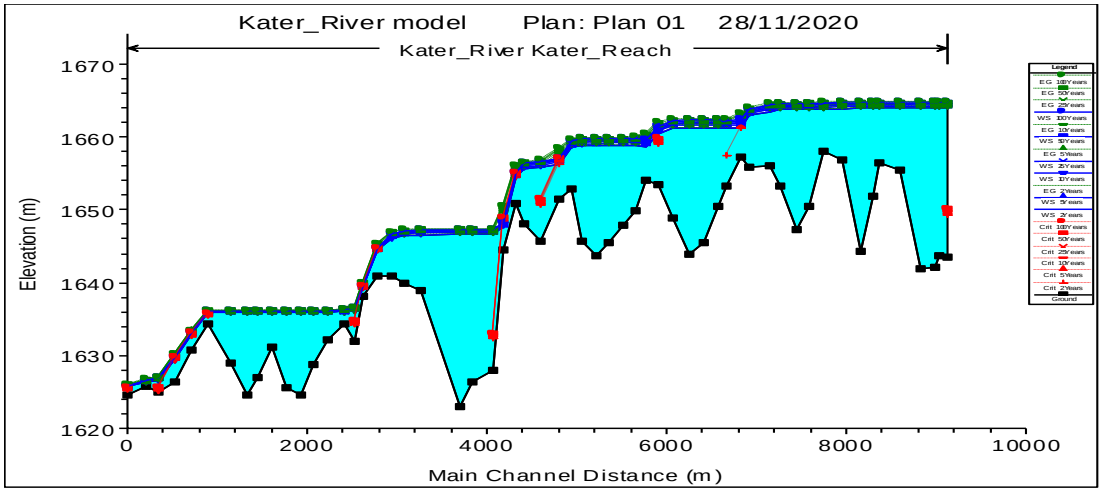

Figure 4-15: Water surface profile for all return periods.

4.5 HEC-GeoRAS Post-processing result

4.5.1 Water Surface TIN Generation

One water surface TIN was created for each selected water surface profile then, the TIN was created based on the water surface elevation at each cross-section and the bounding polygon data specified in the RAS GIS export file. The water surface TIN was generated without considering the terrain surface. After a water surface TIN has been created with water surface elevation for the selected profile, now it is added to the map

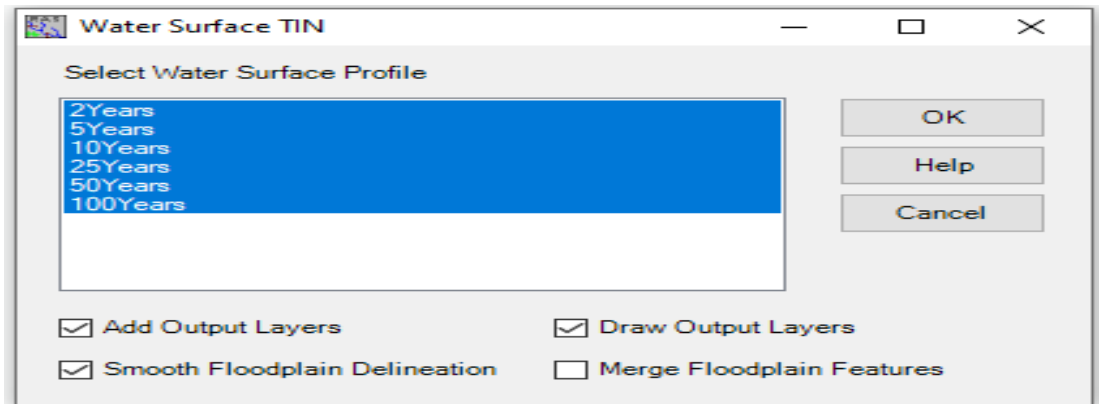

Figure 4-16: Water surface profile selection in HEC-GeoRAS

As shown in Figure: 4.16 and 4.17 the Arc-GIS triangulation method creates the surface TIN using cross-sectional cut lines and connecting the outer points of the bounding polygon so that the TIN was included in an area outside the possible inundation. The water surface TIN was generated using Arc GIS for flow profile used in HEC-RAS and indicated as in figure4.16 and 4.17.

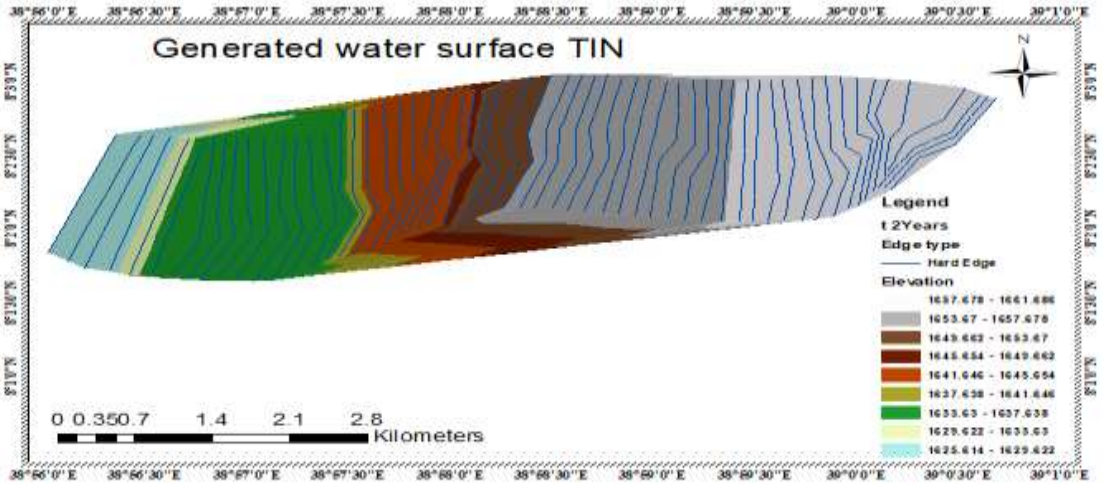

Figure 4-17: Water surface TIN generated for 2-year peak flood

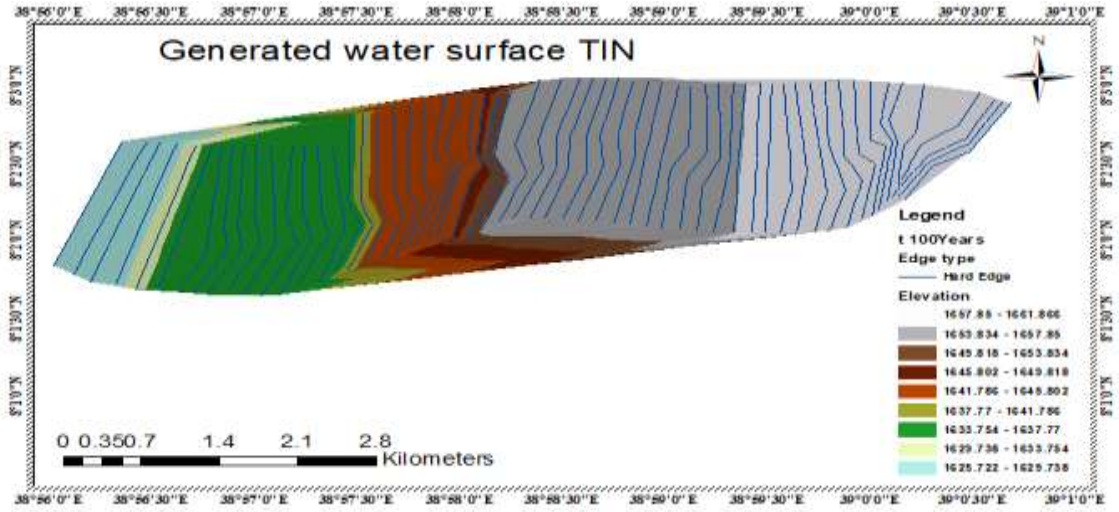

Figure 4-18: Water surface TIN generated for 100-year peak flood.

4.5.2 Flood Inundation Area

Areas inundated by flooding occur wherever the elevation of the floodwater exceeds that of the land. To delineate these areas, we will create surface models of the floodwater and land surface and then compare the two elevations.

The GIS data exported from HEC-RAS in the RASexport.sdf file format was converted to file.xml so that it was easy to process in Arc GIS for the final flood inundation mapping.

After converting the file to Arc GIS compatible using 'Import RAS SDF File' which is one of the HEC-Geo RAS menus, the HEC-Geo RAS layer setup was adjusted and the

RAS data was imported and then flood inundation mapping was generated. The result indicated that a 2 year return period frequency storm inundates 2.86km2 of the proposed flood plain with the minimum and maximum water depth of 0.00085m and 21.64m respectively. Maximum flood coverage resulted for 100 years return period frequency storm and it inundates about 3.01km2 with a minimum and maximum water depth of 0.00024m to 21.79m respectively. Figure 4.18 indicates the flood inundation area of Ketar river flood plain both for 2 years and 100 years return period and APPENDIX_D shown the flood inundation mapping of the sample profiles.

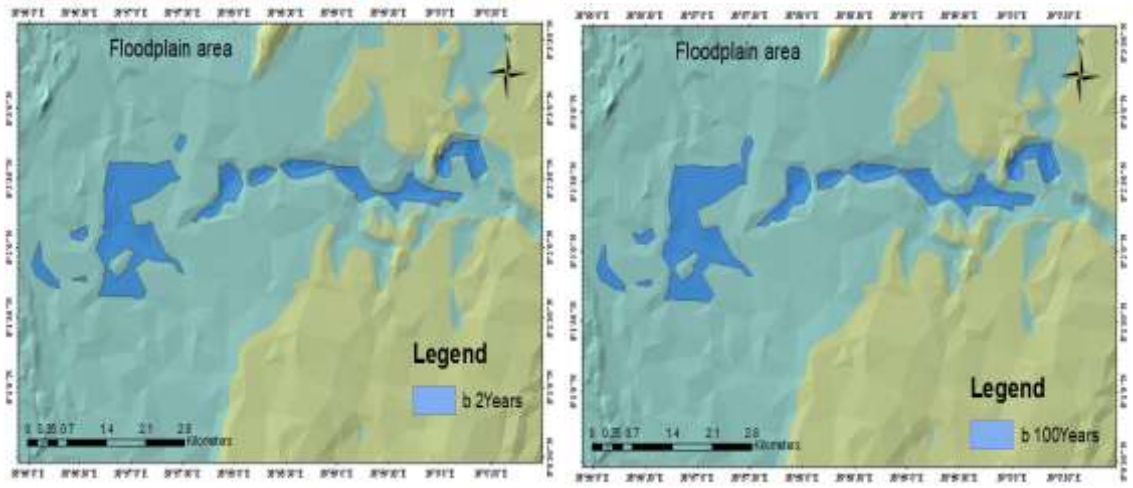

Figure 4-19: Flood inundation area for 2 and 100-year peak flow profile

The inundated area for each return period and the expected peak flood was indicated as in the table below

Table 4-4: Flood inundated area forexpected peak flood

S/No	Return period	24hrs rainfall depth (mm)	Peakflow (m3/s)	Area (km2)
1	2	47.54	198.5	2.86
2	5	59.61	224.1	2.91
3	10	67.66	242.9	2.94
4	25	77.92	251.8	2.95
5	50	85.62	267.5	2.98
6	100	93.35	283.5	3.01

Table 4.4 indicates the flood inundation area of the Ketar river flood plain. According to this table, about 2.86km2 area of the flood plain was to be inundated by 198.5m3/s after 2 years, and about 3.01km2 area of the plain was expected to be covered by 283.5m3/s after 100 years. Therefore, appropriate flood management practice is required to control the future flooding problem of this area and it needs further investigation to identify the most recommended flood protection means that may be structural or non-structural.

4.5.3 Flood Hazard Map

The Flood Hazard map which is reclassified into different hazard levels by considering its floodplain depth of 2 and 100 years return period is as a sample in Figures5.19 and 5.20. For sample peak floods, it is indicated in the APPENDIX-D. The hazard level of water depth from 0-1 m is low level, from 1-2 m is moderate, from 2-3 m is significant and greater than 3 m is very high hazard level.(Niguse and Adhanom, 2019).

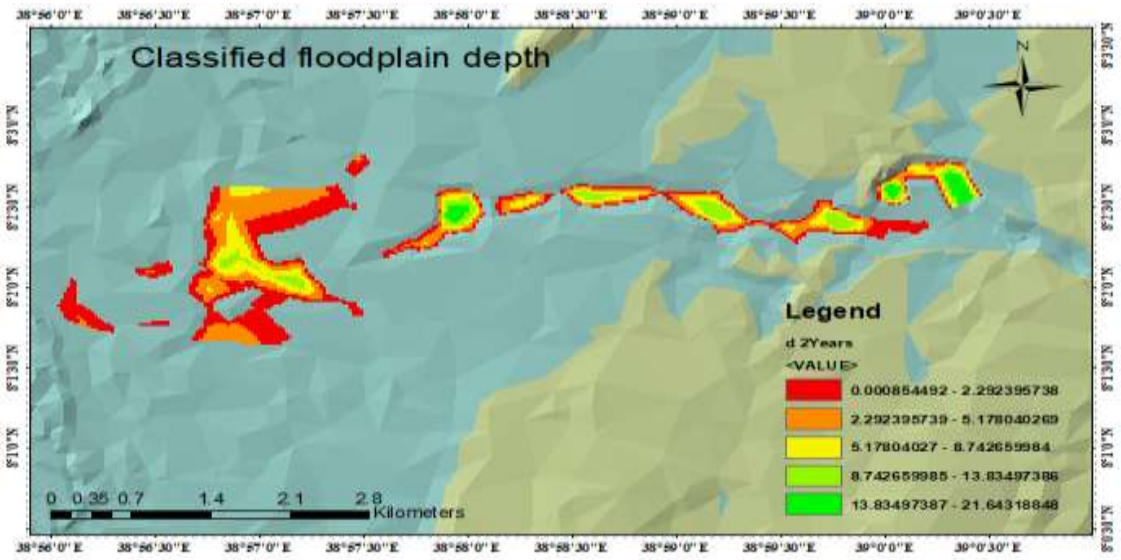

Figure 4-20: Flood hazard map for 2-year peak flood

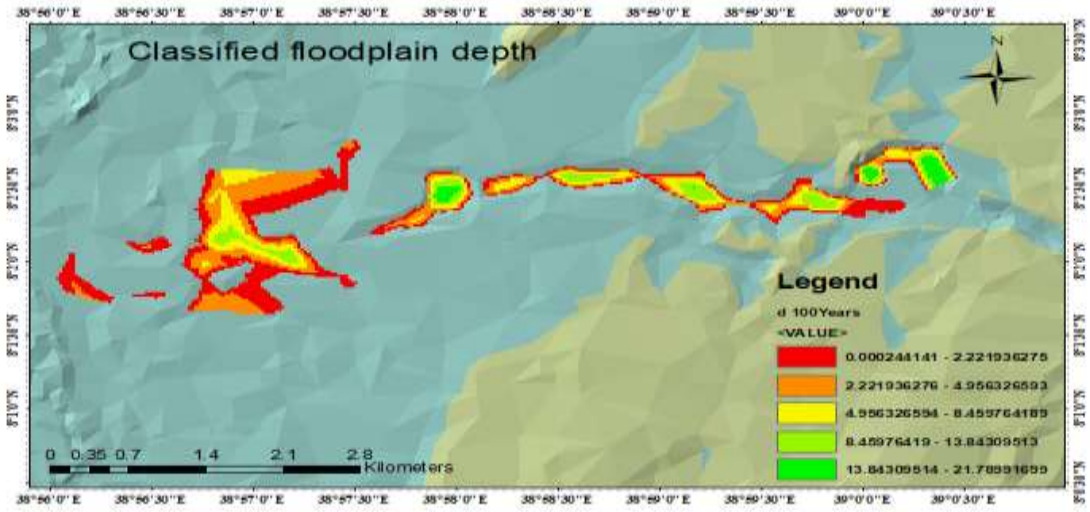

Figure 4-21: Flood hazard map for 100-year peak flood

4.5.4 Flood Vulnerability Map

Vulnerability can be defined as the degree to which people, property, environment, social and economic activities are subjected to harm or being exposed to any destructive factors which indicate the degree of exposure for the hazard problem.

The flood vulnerability is affected by the land use/cover characteristics of the areas under the influence of flood i.e., a flood of the same exceedance probability will have different levels of vulnerability according to the land use characteristics and potential for damage. Therefore, the vulnerability analysis consists of identifying the land use areas(table 3.2) under the potential influence of a flood of a particular return period

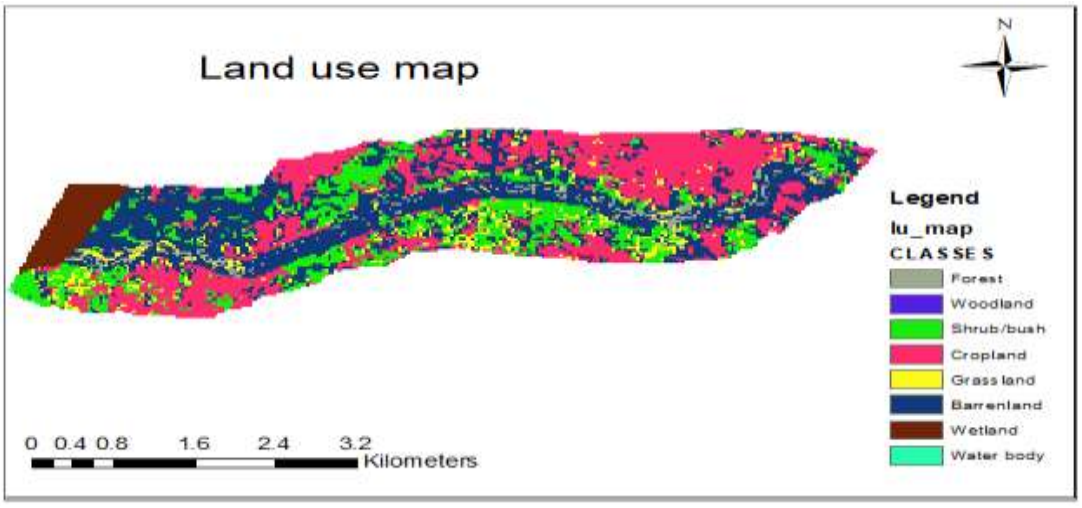

Figure 4-22: Study area land use map

4.5.5 Flood Risk Mapping

The flood risk mapping is the combination of flood hazard map and vulnerability map. Flood hazard map is any flood inundated coverage over the given area which may or may not cause impact; whereas flood risk map is the product of flood hazard map and vulnerability maps. When the inundated area of the flood hazard map has different economic activity (land uses and building points) the flood hazard maps and flood risk maps are the same. This paper justifies this fact which shows that in the study area the land is covered by different farm-land for agricultural activity, building points(houses), roads, forests, etc.as observed from Google earth and site observation.Therefore, the Flood hazard map is the same as the Flood risk map in the case of this study area.

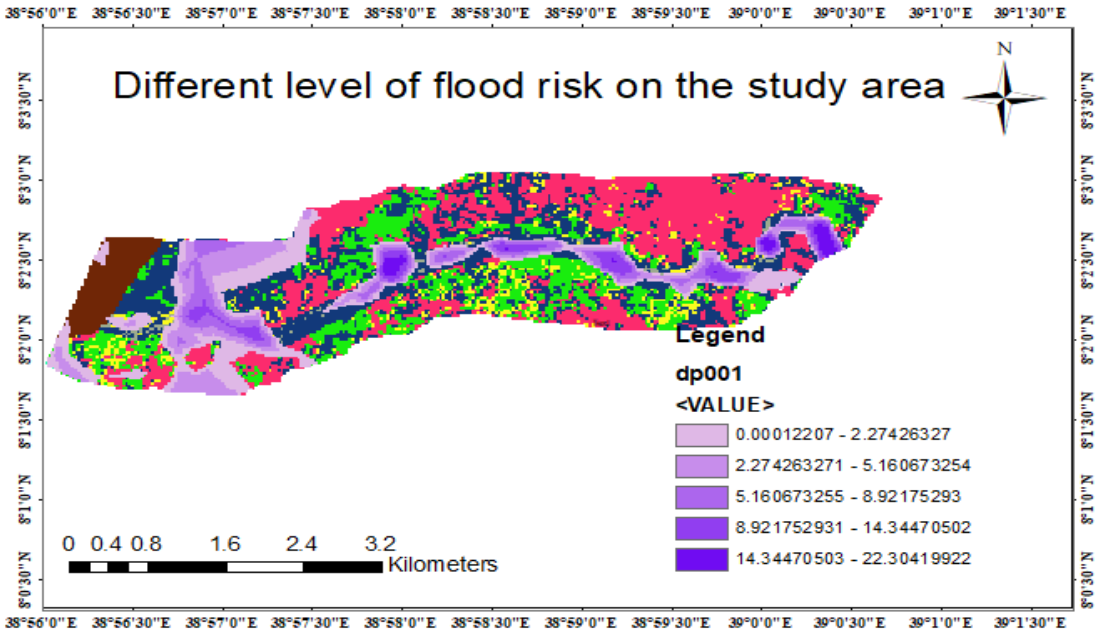

Figure 4-23: Flood risk map for the 100-year peak flood onthe land use map.

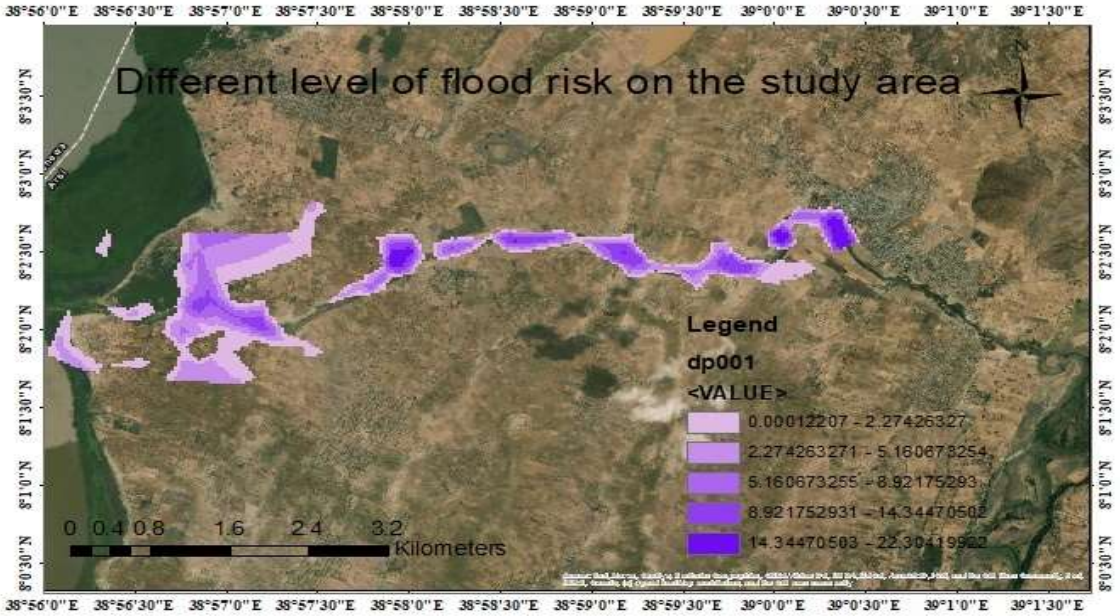

Figure 4-24: Flood risk map for a 100-year peak flood on Google earth image.

CHAPTER 5 CONCLUSIONS AND RECOMMENDATIONS

5.1 Conclusion

Rainfall-runoff modeling is the mathematical representation of hydrological response by the watershed toward the received precipitation considering all the watershed parameters. In this study HEC-HMS,a hydrologic modeling system was used to develop rainfall-runoff modeling for Ketar watershed Oromia regional state, Ethiopia. For this study, five meteorological stations (Assela, Kulumsa, Bekoji, Keter Genet, and Ogelcho) that were found near and in the vicinity were used for meteorological data preparation of the model. All watershed characteristics such as elevation, slope, drainage line network, stream network, flow direction, flow accumulation, sub-basins, and watershed delineation were extracted using an Arc GIS extension called HEC-Geo HMS. The model was processed using the meteorological data and historical flow data collected from different sources as indicated under chapter three. This hydro-meteorological data was classified into two parts; one part for calibration and the second part for model validation. The model performance was evaluated using Nash Sutcliff efficiency and coefficient of determination and the model was well performed for the entered hydro-meteorological data and parameters used. After approving the model performance, peak flood frequency analysis for 2, 5, 10, 25, 50, and 100 years return period was carried out using the 24 hr rainfall depth obtained from IDF curve of the Ethiopian rainfall region adopted from ERA drainage manual for Ketar watershed. Using this peak flood as a profile, a river analysis system was executed using HEC-RAS for 2, 5,10,25,50, and 100 years return period. Triangular irregular network (TIN) was used for river geometry and cross-section extracting. The extracted river geometry together with the flow profile was used in HEC-RAS for computation of water surface elevation and flood inundation areas. Lastly, by using Google earth image and land use map of the study area as a background, the flood hazard map and flood risk map is developed. The obtained final result indicated that most of the Ketar river flood plain of the study area, especially the downstream of Abura gauging station, was under the impact of flood problem and to the minimum about 2.86 km2 under flood inundation that is expected to be faced after 2 years to the maximum of about 3.01 km2 after 100 years.

5.2 Recommendation

The meteorological (Precipitation and streamflow) data used for this study was collected with some missing values. These missing values were filled by using different data filling techniques and these techniques were based on some assumptions. As the assumption was based on personal judgment, there may be some bias in data values which affects the expected outcome. Therefore, it is better if someone uses data with no gap if possible or data with minimum missing value or actual measurement is taken from the study area. HEC-HMS contains different methods for precipitation loss modeling, transformation, flood routing, and base flow computing method. These methods require different input parameters and they produce different outputs. Therefore, it is strongly recommended that one should be reasonable for selecting each method and to choose appropriate parameters. For hydraulic model development, HEC-RAS needs river geometry and river cross-section, manning's roughness coefficient for precise computations of water surface elevation, water depth in the river, velocity of flow, and flood inundation area.For this study, river geometry was extracted from a TIN of the specified flood plain, and manning's roughness coefficient was determined by the cowan method for the main channel and floodplain. Finally, the single calculated manning value was used for all cross-sections. But the river geometry was fluctuating from time to time due to different land use management. Therefore, it is more profitable for someone to conduct a proper and detailed field survey to collect manning value for each cross-section and also carried out some experiments on it to investigate the actual manning's roughness coefficient.Also, limitation of some data like observed water level at the downstream of study area for hydraulic model make a difficulties of model calibration.For accurate extraction of river geometry and flood risk mapping, HEC-GeoRAS requires high precision, digital terrain model. So it is more preferable if someone uses a high precision digital terrain model during hydraulic model development and flood inundation mapping using HEC-GeoRAS. As it was discussed under chapter four of this document, the Ketar river floodplain was under flood problem. On the other hand, as this area is an agricultural area a lot of people were living over there. These people were frequently exposed to flood risk especially, during the summer season every year. Therefore for the safety of these people and their property, the effective non-structural flood mitigation measure such as early flood warning and early evacuation should be adopted

REFERENCES

[1] Damtew Fufa Tufa, Yerramsetty Abbulu, and G.V.R.Srinivasa Rao,2015. HYDROLOGICAL IMPACTS DUE TO LAND-USE AND LAND-COVER CHANGES OF KETAR WATERSHED, LAKE ZIWAY CATCHMENT, ETHIOPIA. International Journal of Civil Engineering and Technology (IJCIET) Volume 6, Issue 10

[2]Pratibha Banstola1*, Bidhan Sapkota2, 2019. Flood Risk Mapping and Analysis Using Hydrodynamic Model HEC-RAS: A Case Study of Daraudi River, Chhepatar, Gorkha, Nepal Grassroots Journal of Natural Resources, Vol. 2 No.3 ISSN:2581-6853.

[3] Zelalem Abera, 2011. Flood Mapping and Modeling on Fogera Flood Plain: A Case Study of Ribb River.

[4] Arghajeet Saha1, D.V.S.Praneeth2, 2016. Flood vulnerability assessment by remote sensing and GIS-based applications in West Bengal: A review. International Research Journal of Engineering and Technology (IRJET) e-ISSN: 2395 -0056 Volume: 03.

[5] Masahiko Haraguchi, and Upmanu Lall, 2013. Flood Risk and impacts future research questions and implications to private investment decision-making for supply chain networks.

[6] Okubay Gidey Adhanom and Amare Gebremedhin Nigusse1*, 2019. Flood hazard and flood risk vulnerability mapping using geo-spatial and MCDA around Adigrat, Tigray Region, Northern Ethiopia Ethiopian Journal of Science (MEJS), V11(1):90-107, ©CNCS, Mekelle University, ISSN:2220-184X Submitted on 30-03-2016 Accepted on 08-11-2018

[7] Getahun and Gebre, 2015. Flood Hazard Assessment and Mapping of Flood Inundation Area of the Awash River Basin in Ethiopia using GIS and HEC-GeoRAS/HEC-RAS Model. Journal of Civil & Environmental Engineering

[8] Yongping Yuan and Kamal Qaiser, 2011. Floodplain Modeling in the Kansas River Basin Using Hydrologic Engineering Center (HEC) Models Impacts of Urbanization and Wetlands for Mitigation. EPA/600/R-11/116

[9] Mohd Talha Anees, Khiruddin Abdullah, Mohd Nawawi Mohd Nordin, Nik Norulaini Nik Ab Rahman, Muhammad Izzuddin Syakir, andMohd. Omar Abdul Kadir, 2017. One- and Two-Dimensional Hydrological Modelling and Their Uncertainties,

[10] Bitew G. Tassew 1,2, Mulugeta A. Belete 1 and K.Miegel, 2019. Application of HEC-HMS Model for Flow Simulation in the Lake Tana Basin: The Case of Gilgel Abay Catchment, Upper Blue Nile Basin.

[11] Asnake Eshetu Gurmu, 2018. Flood Modeling And Mapping Of Lower Omo Gibe River Basin. A Thesis Submitted to The Department of Civil Engineering for the Partial Fulfillment of the Requirements for the Degree of Master of Science in Civil Engineering (Hydraulic Engineering) ADDIS ABABA SCIENCE AND TECHNOLOGY UNIVERSITY.

[12] Brhane Hagos, 2012. Hydraulic Modeling and Flood Mapping Of Fogera Flood Plain: A Case Study of Gumera River. A Thesis Submitted to the School of Graduate Studies of Addis Ababa University in Partial Fulfillment of the Requirements for the Degree of Master of Science in Hydropower Engineering.

[13] Wana Geyisa, 2018. Rainfall-Runoff Modeling Using Hec-Hms For Flood Inundation Mapping; The Case Of Awash Bello Sub Basin, Upper Awash River Basin, Ethiopia,

[14] Davis, CA 95616 USA, 2018. Hydrologic Modeling System HEC-HMS User's Manual Version 4.3 US Army Corps of Engineers Institute for Water Resources Hydrologic Engineering Center

[15]"Mohammad-Taghi Sattari, Ali Rezazadeh-Joudi, and Andrew Kusiak", 2016. Assessment of different methods for the estimation of missing data in precipitation studies. Hydrology Research ·

[16]"Younghyun Cho", 2018. A spatially distributed Clark's unit hydrograph based hybrid hydrologic model (Distributed-Clark) Article *in* Hydrological Sciences Journal/Journal des Sciences Hydrologiques

[17] Daniel Che1; Mandar Nangare2; and Larry W. Mays, F.ASCE3, 2014. Determination of Clark's Unit Hydrograph Parameters for Watersheds. DOI: American Society of Civil Engineers.

[18]" Muluken LE*", 2020. Techniques of Filling Missing Values of Daily and Monthly Rain Fall Data. SF Journal of Environmental and Earth Science Science Forecast Publications LLC., | https://scienceforecastoa.com/ 2020 | Volume 3 | Edition 1 |

[19].Dawit Sisay, 2015. Flood Risk Analysis in Illu Floodplain, Upper Awash River Basin, Ethiopia A Thesis Submitted to the School of Graduate Studies of Addis Ababa University in Partial Fulfillment of the Requirements for the Degree of Master of Science in Hydraulic Engineering.

[20] Arekhi Saleh, Rostamizad Ghobad, and Rostami Noredin, 2011. Evaluation of HEC-HMS methods in surface runoff simulation (Case study: Kan watershed, Iran).

[21] Edsel B. Daniel, Janey V. Camp, Eugene J. Le Boeuf*, Jessica R. Penrod, James P. Dobbins, and Mark D. Abkowitz, 2011. Watershed Modeling and its Applications: A State-of-the-Art Review

[22] Eric Tate, 1999. Floodplain Mapping Using HEC-RAS and Arc View GIS. M.S.E. Graduate Research Assistant and David Maidment, Ph.D. Principal Investigator.

[23] Feldman, 2000. Hydrologic Modeling System HEC-HMS Technical Reference manual

[24]Arash Asadi* And Jahangir Porhemat1, 2013. Calibration, Verification,And Sensitivity Analysis Of The Hec-Hms Hydrologie Model (Study Area: Kabkian Basin And Delibajak Subbasin), Iran**.**

[25**]** Ammar Adhama,c,∗, Jan G. Wesselinga, Rasha Abeda, Michel Riksena, Mohamed Ouessarb, Coen J. Ritsema, 2019. Assessing the impact of climate change on rainwater harvesting in the Oum Zessar watershed in Southeastern Tunisia.

[26] HOSSEIN M.V. SAMANI and G.A. SHAMSIPOUR, 2004. Hydrologic flood routing in branched river systems via nonlinear optimization. Journal of Hydraulic Research Vol. 42, No. 1, pp. 55–59

[27] Md. Motaleb Hossain, 2014. Analysis of Flood Routing. Department of Mathematics, Dhaka University, Dhaka 1000, Bangladesh.

[28] Francisco Olivera and David Maidment, 1999. Geographic information systems (GIS)-based spatially distributed model for runoff routing. WATER RESOURCES RESEARCH, VOL. 35, NO. 4, PAGES 1155–1164.

[29] Gary W. Brunner, CEIWR-HEC, 2016. HEC-RAS River Analysis System User's Manual Version 5.0.

[30] Cameron T. Ackerman, P.E, 2009. HEC-GeoRAS GIS Tools for support of HEC-RAS using Arc GIS User's Manual.

[31] Yitea Seneshaw Getahun and Sintayehu Legesse Gebre, 2015. Flood Hazard Assessment and Mapping of Flood Inundation Area of the Awash River Basin in Ethiopia using GIS and HEC-GeoRAS/HEC-RAS Model.

[32] Joseph OLALEKAN Olusina, 2013. Modeling Hydrological Functions using Digital Elevation Model (DEM) and Soil Conservation Service (SCS) Model Article ·

[33]. Mohammad Taghi Sattari and Ali Rezazadeh Joudi, 2016. Assessment of different methods for the estimation of missing data in precipitation studies Articlein Hydrology Research ·

[34].El Hadj MOKHTARI1) ABCDE, Boualem REMINI2) DE , Saad Abdelamir HAMOUDI1) DF,2016. Modeling of the rain–flow by hydrological modeling software system HEC-HMS – watershed's case of wadi Cheliff-Ghrib, Algeria. No. 30 (VII-IX): 87–100 © Institute of Technology and Life Sciences, PL ISSN 1429–7426.

[35]. F. Saleh a,b,⇑ , A. Ducharne a, N. Flipo b, L. Oudin a, E. Ledoux, 2013. Impact of river bed morphology on discharge and water levels simulated by a 1D Saint–Venant hydraulic model at a regional scale.Journal of HydrologyVolume 476, Pages 169-177

[36].'ERCS',2010. Ethiopia: Floods final report emergency appeal no. March 2010. Period covered by this Final Report: 18 August 2006 to 30 September 2007;

[37]. Nurlan Ongdas, Farida Akiyanova *, Yergali Karakulov, Altynay Muratbayeva, and Nurlybek Zinabdin, 2020. Application of HEC-RAS (2D) for Flood Hazard Maps Generation for Yesil (Ishim) River in Kazakhstan.

[38] Chala Hailu Sime[1] · Tamene Adugna Demissie[1] · Fayera Gudu Tufa[1],2020. Surface Runoff Modeling In Ketar Watershed, Ethiopia.Hydraulic And Water Resources Engineering Department, Civil And Environmental Engineering Faculty, Jimma Institute Of Technology, Jimma University, Jimma, Ethiopia.

[39] Sina Alaghmand*, Rozi bin Abdullah and Ismail Abustan, 2012. Comparison between capabilities of HEC-RAS and MIKE11 hydraulic models in river flood risk modeling (a case study of Sungai Kayu Ara River basin, Malaysia Int. J. Hydrology Science and Technology, Vol. 2, No. 3

[40] Eliyas, 2018. Floodplain Mapping And Modeling For Geray River, Addis Ababa Science And Technology University.

[41] "Lusajo H Mfwango*, Catherine J Salim and Shija Kazumba", 2018. Estimation of Missing River Flow Data for Hydrologic Analysis: The Case of Great Ruaha River Catchment.

[42] David Ford, Nathan Pingel, J. J. DeVries, 2008. Updated by HEC. Hydrologic Modeling System HEC-HMS Applications Guide.

[43] Matthew J. Fleming, James H. Doan, 2009. HEC-GeoHMS Geospatial Hydrologic Modeling Extension version 4.2.

[44]. Ethiopian Red Cross Society (ERCS). 2012. Disaster Preparedness, Unit Major Activities between 2007-2010 and Pan of 2011-2015. The report, Addis Ababa, Ethiopia.

[45''Revised Flood Alert'', 2018. Federal Democratic Republic of Ethiopia National Disaster Risk Management Commission, Early Warning, and Emergency Response Directorate Revised Flood Alert. Flood incident in Hargelle woreda (Afder zone).

[46] Special Report'', East Africa 2020 flood impacts on agriculture Updated May 19th, 2020. SPECIAL REPORT.19"Ethiopia: Floods - Apr 2020." ReliefWeb, May 6, 2020.

[47] M.Fleming and T.Brauer,August 2016. Hydrologic modeling system HEC-HMS Quickstart Guide.

[48] Elizabeth M. shaw, 1988. Hydrology in practice. Third edition

[49] U.SArmy Corps of Engineers, August 2016. Hydrologic modeling system HEC-HMS Validation Guide version 4.2

[50] Zaid Wolde Gebriel Director General, 2013. Drainage Design Manual-2013. Ethiopia Roads Authority Addis Ababa, 2013

[51]''ERCS'',2010. Ethiopia: Floods Final report Emergency appeal no. MDRET003 GLIDE no. FL-2006-000112-ETH 4 March 2010. Period covered by this Final Report: 18 August 2006 to 30 September 2007

APPENDIX

APPENDIX-A Double mass curve of stations of Ketar watershed

TableA1: Mean annual precipitations for each Stations

Year	Assela	Kulumsa	Keter Genet	Ogelcho	Bekoji
1988	2.480874	2.389071	2.484699	4.063661	3.191865
1989	3.185205	2.510411	2.184932	2.657808	2.953425
1990	2.651233	2.69589	2.493425	2.573699	2.908278
1991	2.147945	2.181644	2.17863	1.930685	2.866025
1992	2.693773	2.211749	2.032514	2.021311	3.152459
1993	2.895342	2.549589	1.933151	2.544384	3.249863
1994	3.015714	1.991781	1.832329	1.614247	2.880548
1995	2.959726	2.375068	1.928219	2.000219	2.824384
1996	3.391803	2.396175	1.99153	2.229508	2.947379
1997	3.16411	2.497534	1.808767	2.047123	2.804857
1998	3.129041	2.39589	2.444414	2.258904	2.838037
1999	2.348493	2.045479	2.023453	1.718868	2.523969
2000	2.901093	2.178962	2.549454	1.966393	3.301612
2001	3.941918	2.572329	2.16	1.927945	3.736871
2002	2.135616	1.940822	1.495616	1.598082	2.568474
2003	2.68137	2.078356	1.672603	2.124658	2.996197

Table A2: Cumulative mean annual precipitation for each station

Year	Assela	Kulumsa	Keter Genet	Ogelcho	Bekoji
2003	2.68137	2.078356	1.672603	2.124658	2.996197
2002	4.816986	4.019178	3.168219	3.72274	5.564671
2001	8.758904	6.591507	5.328219	5.650685	9.301542
2000	11.66	8.770469	7.877673	7.617078	12.60315
1999	14.00849	10.81595	9.901126	9.335946	15.12712
1998	17.13753	13.21184	12.34554	11.59485	17.96516
1997	20.30164	15.70937	14.15431	13.64197	20.77002
1996	23.69344	18.10555	16.14584	15.87148	23.7174
1995	26.65317	20.48062	18.07406	17.8717	26.54178
1994	29.66888	22.4724	19.90638	19.48595	29.42233
1993	32.56423	25.02199	21.83954	22.03033	32.67219
1992	35.258	27.23373	23.87205	24.05164	35.82465
1991	37.40594	29.41538	26.05068	25.98233	38.69067
1990	40.05718	32.11127	28.5441	28.55603	41.59895
1989	43.24238	34.62168	30.72904	31.21383	44.55238
1988	45.72326	37.01075	33.21373	35.2775	47.74424

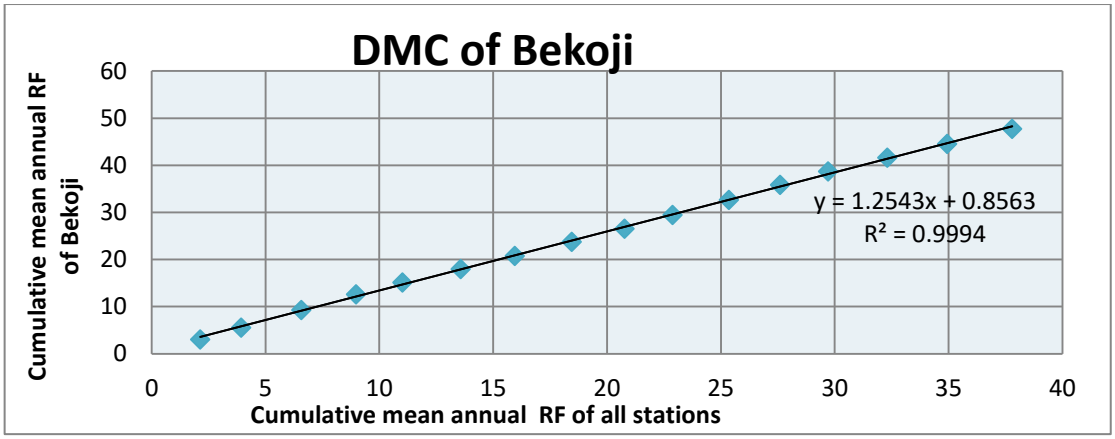

Figure A3: DMC for Bekoji

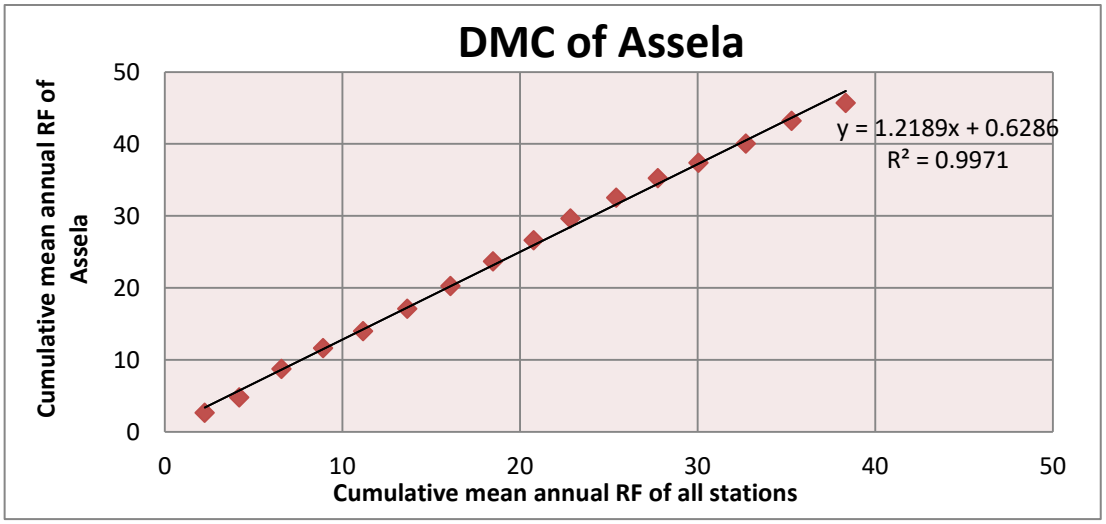

Figure A4: DMC for Assela

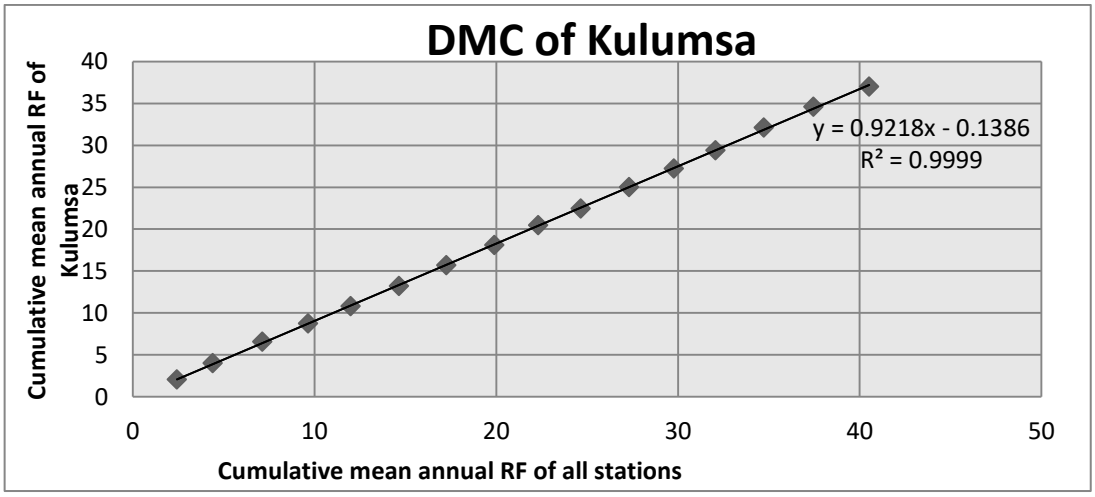

Figure A5: DMC for Kulumsa

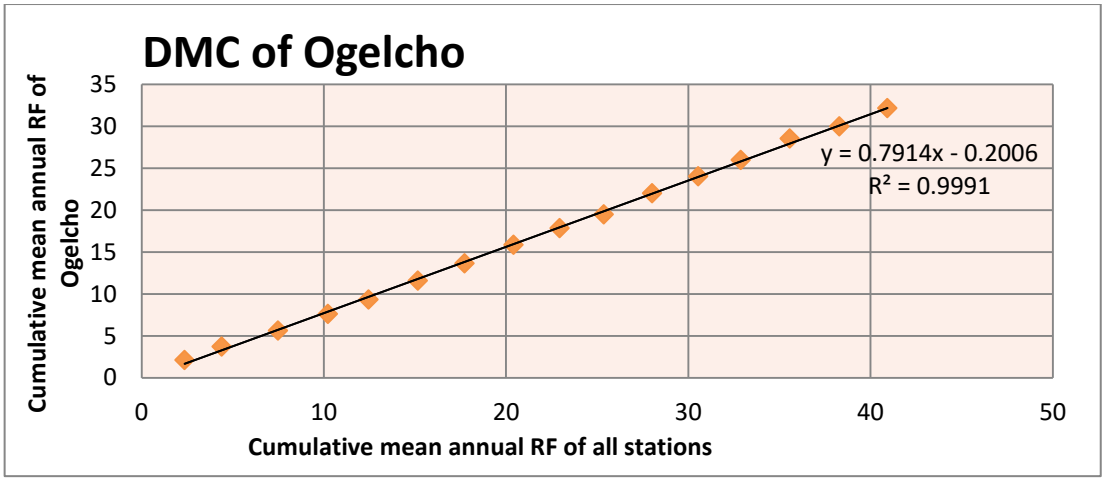

Figure A6: DMC for Ogelcho

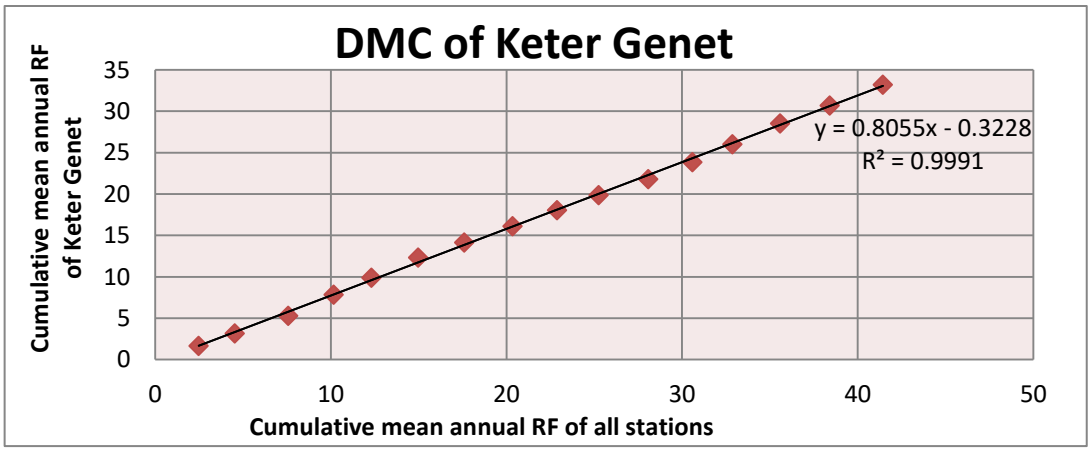

Figure A7: DMC for Keter Genet

APPENDIX-B HEC-HMS Output flow hydrograph

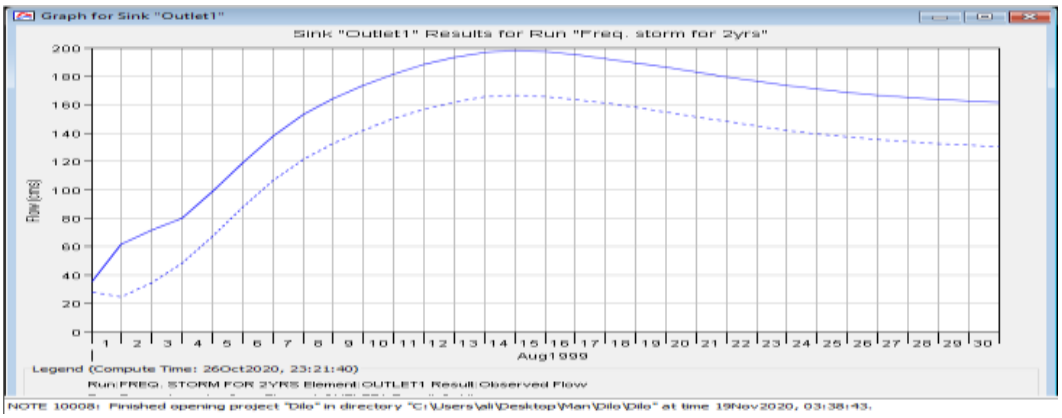

Figure B1: 2-year storm flow hydrograph

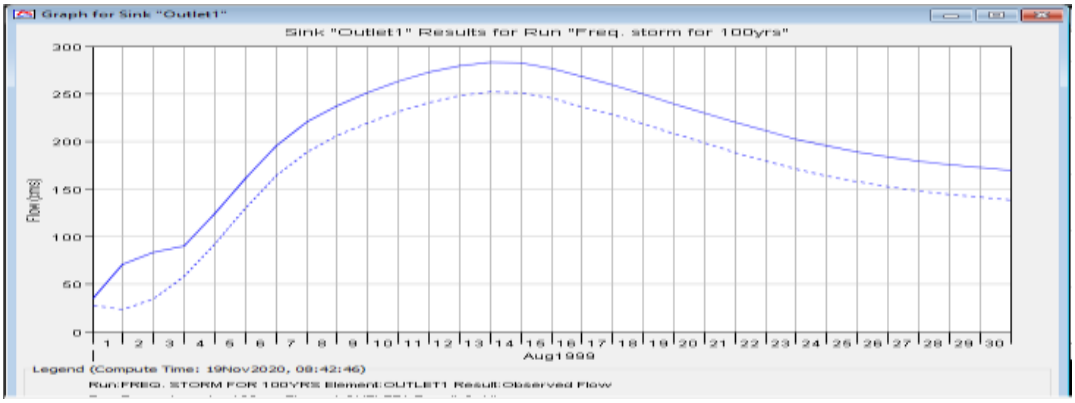

Figure B2: 100-year storm flow hydrograph

APPENDIX-C HEC-RAS Output

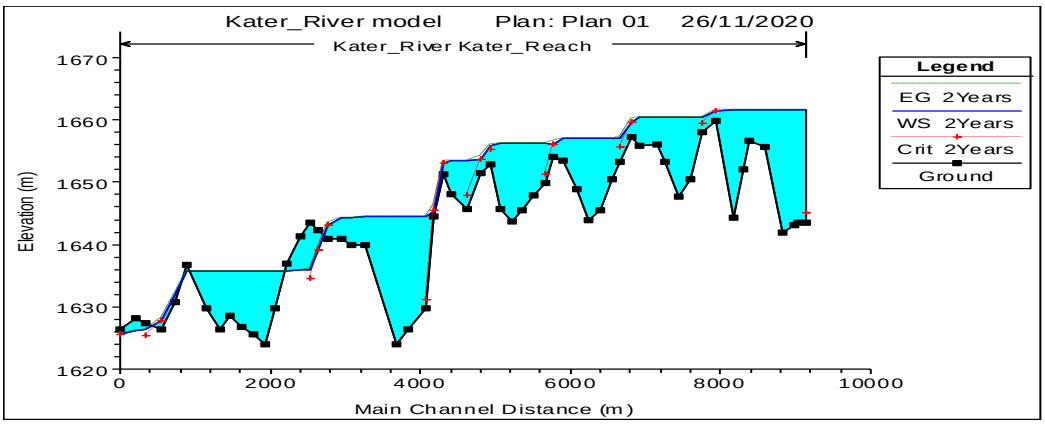

Figure C1 Water surface profile for 2-year peak flood

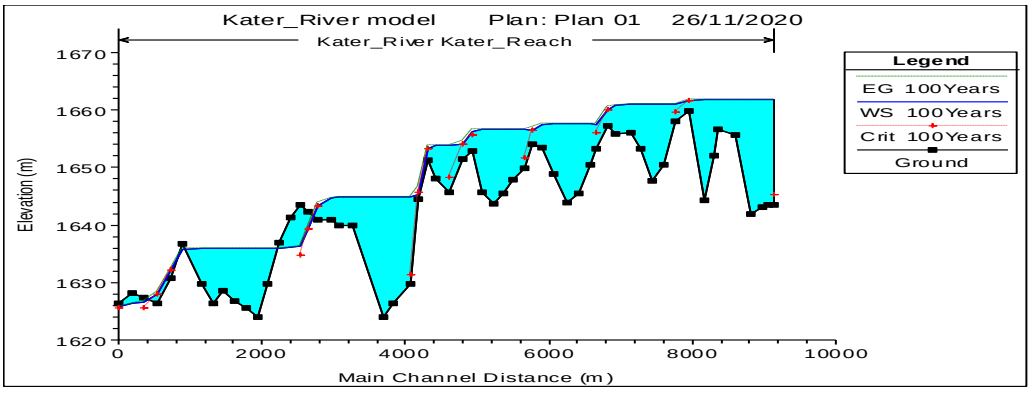

Figure C2: Water surface profile for100-year peak flood

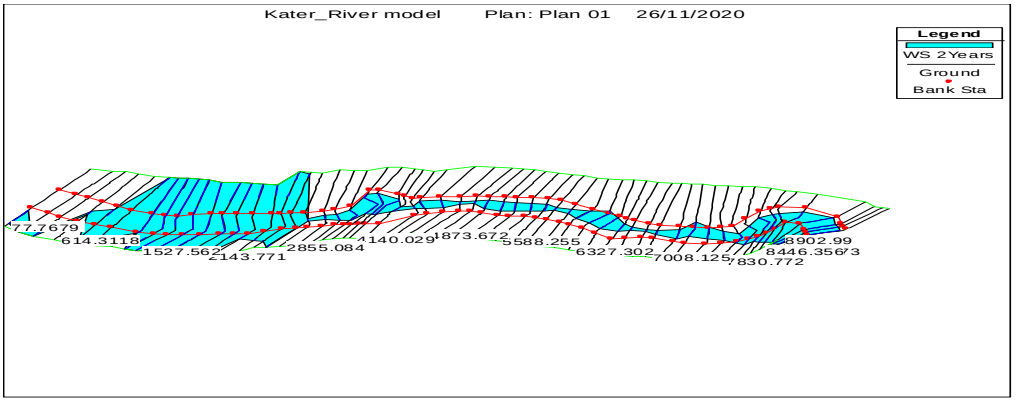

Figure C3: 3D View the 2-year peak flood

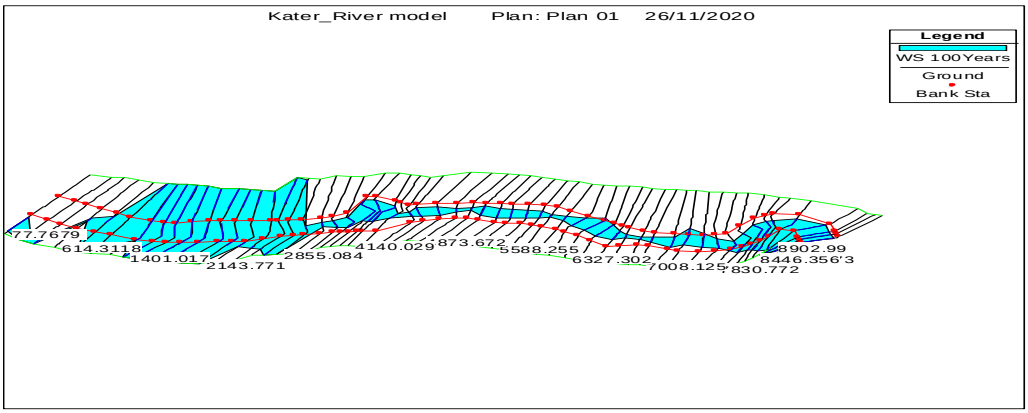

Figure C4: 3D View of the 100-year peak flood

Table C1: Summary output tables by different flow profile

Reach	River Sta	Profile	Q Total	Min Ch El	W.S. Elev	Crit W.S.	E.G. Elev	E.G. Slope	Vel Chnl	Flow Area	Top Width	Froude # Chl
			(m3/s)	(m)	(m)	(m)	(m)	(m/m)	(m/s)	(m2)	(m)	
Kater_Reach	9204.5	2Years	198.5	1643.5	1661.69	1645	1662	0	0.06	3424.9	311.02	0.01
Kater_Reach	9204.5	5Years	224.1	1643.5	1661.74	1645	1662	0	0.07	3442.4	311.65	0.01
Kater_Reach	9204.5	10Years	242.9	1643.5	1661.78	1645	1662	0	0.07	3455	312.1	0.01
Kater_Reach	9204.5	25Years	251.8	1643.5	1661.8	1645	1662	1E-06	0.07	3460.8	312.31	0.01
Kater_Reach	9204.5	50Years	267.5	1643.5	1661.83	1645	1662	1E-06	0.08	3470.9	312.68	0.01
Kater_Reach	9204.5	100Years	283.5	1643.5	1661.87	1645	1662	1E-06	0.08	3481	313.04	0.01
Kater_Reach	9121.9	2Years	198.5	1643.51	1661.69		1662	0	0.05	3730.7	400.6	0
Kater_Reach	9121.9	5Years	224.1	1643.51	1661.74		1662	0	0.06	3753.3	406.05	0.01
Kater_Reach	9121.9	10Years	242.9	1643.51	1661.78		1662	0	0.07	3769.8	409.98	0.01
Kater_Reach	9121.9	25Years	251.8	1643.51	1661.8		1662	0	0.07	3777.3	411.76	0.01
Kater_Reach	9121.9	50Years	267.5	1643.51	1661.83		1662	0	0.07	3790.8	414.92	0.01
Kater_Reach	9121.9	100Years	283.5	1643.51	1661.87		1662	1E-06	0.08	3804.2	418.04	0.01
Kater_Reach	9061.6	2Years	198.5	1643.08	1661.69		1662	0	0.05	3751.5	457.63	0

Kater_Reach	9061.6	5Years	224.1	1643.08	1661.74		1662	0	0.06	3777.5	468.03	0.01
Kater_Reach	9061.6	10Years	242.9	1643.08	1661.78		1662	0	0.06	3796.6	475.53	0.01
Kater_Reach	9061.6	25Years	251.8	1643.08	1661.8		1662	0	0.07	3805.3	478.93	0.01
Kater_Reach	9061.6	50Years	267.5	1643.08	1661.83		1662	0	0.07	3821	484.97	0.01
Kater_Reach	9061.6	100Years	283.5	1643.08	1661.87		1662	0	0.08	3836.7	490.93	0.01
Kater_Reach	8903	2Years	198.5	1642	1661.69		1662	0	0.06	3601	316.78	0.01
Kater_Reach	8903	5Years	224.1	1642	1661.74		1662	0	0.06	3618.9	321.22	0.01
Kater_Reach	8903	10Years	242.9	1642	1661.78		1662	0	0.07	3632	324.41	0.01
Kater_Reach	8903	25Years	251.8	1642	1661.8		1662	0	0.07	3638	325.87	0.01
Kater_Reach	8903	50Years	267.5	1642	1661.83		1662	1E-06	0.07	3648.6	328.44	0.01
Kater_Reach	8903	100Years	283.5	1642	1661.87		1662	1E-06	0.08	3659.2	330.98	0.01
Kater_Reach	8676.3	2Years	198.5	1655.65	1661.68		1662	4E-05	0.28	729.24	271.39	0.05
Kater_Reach	8676.3	5Years	224.1	1655.65	1661.74		1662	5E-05	0.31	744.32	276.38	0.05
Kater_Reach	8676.3	10Years	242.9	1655.65	1661.78		1662	5E-05	0.33	755.33	279.96	0.06
Kater_Reach	8676.3	25Years	251.8	1655.65	1661.8		1662	5E-05	0.34	760.43	281.61	0.06
Kater_Reach	8676.3	50Years	267.5	1655.65	1661.83		1662	6E-05	0.36	769.4	284.48	0.06
Kater_Reach	8676.3	100Years	283.5	1655.65	1661.86		1662	7E-05	0.38	778.34	287.31	0.06
Kater_Reach	8446.4	2Years	198.5	1656.64	1661.65		1662	3E-04	0.56	383.75	272.2	0.12
Kater_Reach	8446.4	5Years	224.1	1656.64	1661.7		1662	3E-04	0.61	397.26	282.83	0.13
Kater_Reach	8446.4	10Years	242.9	1656.64	1661.74		1662	4E-04	0.65	407.29	290.47	0.14
Kater_Reach	8446.4	25Years	251.8	1656.64	1661.75		1662	4E-04	0.67	411.9	293.92	0.14
Kater_Reach	8446.4	50Years	267.5	1656.64	1661.78		1662	4E-04	0.7	420.07	299.93	0.15
Kater_Reach	8446.4	100Years	283.5	1656.64	1661.81		1662	4E-04	0.73	428.28	305.85	0.16
Kater_Reach	8383.5	2Years	198.5	1652.06	1661.66		1662	7E-06	0.14	1432.5	430.43	0.02
Kater_Reach	8383.5	5Years	224.1	1652.06	1661.71		1662	8E-06	0.16	1454.4	440.82	0.02
Kater_Reach	8383.5	10Years	242.9	1652.06	1661.75		1662	1E-05	0.17	1470.5	448.32	0.03
Kater_Reach	8383.5	25Years	251.8	1652.06	1661.76		1662	1E-05	0.18	1478	451.76	0.03
Kater_Reach	8383.5	50Years	267.5	1652.06	1661.79		1662	1E-05	0.19	1490.9	457.63	0.03
Kater_Reach	8383.5	100Years	283.5	1652.06	1661.82		1662	1E-05	0.19	1504	463.47	0.03
Kater_Reach	8240	2Years	198.5	1644.25	1661.66		1662	0	0.05	4070.3	446.72	0
Kater_Reach	8240	5Years	224.1	1644.25	1661.71		1662	0	0.06	4093.1	456.01	0.01
Kater_Reach	8240	10Years	242.9	1644.25	1661.75		1662	0	0.06	4109.9	462.72	0.01
Kater_Reach	8240	25Years	251.8	1644.25	1661.76		1662	0	0.06	4117.5	465.76	0.01
Kater_Reach	8240	50Years	267.5	1644.25	1661.79		1662	0	0.07	4131	471.05	0.01
Kater_Reach	8240	100Years	283.5	1644.25	1661.82		1662	0	0.07	4144.3	476.22	0.01
Kater_Reach	8022.1	2Years	198.5	1659.85	1661.44	1661	1662	0.029	2.21	106.58	250.42	0.98
Kater_Reach	8022.1	5Years	224.1	1659.85	1661.48	1661	1662	0.029	2.28	115.43	253.48	0.99
Kater_Reach	8022.1	10Years	242.9	1659.85	1661.5	1662	1662	0.03	2.37	119.97	255.04	1.02
Kater_Reach	8022.1	25Years	251.8	1659.85	1661.51	1662	1662	0.031	2.39	122.82	256.01	1.02

Kater_Reach	8022.1	50Years	267.5	1659.85	1661.53	1662	1662	0.031	2.43	127.71	257.67	1.03
Kater_Reach	8022.1	100Years	283.5	1659.85	1661.55	1662	1662	0.031	2.46	132.79	259.39	1.03
Kater_Reach	7830.8	2Years	198.5	1657.96	1660.46	1659	1661	0.001	0.88	238.06	223.01	0.25
Kater_Reach	7830.8	5Years	224.1	1657.96	1660.62	1660	1661	0.001	0.86	275.71	228.3	0.23
Kater_Reach	7830.8	10Years	242.9	1657.96	1660.74	1660	1661	0.001	0.85	301.87	231.91	0.22
Kater_Reach	7830.8	25Years	251.8	1657.96	1660.79	1660	1661	0.001	0.85	314.17	233.59	0.22
Kater_Reach	7830.8	50Years	267.5	1657.96	1660.88	1660	1661	9E-04	0.85	335.51	236.47	0.21
Kater_Reach	7830.8	100Years	283.5	1657.96	1660.97	1660	1661	9E-04	0.84	356.22	239.23	0.21
Kater_Reach	7667	2Years	198.5	1650.52	1660.48		1660	6E-06	0.16	1253.4	213.03	0.02
Kater_Reach	7667	5Years	224.1	1650.52	1660.64		1661	7E-06	0.17	1288.7	216	0.02
Kater_Reach	7667	10Years	242.9	1650.52	1660.76		1661	8E-06	0.18	1313.2	218.04	0.02
Kater_Reach	7667	25Years	251.8	1650.52	1660.81		1661	8E-06	0.19	1324.6	218.98	0.02
Kater_Reach	7667	50Years	267.5	1650.52	1660.9		1661	9E-06	0.2	1344.4	220.6	0.03
Kater_Reach	7667	100Years	283.5	1650.52	1660.99		1661	9E-06	0.21	1363.6	222.17	0.03
Kater_Reach	7520.1	2Years	198.5	1647.72	1660.48		1660	1E-06	0.08	2508.2	286.27	0.01
Kater_Reach	7520.1	5Years	224.1	1647.72	1660.65		1661	1E-06	0.09	2555.5	288.1	0.01
Kater_Reach	7520.1	10Years	242.9	1647.72	1660.76		1661	1E-06	0.1	2588.1	289.35	0.01
Kater_Reach	7520.1	25Years	251.8	1647.72	1660.81		1661	1E-06	0.1	2603.3	289.93	0.01
Kater_Reach	7520.1	50Years	267.5	1647.72	1660.9		1661	1E-06	0.1	2629.5	294.64	0.01
Kater_Reach	7520.1	100Years	283.5	1647.72	1660.99		1661	1E-06	0.11	2655.4	302.1	0.01
Kater_Reach	7349.2	2Years	198.5	1653.23	1660.48		1660	6E-06	0.15	1469	364.71	0.02
Kater_Reach	7349.2	5Years	224.1	1653.23	1660.64		1661	7E-06	0.16	1529.4	369.59	0.02
Kater_Reach	7349.2	10Years	242.9	1653.23	1660.76		1661	8E-06	0.17	1571.3	372.94	0.02
Kater_Reach	7349.2	25Years	251.8	1653.23	1660.81		1661	8E-06	0.18	1590.8	374.49	0.02
Kater_Reach	7349.2	50Years	267.5	1653.23	1660.9		1661	8E-06	0.18	1624.5	377.15	0.02
Kater_Reach	7349.2	100Years	283.5	1653.23	1660.98		1661	9E-06	0.19	1657.3	379.72	0.03
Kater_Reach	7223.6	2Years	198.5	1655.99	1660.47		1660	2E-04	0.45	438.61	208.9	0.1
Kater_Reach	7223.6	5Years	224.1	1655.99	1660.63		1661	2E-04	0.47	473.57	219.26	0.1
Kater_Reach	7223.6	10Years	242.9	1655.99	1660.74		1661	2E-04	0.49	498.54	226.37	0.1
Kater_Reach	7223.6	25Years	251.8	1655.99	1660.79		1661	2E-04	0.49	510.38	229.67	0.11
Kater_Reach	7223.6	50Years	267.5	1655.99	1660.88		1661	2E-04	0.5	531.07	235.32	0.11
Kater_Reach	7223.6	100Years	283.5	1655.99	1660.97		1661	2E-04	0.51	551.55	240.78	0.11
Kater_Reach	7008.1	2Years	198.5	1655.82	1660.38		1660	5E-04	0.76	260.09	113.97	0.16
Kater_Reach	7008.1	5Years	224.1	1655.82	1660.54		1661	5E-04	0.81	278.33	117.9	0.17
Kater_Reach	7008.1	10Years	242.9	1655.82	1660.65		1661	5E-04	0.83	291.18	120.59	0.17
Kater_Reach	7008.1	25Years	251.8	1655.82	1660.7		1661	5E-04	0.85	297.24	121.84	0.17
Kater_Reach	7008.1	50Years	267.5	1655.82	1660.79		1661	6E-04	0.87	307.79	123.98	0.18
Kater_Reach	7008.1	100Years	283.5	1655.82	1660.87		1661	6E-04	0.89	318.16	126.05	0.18

Kater_Reach	6894.4	2Years	198.5	1657.19	1659.59	1660	1660	0.023	3.45	57.62	48.11	1.01
Kater_Reach	6894.4	5Years	224.1	1657.19	1659.71	1660	1660	0.023	3.52	63.58	50.54	1
Kater_Reach	6894.4	10Years	242.9	1657.19	1659.79	1660	1660	0.022	3.57	67.99	52.26	1
Kater_Reach	6894.4	25Years	251.8	1657.19	1659.83	1660	1660	0.022	3.61	69.83	52.97	1
Kater_Reach	6894.4	50Years	267.5	1657.19	1659.88	1660	1661	0.022	3.67	72.87	54.11	1.01
Kater_Reach	6894.4	100Years	283.5	1657.19	1659.95	1660	1661	0.022	3.71	76.49	55.44	1.01
Kater_Reach	6737.6	2Years	198.5	1653.26	1657.09	1656	1657	0.002	1.35	147.57	78.51	0.31
Kater_Reach	6737.6	5Years	224.1	1653.26	1657.23	1656	1657	0.002	1.41	159.3	81.73	0.32
Kater_Reach	6737.6	10Years	242.9	1653.26	1657.34	1656	1657	0.002	1.45	167.66	83.96	0.33
Kater_Reach	6737.6	25Years	251.8	1653.26	1657.38	1656	1657	0.002	1.47	171.4	84.93	0.33
Kater_Reach	6737.6	50Years	267.5	1653.26	1657.46	1656	1658	0.002	1.5	178.1	86.65	0.33
Kater_Reach	6737.6	100Years	283.5	1653.26	1657.53	1656	1658	0.002	1.53	184.78	88.33	0.34
Kater_Reach	6642.4	2Years	198.5	1650.49	1657.14		1657	3E-05	0.27	723.84	197.23	0.05
Kater_Reach	6642.4	5Years	224.1	1650.49	1657.29		1657	4E-05	0.3	753.88	201.26	0.05
Kater_Reach	6642.4	10Years	242.9	1650.49	1657.39		1657	4E-05	0.31	774.93	204.03	0.05
Kater_Reach	6642.4	25Years	251.8	1650.49	1657.44		1657	4E-05	0.32	784.28	205.25	0.05
Kater_Reach	6642.4	50Years	267.5	1650.49	1657.52		1658	5E-05	0.33	800.9	207.4	0.05
Kater_Reach	6642.4	100Years	283.5	1650.49	1657.6		1658	5E-05	0.35	817.34	209.51	0.06
Kater_Reach	6482	2Years	198.5	1645.42	1657.14		1657	1E-06	0.09	2302.1	309.96	0.01
Kater_Reach	6482	5Years	224.1	1645.42	1657.29		1657	2E-06	0.1	2349.1	312.81	0.01
Kater_Reach	6482	10Years	242.9	1645.42	1657.4		1657	2E-06	0.1	2381.8	314.77	0.01
Kater_Reach	6482	25Years	251.8	1645.42	1657.44		1657	2E-06	0.11	2396.2	315.64	0.01
Kater_Reach	6482	50Years	267.5	1645.42	1657.52		1658	2E-06	0.11	2421.8	317.16	0.01
Kater_Reach	6482	100Years	283.5	1645.42	1657.6		1658	2E-06	0.12	2446.9	318.65	0.01
Kater_Reach	6327.3	2Years	198.5	1643.94	1657.14		1657	1E-06	0.08	2596.9	358.21	0.01
Kater_Reach	6327.3	5Years	224.1	1643.94	1657.29		1657	1E-06	0.09	2651.3	362.65	0.01
Kater_Reach	6327.3	10Years	242.9	1643.94	1657.4		1657	1E-06	0.09	2689.2	365.71	0.01
Kater_Reach	6327.3	25Years	251.8	1643.94	1657.44		1657	1E-06	0.09	2705.9	367.05	0.01
Kater_Reach	6327.3	50Years	267.5	1643.94	1657.52		1658	1E-06	0.1	2735.7	369.42	0.01
Kater_Reach	6327.3	100Years	283.5	1643.94	1657.6		1658	2E-06	0.1	2765	371.74	0.01
Kater_Reach	6153.1	2Years	198.5	1648.96	1657.14		1657	2E-05	0.21	941.72	226.46	0.03
Kater_Reach	6153.1	5Years	224.1	1648.96	1657.29		1657	2E-05	0.23	976	229.17	0.04
Kater_Reach	6153.1	10Years	242.9	1648.96	1657.39		1657	2E-05	0.24	999.9	231.05	0.04
Kater_Reach	6153.1	25Years	251.8	1648.96	1657.44		1657	2E-05	0.25	1010.4	231.86	0.04
Kater_Reach	6153.1	50Years	267.5	1648.96	1657.52		1658	2E-05	0.26	1029.1	233.31	0.04
Kater_Reach	6153.1	100Years	283.5	1648.96	1657.6		1658	3E-05	0.27	1047.6	234.73	0.04
Kater_Reach	5989.1	2Years	198.5	1653.37	1657.07		1657	0.001	1.09	181.82	98.31	0.26
Kater_Reach	5989.1	5Years	224.1	1653.37	1657.21		1657	0.001	1.14	196.19	102.07	0.26
Kater_Reach	5989.1	10Years	242.9	1653.37	1657.31		1657	0.001	1.18	206.39	104.66	0.27

Kater_Reach	5989.1	25Years	251.8	1653.37	1657.35		1657	0.001	1.19	210.92	105.79	0.27
Kater_Reach	5989.1	50Years	267.5	1653.37	1657.43		1658	0.001	1.22	219.07	107.79	0.27
Kater_Reach	5989.1	100Years	283.5	1653.37	1657.5		1658	0.001	1.25	227.18	109.74	0.28
Kater_Reach	5838.2	2Years	198.5	1654.09	1656.04	1656	1657	0.024	3.22	61.72	58.6	1
Kater_Reach	5838.2	5Years	224.1	1654.09	1656.14	1656	1657	0.024	3.31	67.79	61.39	1
Kater_Reach	5838.2	10Years	242.9	1654.09	1656.21	1656	1657	0.023	3.37	72.07	63.29	1.01
Kater_Reach	5838.2	25Years	251.8	1654.09	1656.25	1656	1657	0.023	3.37	74.63	64.39	1
Kater_Reach	5838.2	50Years	267.5	1654.09	1656.31	1656	1657	0.023	3.42	78.32	65.96	1
Kater_Reach	5838.2	100Years	283.5	1654.09	1656.36	1656	1657	0.023	3.45	82.09	67.51	1
Kater_Reach	5732.1	2Years	198.5	1649.89	1656.18	1651	1656	5E-05	0.34	578.87	154.71	0.06
Kater_Reach	5732.1	5Years	224.1	1649.89	1656.33	1651	1656	6E-05	0.37	602.72	157.73	0.06
Kater_Reach	5732.1	10Years	242.9	1649.89	1656.43	1651	1656	6E-05	0.39	618.6	159.7	0.06
Kater_Reach	5732.1	25Years	251.8	1649.89	1656.48	1652	1656	7E-05	0.4	625.98	160.61	0.07
Kater_Reach	5732.1	50Years	267.5	1649.89	1656.56	1652	1657	7E-05	0.42	639.66	162.28	0.07
Kater_Reach	5732.1	100Years	283.5	1649.89	1656.64	1652	1657	7E-05	0.43	653.13	163.91	0.07
Kater_Reach	5588.3	2Years	198.5	1647.82	1656.18		1656	2E-05	0.25	803.22	173.77	0.04
Kater_Reach	5588.3	5Years	224.1	1647.82	1656.33		1656	2E-05	0.27	829.9	176.75	0.04
Kater_Reach	5588.3	10Years	242.9	1647.82	1656.43		1656	3E-05	0.29	847.65	178.7	0.04
Kater_Reach	5588.3	25Years	251.8	1647.82	1656.47		1656	3E-05	0.29	855.86	179.6	0.04
Kater_Reach	5588.3	50Years	267.5	1647.82	1656.56		1657	3E-05	0.31	871.14	181.26	0.04
Kater_Reach	5588.3	100Years	283.5	1647.82	1656.64		1657	3E-05	0.32	886.13	182.87	0.05
Kater_Reach	5433.3	2Years	198.5	1645.57	1656.17		1656	8E-06	0.18	1132.6	202.79	0.02
Kater_Reach	5433.3	5Years	224.1	1645.57	1656.33		1656	9E-06	0.19	1163.6	205.54	0.03
Kater_Reach	5433.3	10Years	242.9	1645.57	1656.43		1656	1E-05	0.21	1184.3	207.35	0.03
Kater_Reach	5433.3	25Years	251.8	1645.57	1656.47		1656	1E-05	0.21	1193.8	208.18	0.03
Kater_Reach	5433.3	50Years	267.5	1645.57	1656.56		1657	1E-05	0.22	1211.4	209.71	0.03
Kater_Reach	5433.3	100Years	283.5	1645.57	1656.64		1657	1E-05	0.23	1228.7	211.2	0.03
Kater_Reach	5301.9	2Years	198.5	1643.64	1656.17		1656	4E-06	0.14	1450.7	224.9	0.02
Kater_Reach	5301.9	5Years	224.1	1643.64	1656.33		1656	5E-06	0.15	1485.1	227.46	0.02
Kater_Reach	5301.9	10Years	242.9	1643.64	1656.43		1656	5E-06	0.16	1507.9	229.14	0.02
Kater_Reach	5301.9	25Years	251.8	1643.64	1656.47		1656	5E-06	0.17	1518.4	229.91	0.02
Kater_Reach	5301.9	50Years	267.5	1643.64	1656.56		1657	6E-06	0.17	1537.9	231.33	0.02
Kater_Reach	5301.9	100Years	283.5	1643.64	1656.64		1657	6E-06	0.18	1556.9	232.71	0.02
Kater_Reach	5139.2	2Years	198.5	1645.61	1656.17		1656	9E-06	0.18	1098.9	208.07	0.03
Kater_Reach	5139.2	5Years	224.1	1645.61	1656.32		1656	1E-05	0.2	1130.7	211.06	0.03
Kater_Reach	5139.2	10Years	242.9	1645.61	1656.42		1656	1E-05	0.21	1151.8	213.02	0.03
Kater_Reach	5139.2	25Years	251.8	1645.61	1656.47		1656	1E-05	0.22	1161.5	213.92	0.03
Kater_Reach	5139.2	50Years	267.5	1645.61	1656.55		1657	1E-05	0.23	1179.6	215.58	0.03
Kater_Reach	5139.2	100Years	283.5	1645.61	1656.64		1657	1E-05	0.24	1197.3	217.19	0.03

Kater_Reach	5020.9	2Years	198.5	1652.95	1655.86	1655	1656	0.008	2.35	84.63	58.13	0.62
Kater_Reach	5020.9	5Years	224.1	1652.95	1655.99	1655	1656	0.008	2.43	92.33	60.71	0.63
Kater_Reach	5020.9	10Years	242.9	1652.95	1656.07	1656	1656	0.009	2.5	97.22	62.3	0.64
Kater_Reach	5020.9	25Years	251.8	1652.95	1656.11	1656	1656	0.009	2.53	99.53	63.09	0.64
Kater_Reach	5020.9	50Years	267.5	1652.95	1656.18	1656	1657	0.009	2.57	104.26	65.04	0.65
Kater_Reach	5020.9	100Years	283.5	1652.95	1656.25	1656	1657	0.009	2.6	108.96	66.91	0.65
Kater_Reach	4873.7	2Years	198.5	1651.57	1653.67	1654	1654	0.024	3.22	61.74	58.78	1
Kater_Reach	4873.7	5Years	224.1	1651.57	1653.77	1654	1654	0.024	3.32	67.5	61.46	1.01
Kater_Reach	4873.7	10Years	242.9	1651.57	1653.85	1654	1654	0.023	3.35	72.6	63.74	1
Kater_Reach	4873.7	25Years	251.8	1651.57	1653.88	1654	1654	0.023	3.37	74.77	64.69	1
Kater_Reach	4873.7	50Years	267.5	1651.57	1653.94	1654	1655	0.023	3.42	78.26	66.18	1
Kater_Reach	4873.7	100Years	283.5	1651.57	1653.99	1654	1655	0.023	3.47	81.64	67.59	1.01
Kater_Reach	4686.4	2Years	198.5	1645.69	1653.52	1648	1654	3E-05	0.27	728.43	186.01	0.04
Kater_Reach	4686.4	5Years	224.1	1645.69	1653.63	1648	1654	4E-05	0.3	749.18	188.64	0.05
Kater_Reach	4686.4	10Years	242.9	1645.69	1653.71	1648	1654	4E-05	0.32	763.85	190.47	0.05
Kater_Reach	4686.4	25Years	251.8	1645.69	1653.75	1648	1654	4E-05	0.33	770.58	191.26	0.05
Kater_Reach	4686.4	50Years	267.5	1645.69	1653.81	1648	1654	4E-05	0.34	782.26	192.64	0.05
Kater_Reach	4686.4	100Years	283.5	1645.69	1653.87	1648	1654	5E-05	0.36	793.89	194	0.06
Kater_Reach	4486.7	2Years	198.5	1648.07	1653.51		1654	5E-05	0.31	632.53	197.64	0.06
Kater_Reach	4486.7	5Years	224.1	1648.07	1653.62		1654	6E-05	0.34	654.29	200.21	0.06
Kater_Reach	4486.7	10Years	242.9	1648.07	1653.7		1654	7E-05	0.36	669.62	202	0.06
Kater_Reach	4486.7	25Years	251.8	1648.07	1653.73		1654	7E-05	0.37	676.67	202.82	0.07
Kater_Reach	4486.7	50Years	267.5	1648.07	1653.79		1654	7E-05	0.39	688.81	204.22	0.07
Kater_Reach	4486.7	100Years	283.5	1648.07	1653.85		1654	8E-05	0.4	700.98	205.62	0.07
Kater_Reach	4392.1	2Years	198.5	1651.32	1653.02	1653	1653	0.026	2.92	67.96	79.83	1.01
Kater_Reach	4392.1	5Years	224.1	1651.32	1653.11	1653	1654	0.025	2.97	75.49	84.13	1
Kater_Reach	4392.1	10Years	242.9	1651.32	1653.17	1653	1654	0.025	3.02	80.51	86.88	1
Kater_Reach	4392.1	25Years	251.8	1651.32	1653.2	1653	1654	0.025	3.04	82.77	88.1	1
Kater_Reach	4392.1	50Years	267.5	1651.32	1653.24	1653	1654	0.025	3.08	86.74	90.18	1
Kater_Reach	4392.1	100Years	283.5	1651.32	1653.28	1653	1654	0.025	3.14	90.43	92.08	1.01
Kater_Reach	4265.2	2Years	198.5	1644.52	1645.25	1646	1646	0.203	4.64	42.76	117.26	2.46
Kater_Reach	4265.2	5Years	224.1	1644.52	1645.28	1646	1646	0.209	4.84	46.28	122	2.51
Kater_Reach	4265.2	10Years	242.9	1644.52	1645.3	1646	1647	0.213	4.98	48.82	125.3	2.55
Kater_Reach	4265.2	25Years	251.8	1644.52	1645.31	1646	1647	0.215	5.04	50	126.81	2.56
Kater_Reach	4265.2	50Years	267.5	1644.52	1645.33	1646	1647	0.218	5.14	52.06	129.4	2.59
Kater_Reach	4265.2	100Years	283.5	1644.52	1645.34	1646	1647	0.221	5.24	54.09	131.89	2.61
Kater_Reach	4140	2Years	198.5	1629.78	1644.42	1631	1644	0	0.05	3990.9	441.01	0.01
Kater_Reach	4140	5Years	224.1	1629.78	1644.57	1631	1645	0	0.06	4058	444.16	0.01

Kater_Reach	4140	10Years	242.9	1629.78	1644.67	1631	1645	0	0.06	4103.4	446.29	0.01
Kater_Reach	4140	25Years	251.8	1629.78	1644.71	1631	1645	0	0.06	4123.8	447.24	0.01
Kater_Reach	4140	50Years	267.5	1629.78	1644.8	1631	1645	1E-06	0.06	4160.1	448.93	0.01
Kater_Reach	4140	100Years	283.5	1629.78	1644.87	1631	1645	1E-06	0.07	4195.6	450.57	0.01
Kater_Reach	3914.2	2Years	198.5	1626.29	1644.42		1644	0	0.03	5717.4	521.51	0
Kater_Reach	3914.2	5Years	224.1	1626.29	1644.57		1645	0	0.04	5796.4	524.22	0
Kater_Reach	3914.2	10Years	242.9	1626.29	1644.67		1645	0	0.04	5850	526.05	0
Kater_Reach	3914.2	25Years	251.8	1626.29	1644.71		1645	0	0.04	5874.1	526.87	0
Kater_Reach	3914.2	50Years	267.5	1626.29	1644.8		1645	0	0.05	5916.8	528.32	0
Kater_Reach	3914.2	100Years	283.5	1626.29	1644.87		1645	0	0.05	5958.6	529.74	0
Kater_Reach	3769.3	2Years	198.5	1623.94	1644.42		1644	0	0.03	6189.7	555.37	0
Kater_Reach	3769.3	5Years	224.1	1623.94	1644.57		1645	0	0.04	6274.1	559.47	0
Kater_Reach	3769.3	10Years	242.9	1623.94	1644.67		1645	0	0.04	6331.2	562.22	0
Kater_Reach	3769.3	25Years	251.8	1623.94	1644.71		1645	0	0.04	6357	563.46	0
Kater_Reach	3769.3	50Years	267.5	1623.94	1644.8		1645	0	0.04	6402.7	565.65	0
Kater_Reach	3769.3	100Years	283.5	1623.94	1644.87		1645	0	0.04	6447.5	567.79	0
Kater_Reach	3341.8	2Years	198.5	1639.99	1644.41		1644	1E-04	0.35	567.75	262.6	0.08
Kater_Reach	3341.8	5Years	224.1	1639.99	1644.56		1645	1E-04	0.37	607.52	265.94	0.08
Kater_Reach	3341.8	10Years	242.9	1639.99	1644.66		1645	1E-04	0.38	634.58	268.19	0.08
Kater_Reach	3341.8	25Years	251.8	1639.99	1644.71		1645	1E-04	0.39	646.82	269.2	0.08
Kater_Reach	3341.8	50Years	267.5	1639.99	1644.79		1645	1E-04	0.4	668.57	270.99	0.08
Kater_Reach	3341.8	100Years	283.5	1639.99	1644.86		1645	1E-04	0.41	689.89	272.74	0.08
Kater_Reach	3158.3	2Years	198.5	1639.85	1644.38		1644	2E-04	0.48	409.41	154.01	0.09
Kater_Reach	3158.3	5Years	224.1	1639.85	1644.53		1645	2E-04	0.52	432.47	157.95	0.1
Kater_Reach	3158.3	10Years	242.9	1639.85	1644.63		1645	2E-04	0.54	448.29	160.86	0.1
Kater_Reach	3158.3	25Years	251.8	1639.85	1644.67		1645	2E-04	0.55	455.5	162.16	0.11
Kater_Reach	3158.3	50Years	267.5	1639.85	1644.75		1645	2E-04	0.57	468.41	164.47	0.11
Kater_Reach	3158.3	100Years	283.5	1639.85	1644.83		1645	2E-04	0.59	481.15	166.72	0.11
Kater_Reach	3031	2Years	198.5	1641	1644.26		1644	0.002	1.19	166.11	100.38	0.3
Kater_Reach	3031	5Years	224.1	1641	1644.4		1644	0.002	1.24	180.4	104.5	0.3
Kater_Reach	3031	10Years	242.9	1641	1644.5		1645	0.002	1.28	190.26	107.26	0.31
Kater_Reach	3031	25Years	251.8	1641	1644.54		1645	0.002	1.29	194.74	108.48	0.31
Kater_Reach	3031	50Years	267.5	1641	1644.61		1645	0.002	1.32	202.86	110.67	0.31
Kater_Reach	3031	100Years	283.5	1641	1644.68		1645	0.002	1.34	210.93	112.81	0.31
Kater_Reach	2855.1	2Years	198.5	1641	1643.03	1643	1644	0.023	3.1	63.94	62.96	0.98
Kater_Reach	2855.1	5Years	224.1	1641	1643.12	1643	1644	0.024	3.22	69.49	65.63	1
Kater_Reach	2855.1	10Years	242.9	1641	1643.19	1643	1644	0.023	3.28	74.09	67.77	1
Kater_Reach	2855.1	25Years	251.8	1641	1643.22	1643	1644	0.023	3.31	76.18	68.72	1
Kater_Reach	2855.1	50Years	267.5	1641	1643.27	1643	1644	0.023	3.35	79.78	70.32	1.01

Kater_Reach	2855.1	100Years	283.5	1641	1643.32	1643	1644	0.023	3.4	83.43	73.87	1.01
Kater_Reach	2707.8	2Years	198.5	1642.25	1639.19	1639	1639	0.039		90.38	179.61	0
Kater_Reach	2707.8	5Years	224.1	1642.25	1639.24	1639	1640	0.038		99.7	188.9	0
Kater_Reach	2707.8	10Years	242.9	1642.25	1639.27	1639	1640	0.038		106.45	196.19	0
Kater_Reach	2707.8	25Years	251.8	1642.25	1639.28	1639	1640	0.039		108.04	198.3	0
Kater_Reach	2707.8	50Years	267.5	1642.25	1639.31	1639	1640	0.038		114.8	203.31	0
Kater_Reach	2707.8	100Years	283.5	1642.25	1639.33	1639	1640	0.038		118.88	206.17	0
Kater_Reach	2612.7	2Years	198.5	1643.58	1636.03	1635	1636	6E-04		339.8	327.62	0
Kater_Reach	2612.7	5Years	224.1	1643.58	1636.1	1635	1636	7E-04		366.67	447.13	0
Kater_Reach	2612.7	10Years	242.9	1643.58	1636.15	1635	1636	8E-04		390.31	530.48	0
Kater_Reach	2612.7	25Years	251.8	1643.58	1636.17	1635	1636	8E-04		402.41	568.44	0
Kater_Reach	2612.7	50Years	267.5	1643.58	1636.21	1635	1636	8E-04		424.95	633.07	0
Kater_Reach	2612.7	100Years	283.5	1643.58	1636.32	1635	1636	0.001		499.03	649.98	0
Kater_Reach	2488	2Years	198.5	1641.22	1635.87		1636	0.004		221.68	313.25	0
Kater_Reach	2488	5Years	224.1	1641.22	1635.93		1636	0.004		239.27	320.68	0
Kater_Reach	2488	10Years	242.9	1641.22	1635.96		1636	0.004		251.88	325.91	0
Kater_Reach	2488	25Years	251.8	1641.22	1635.98		1636	0.004		257.57	328.24	0
Kater_Reach	2488	50Years	267.5	1641.22	1636.01		1636	0.004		267.55	332.29	0
Kater_Reach	2488	100Years	283.5	1641.22	1636.04		1636	0.004		277.55	336.3	0
Kater_Reach	2301.9	2Years	198.5	1636.9	1635.83		1636	1E-04		742.37	458.63	0
Kater_Reach	2301.9	5Years	224.1	1636.9	1635.88		1636	1E-04		764.58	465.26	0
Kater_Reach	2301.9	10Years	242.9	1636.9	1635.91		1636	2E-04		780.23	469.88	0
Kater_Reach	2301.9	25Years	251.8	1636.9	1635.93		1636	2E-04		787.24	471.93	0
Kater_Reach	2301.9	50Years	267.5	1636.9	1635.95		1636	2E-04		799.3	475.44	0
Kater_Reach	2301.9	100Years	283.5	1636.9	1635.98		1636	2E-04		811.37	478.93	0
Kater_Reach	2143.8	2Years	198.5	1629.84	1635.83		1636	9E-06	0.14	1904.2	808.44	0.02
Kater_Reach	2143.8	5Years	224.1	1629.84	1635.88		1636	1E-05	0.15	1943.1	817.99	0.03
Kater_Reach	2143.8	10Years	242.9	1629.84	1635.91		1636	1E-05	0.16	1970.3	824.62	0.03
Kater_Reach	2143.8	25Years	251.8	1629.84	1635.93		1636	1E-05	0.16	1982.5	827.57	0.03
Kater_Reach	2143.8	50Years	267.5	1629.84	1635.95		1636	1E-05	0.17	2003.5	832.62	0.03
Kater_Reach	2143.8	100Years	283.5	1629.84	1635.98		1636	2E-05	0.18	2024.4	837.62	0.03
Kater_Reach	2005.9	2Years	198.5	1624.04	1635.83		1636	1E-06	0.06	4482.6	1186	0.01
Kater_Reach	2005.9	5Years	224.1	1624.04	1635.88		1636	1E-06	0.06	4539.5	1195	0.01
Kater_Reach	2005.9	10Years	242.9	1624.04	1635.91		1636	1E-06	0.07	4579.4	1201.3	0.01
Kater_Reach	2005.9	25Years	251.8	1624.04	1635.93		1636	1E-06	0.07	4597	1204.1	0.01
Kater_Reach	2005.9	50Years	267.5	1624.04	1635.95		1636	1E-06	0.07	4627.5	1208.8	0.01
Kater_Reach	2005.9	100Years	283.5	1624.04	1635.98		1636	1E-06	0.08	4658	1213.6	0.01
Kater_Reach	1847.1	2Years	198.5	1625.64	1635.83		1636	1E-06	0.07	3996.5	1453.3	0.01

Kater_Reach	1847.1	5Years	224.1	1625.64	1635.88		1636	2E-06	0.07	4066.2	1465.5	0.01
Kater_Reach	1847.1	10Years	242.9	1625.64	1635.91		1636	2E-06	0.08	4115	1472.9	0.01
Kater_Reach	1847.1	25Years	251.8	1625.64	1635.93		1636	2E-06	0.08	4136.5	1476.2	0.01
Kater_Reach	1847.1	50Years	267.5	1625.64	1635.95		1636	2E-06	0.08	4173.9	1481.9	0.01
Kater_Reach	1847.1	100Years	283.5	1625.64	1635.98		1636	3E-06	0.09	4211.3	1487.6	0.01
Kater_Reach	1696.6	2Years	198.5	1626.68	1635.83		1636	1E-06	0.05	4882	1675.6	0.01
Kater_Reach	1696.6	5Years	224.1	1626.68	1635.88		1636	1E-06	0.06	4962.6	1707	0.01
Kater_Reach	1696.6	10Years	242.9	1626.68	1635.91		1636	1E-06	0.06	5019.8	1729	0.01
Kater_Reach	1696.6	25Years	251.8	1626.68	1635.93		1636	2E-06	0.06	5045.1	1738.6	0.01
Kater_Reach	1696.6	50Years	267.5	1626.68	1635.95		1636	2E-06	0.07	5089.3	1755.3	0.01
Kater_Reach	1696.6	100Years	283.5	1626.68	1635.98		1636	2E-06	0.07	5133.4	1764.6	0.01
Kater_Reach	1527.6	2Years	198.5	1628.65	1635.83		1636	0	0.03	6483.9	1449	0.01
Kater_Reach	1527.6	5Years	224.1	1628.65	1635.88		1636	0	0.04	6553.1	1457	0.01
Kater_Reach	1527.6	10Years	242.9	1628.65	1635.91		1636	1E-06	0.04	6601.7	1462.5	0.01
Kater_Reach	1527.6	25Years	251.8	1628.65	1635.93		1636	1E-06	0.04	6622.9	1464.9	0.01
Kater_Reach	1527.6	50Years	267.5	1628.65	1635.95		1636	1E-06	0.04	6660	1469.1	0.01
Kater_Reach	1527.6	100Years	283.5	1628.65	1635.98		1636	1E-06	0.04	6696.8	1473.3	0.01
Kater_Reach	1401	2Years	198.5	1626.43	1635.83		1636	0	0.02	7795.1	1614.7	0
Kater_Reach	1401	5Years	224.1	1626.43	1635.88		1636	0	0.03	7872.1	1617.3	0
Kater_Reach	1401	10Years	242.9	1626.43	1635.91		1636	0	0.03	7926	1619	0
Kater_Reach	1401	25Years	251.8	1626.43	1635.93		1636	0	0.03	7949.6	1619.8	0
Kater_Reach	1401	50Years	267.5	1626.43	1635.95		1636	0	0.03	7990.6	1621.2	0
Kater_Reach	1401	100Years	283.5	1626.43	1635.98		1636	0	0.03	8031.2	1622.5	0.01
Kater_Reach	1229.7	2Years	198.5	1629.75	1635.83		1636	1E-06	0.04	5256.3	1365.4	0.01
Kater_Reach	1229.7	5Years	224.1	1629.75	1635.88		1636	1E-06	0.05	5321.2	1367.2	0.01
Kater_Reach	1229.7	10Years	242.9	1629.75	1635.91		1636	1E-06	0.05	5366.6	1368.4	0.01
Kater_Reach	1229.7	25Years	251.8	1629.75	1635.93		1636	1E-06	0.05	5386.5	1368.9	0.01
Kater_Reach	1229.7	50Years	267.5	1629.75	1635.95		1636	1E-06	0.05	5421.2	1369.9	0.01
Kater_Reach	1229.7	100Years	283.5	1629.75	1635.98		1636	1E-06	0.06	5455.5	1370.8	0.01
Kater_Reach	967.42	2Years	198.5	1636.8	1635.68		1636	0.028		122.95	303.31	0
Kater_Reach	967.42	5Years	224.1	1636.8	1635.72		1636	0.028		135.46	322.55	0
Kater_Reach	967.42	10Years	242.9	1636.8	1635.75		1636	0.027		145.56	339.76	0
Kater_Reach	967.42	25Years	251.8	1636.8	1635.77		1636	0.027		149.8	346.73	0
Kater_Reach	967.42	50Years	267.5	1636.8	1635.79		1636	0.027		157.74	359.4	0
Kater_Reach	967.42	100Years	283.5	1636.8	1635.81		1636	0.027		165.78	364.95	0
Kater_Reach	798.5	2Years	198.5	1630.8	1632		1632	0.018	1.91	105.85	193.85	0.79
Kater_Reach	798.5	5Years	224.1	1630.8	1632.05	1632	1632	0.018	1.98	115.87	202.6	0.8
Kater_Reach	798.5	10Years	242.9	1630.8	1632.08	1632	1632	0.018	2.04	122.28	207.46	0.81
Kater_Reach	798.5	25Years	251.8	1630.8	1632.09	1632	1632	0.018	2.06	125.63	209.96	0.81

Kater_Reach	798.5	50Years	267.5	1630.8	1632.12	1632	1632	0.018	2.1	131.12	213.99	0.81
Kater_Reach	798.5	100Years	283.5	1630.8	1632.15	1632	1632	0.018	2.14	136.88	218.13	0.82
Kater_Reach	614.31	2Years	198.5	1626.28	1627.79	1628	1628	0.027	2.74	72.4	96.22	1.01
Kater_Reach	614.31	5Years	224.1	1626.28	1627.86	1628	1628	0.026	2.81	79.8	101.01	1.01
Kater_Reach	614.31	10Years	242.9	1626.28	1627.91	1628	1628	0.026	2.85	85.32	103.71	1
Kater_Reach	614.31	25Years	251.8	1626.28	1627.94	1628	1628	0.026	2.87	87.61	104.63	1
Kater_Reach	614.31	50Years	267.5	1626.28	1627.98	1628	1628	0.025	2.91	91.85	106.32	1
Kater_Reach	614.31	100Years	283.5	1626.28	1628.01	1628	1628	0.025	2.96	95.85	107.89	1
Kater_Reach	426.57	2Years	198.5	1627.32	1626.33	1625	1626	0.003		182.79	140.33	0
Kater_Reach	426.57	5Years	224.1	1627.32	1626.42	1625	1626	0.003		196.16	145.37	0
Kater_Reach	426.57	10Years	242.9	1627.32	1626.48	1625	1627	0.003		205.75	148.89	0
Kater_Reach	426.57	25Years	251.8	1627.32	1626.51	1625	1627	0.003		210.21	150.49	0
Kater_Reach	426.57	50Years	267.5	1627.32	1626.57	1626	1627	0.003		217.98	153.25	0
Kater_Reach	426.57	100Years	283.5	1627.32	1626.62	1626	1627	0.003		225.74	155.95	0
Kater_Reach	279.28	2Years	198.5	1628.12	1626.13		1626	8E-04		301.86	196.42	0
Kater_Reach	279.28	5Years	224.1	1628.12	1626.21		1626	9E-04		316.9	199.27	0
Kater_Reach	279.28	10Years	242.9	1628.12	1626.26		1626	1E-03		327.57	201.26	0
Kater_Reach	279.28	25Years	251.8	1628.12	1626.28		1626	1E-03		332.5	202.18	0
Kater_Reach	279.28	50Years	267.5	1628.12	1626.33		1626	0.001		340.99	203.75	0
Kater_Reach	279.28	100Years	283.5	1628.12	1626.37		1626	0.001		349.3	205.27	0
Kater_Reach	77.768	2Years	198.5	1626.3	1625.61	1625	1626	0.018		151.26	358.59	0
Kater_Reach	77.768	5Years	224.1	1626.3	1625.65	1626	1626	0.018		163.63	364.17	0
Kater_Reach	77.768	10Years	242.9	1626.3	1625.67	1626	1626	0.018		172.51	368.13	0
Kater_Reach	77.768	25Years	251.8	1626.3	1625.68	1626	1626	0.018		176.63	369.95	0
Kater_Reach	77.768	50Years	267.5	1626.3	1625.7	1626	1626	0.018		183.77	373.08	0
Kater_Reach	77.768	100Years	283.5	1626.3	1625.72	1626	1626	0.018		190.96	376.21	0

APPENDIX-D FloodplainMapping

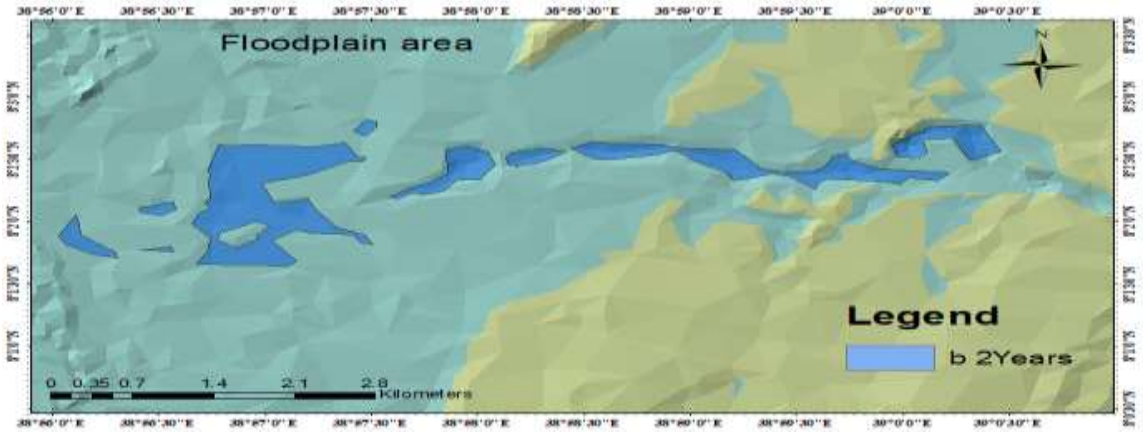

FigureD1: Floodplain area map from 2-year peak flood

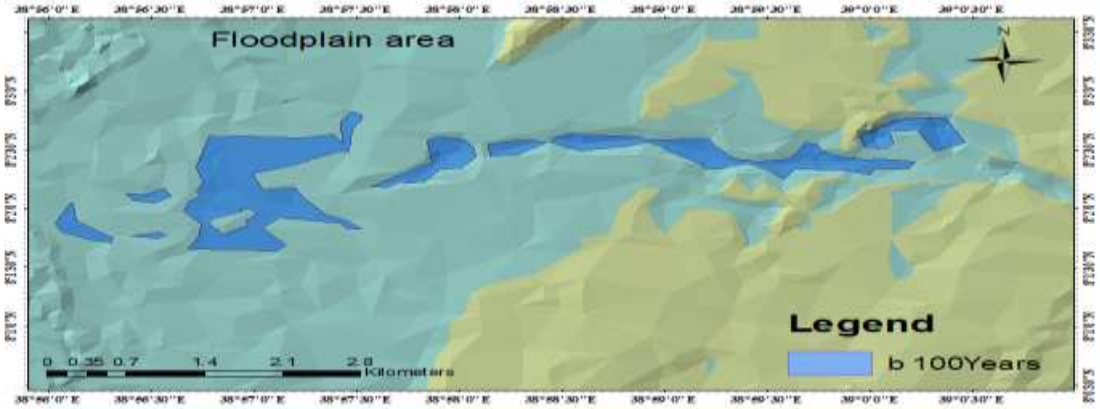

FigureD2: Floodplain area map from 100-year peak flood

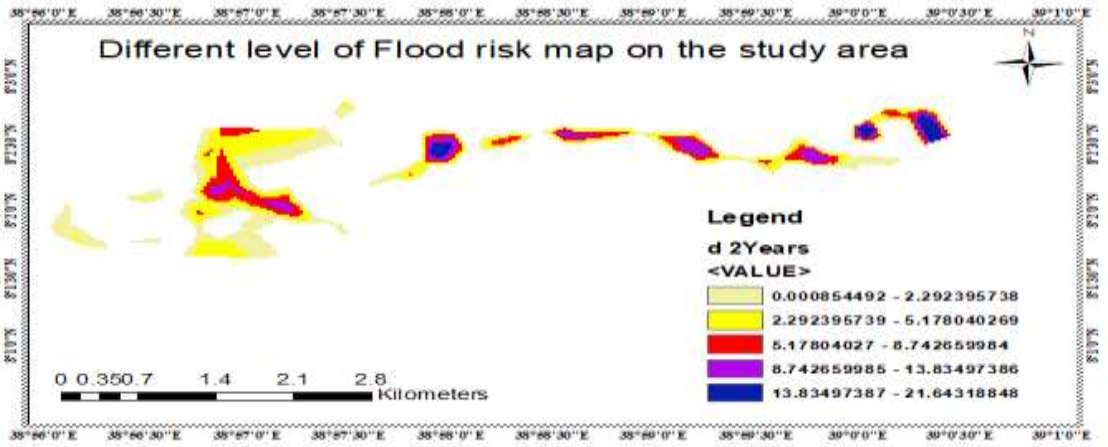

Figure D3: Flood risk map from 2-year peak flood

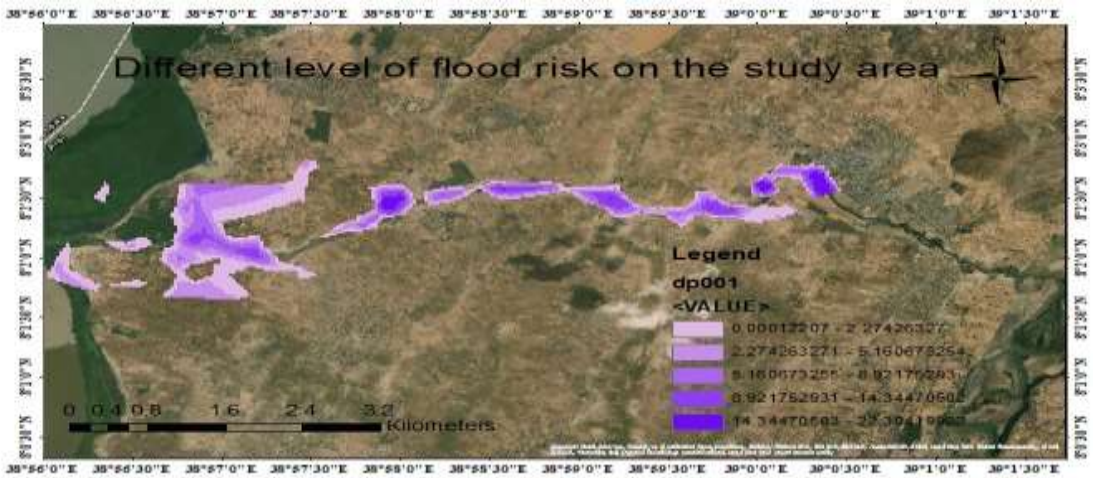

Figure D4: Flood risk map from 100-year peak flood